The role of P2X7 receptor in anxiety and depression: characterization of transgenic mouse models

Lidia Urbina Treviño

Graduate School of Systemic Neurosciences

LMU Munich

Dissertation at the

Graduate School of Systemic Neurosciences

Ludwig-Maximilians-Universität München

November 2021

Supervisor: Dr Jan Deussing.

Max Planck Institute of Psychiatry

First Reviewer: Dr Jan Deussing

Second Reviewer: Prof Dr Annette Nicke

External Reviewer: Prof Dr Beata Sperlagh

Date of Submission: 26th November 2021

Date of Defense: 7th March 2022

Table of contents

1. Abbreviations

^{35}S-UTP: Sulfur-labeled uridine triphosphate

ATP: Adenosine triphosphate

BBG: Coomassie Brilliant Blue G

BD: Bipolar disorder

BDNF: Brain-derived neurotrophic factor

BzATP: 2',3'-O-(benzoyl-4-benzoyl)-ATP

CNS: Central nervous system

CSDS: Chronic social defeat stress

Ct: Crossing points

CUS: Chronic unpredictable stressor

DEPC: Diethyl pyrocarbonate

dNTPs: Deoxyribonucleotides

DTT: Dithiothreitol

eATP: Extracellular ATP

ECS: Extracellular space

EGFP: Enhanced green fluorescent protein

EPM: Elevated plus maze

ERT2: Modified ligand binding domain of the estrogen receptor

FBS: Fetal bovine serum

FST: Forced swim test

HA-Tag/Ribotag: Hemagglutinin tag

HCL: Home cage locomotion test

hKO: conditional humanized P2X7R KO

hP2X7R/hWT: humanized P2X7R

HPA axis: Hypothalamic-pituitary-adrenal axis

IKMC: International Knockout Mouse Consortium

IL-1β: Interleukine 1-beta

IL-6: Interleukine 6

ISH: *In situ* hybridization

KO: Knockout

LDB: Light-dark box

LPS: Lipopolysaccharide

MDD: Major depressive disorder

Micro-KO: Microglia-specific P2X7R KO

NaPyr: Sodium pyruvate

NEAA: Non-essential amino acids

nEGFP: Nuclear EGFP

NGS: Normal goat serum

NT: Non-treated

OFT: Open field test

OH-TAM: (Z)-4-Hydroxytamoxifen

P/S: Penicillin / Streptomycin

P2X4R: Purinergic P2X4 receptor

P2X7R: Purinergic P2X7 receptor

P2X7R-KO: P2X7R-knockout

PCR: Polymerase chain reaction

PDL: Poly-D-Lysine

PFA: Paraformaldehyde

ROS: Reactive oxygen species

RT-qPCR: Real time quantitative PCR

RT: Room temperature

SAT: Social avoidance test

sEGFP: Soluble EGFP

SEM: Standard error of the mean

SNP: Single-nucleotide polymorphism

SPT: Sucrose preference test

TNF-α: Tumor necrosis factor alpha

WT: wildtype

2. Abstract

Major depression (MDD) is a common psychiatric disorder and currently one of the main causes of disability worldwide. It is a multifactorial disease where both genetic and environmental factors have an impact on its development and outcome. One of the genes that has previously been linked to MDD is the purinergic P2X7 receptor (P2X7R). Earlier studies have suggested that P2X7R inactivation ameliorates anxiety- and depressive-like behaviors in mice. To further substantiate the evidence, we carried out a behavioral assessment of humanized P2X7R mice and thereof derived P2X7R knockout (P2X7R-KO) mice. Full inactivation of P2X7R did not produce major effects in anxiety, anhedonia or coping behaviors neither under baseline, acute stress, nor chronic stress conditions. The same was true for a microglia-specific P2X7R-KO mouse line, validated *in vitro*, which presented increased locomotion, but no variation in any other behavioral readout under baseline or chronic stress conditions. Furthermore, two P2X7R reporter mouse lines were characterized, one expressing soluble EGFP under a P2X7R promoter (sEGFP), and another expressing a P2X7-EGFP fusion protein. Both mouse lines showed overexpression of P2X7R. However, the sEGFP mice also presented P2X4R overexpression and ectopic reporter gene expression, which was not the case for the P2X7-EGFP line. Additionally, a third potential reporter mouse line expressing CreERT2 under the regulatory control of the endogenous P2X7R locus was analyzed. The detailed characterization revealed a lack of functionality, which was ascribed to an aberrant insertion of the targeting construct in the P2X7R locus. The P2X7-EGFP and sEGFP lines were also used to assess the behavioral consequences of P2X7R overexpression under baseline conditions. However, neither line presented significant alterations in depressive or anxiety-related phenotypes compared to control littermates. This study illustrates the great potential but also caveats of different transgenic mouse lines to assess P2X7R expression and to determine the impact of P2X7R activity on behavioral phenotypes.

3. Introduction

3.1 *Major depressive disorder*

Major depressive disorder (MDD) is a highly prevalent psychiatric disorder affecting around 2-6% of the global population. Specifically, 4.1% of women and 2.6% of men are estimated to present the disorder. This means that approximately 260 million people are currently suffering from depression (Kessler et al. 1993; Sassarini 2016; Ritchie & Roser 2018). Nowadays, MDD is responsible for an average of 7.5% of total years of disability, which is why it is considered the main source of disability by the World Health Organization. Furthermore, it is responsible for approximately 800,000 deaths by suicide per year worldwide, making it the leading cause of death among young people (WHO, 2017). MDD not only produces great societal burden, but also economic. On average, the estimated yearly, total costs of MDD are around 8,000 to 16,000 USD per person (Chow et al., 2019). In the United States alone, an approximate 210 million USD was spent in 2010 in direct and indirect costs as a consequence of MDD (Greenberg et al., 2015).

The severe consequences resulting from an undetected or untreated depressive disorder highlight the importance of an accurate diagnosis and screening process. Some of the most common symptoms of MDD are low mood, anhedonia, hopelessness, guilt, low self-esteem, fluctuations in appetite and sleep, lack of energy and focus, irritability, and thoughts of death (American Psychiatric Association. Diagnostic and Statistical Manual of Mental Disorders, 5th Edition: DSM-5, 2013). In order to diagnose a depressive episode, there must be clear, significant changes that cause distress or impairment and last for a period of at least 2 weeks. However, the psychiatric symptoms as well as the somatization of depression can vary greatly from person to person. Furthermore, depression often arises as a comorbidity of other disorders, which can make the diagnosis much more complex due to common symptomatology among the different conditions. These facts, combined with an inadequate understanding of the complexities underlying a depressive episode, render its diagnosis extremely challenging.

Due to the high interpersonal variability of MDD, finding an effective treatment can be a demanding task. The most effective, widespread treatments available can be divided in pharmacological and psychological therapy. Currently, medications employed to treat MDD aim to maintain elevated concentrations of monoamines in the synaptic cleft, either by

inhibiting the reuptake (i.e. selective serotonin reuptake inhibitors, tricyclic antidepressants) or by preventing the enzymatic processing of these substances (i.e. monoamine oxidase inhibitors) (Otte et al., 2016). Even though these medications have improved the quality of life of many who suffer from MDD, they also bear limitations. The full pharmacological effect of available antidepressants can take from weeks to months (Machado-Vieira et al., 2010) and the lack of noticeable changes during these first few weeks of treatment increases the danger for treatment drop-out, self-harm and suicide (Jick et al., 2004; Rohden et al., 2017; Simon et al., 2006). Moreover, long-term use of these drugs can cause adverse side effects such as nausea, weight gain, fatigue and sexual dysfunction (Cassano & Fava, 2004; Ferguson, 2001), which often lead to treatment dropout. Despite the drawbacks of the pharmacological treatment, it is known that it can be quite an effective therapy for MDD, even more so when it is delivered in combination with psychotherapy (Cuijpers et al., 2020). The main limitation of the currently available antidepressant treatments is their lack of overall effectivity, even when it consists of combination therapy. Only 30-50% of treated patients experience full remission of MDD, leaving a large subset of the affected population without a functional treatment. This is referred to as treatment-resistant depression (McIntyre et al., 2014).

Although there are certain factors that can serve as predictors of MDD outcome and treatment response (Kraus et al., 2019), there is no singular causative element defined for MDD. It is known that environmental factors have a great influence on its appearance: there is a high correlation between stressful events such as early life adversity, physical or psychological abuse and traumatic events, and development of MDD (Dube et al. 2001; Kessler et al. 1997). In addition, there are genetic factors that can prompt the appearance of MDD. Twin studies indicate a heritability around 35%, which is significantly higher in in women than men (Kendler et al., 2006; Sullivan et al., 2000). Due to the polygenic nature of MDD, its heterogeneity, the low relative effect of individual genes and the interaction between environment and genes, it has been difficult to identify single candidate genes (Kupfer et al., 2012; Lopizzo et al., 2015). However, studies have pinpointed gene variants that are potential risk factors for MDD development (Shadrina et al. 2018). Among them is the purinergic P2X7 receptor (P2X7R) which is a key player in the activation of the inflammatory response in the central nervous system (CNS). For the sake of simplicity, during this dissertation all the elements from the *P2rx7* gene to the receptor protein will be referred to as P2X7R.

3.2 *Neuroinflammation*

Neuroinflammation is a physiological process that has the function to restore homeostasis in the CNS when it suffers from a challenge such as an infection, cell stress or physical trauma. However, the immune system can be a source of pathology when it responds to a non-threatening stimulus or when this response is exacerbated (Rosenblat et al., 2015). Transient, controlled production of inflammatory cytokines in the brain is involved in plasticity, tissue repair and neuroprotection. In contrast, sustained neuroinflammation has been linked to neurodegenerative disorders, aging, anxiety and depression (Dantzer et al., 2008; Di Benedetto et al., 2017; DiSabato et al., 2016).

Microglial cells are the main inflammatory cell type in the CNS. They are the resident macrophages in the brain and spinal cord, comprising approximately 10% of the total cells in these structures. When there is cellular stress due to pathogens or trauma, microglia become activated, migrate towards the pathological stimulus, and provide three types of response. First, they produce neurotrophic factors that contribute to brain tissue repair. Secondly, they are responsible for the elimination of pathogens and potentially harming elements such as dead cells or aggregates via phagocytosis. Finally, they produce inflammatory cytokines and chemokines, which will lead to proliferation, activation and migration of leukocytes to the brain (Colonna & Butovsky, 2017). These include Interleukin 1 beta (IL-1β), tumor necrosis factor alpha (TNF-α) and reactive oxygen species (ROS). Transient production and secretion of these factors is necessary for the defense against pathology, but sustained or chronic production is potentially neurotoxic and leads to neuronal dysfunction (Lyman et al., 2014). In fact, abnormal activation of microglia has been linked to neurodegenerative disorders as well as psychiatric disorders such as depression and schizophrenia (Shabab et al., 2017).

3.3 *The P2X7 Receptor*

3.3.1 *General characteristics*

P2X7R belongs to the P2X family, that is formed by 7 members (P2X1-7), all of which are trimeric ligand-gated ion channels that respond to extracellular adenosine triphosphate (ATP). Each subunit has two transmembrane domains with intracellular C and N-termini and a large ectodomain (Figure 1 A). Each of the three ATP binding sites are formed between the interfaces of two subunits, which contain highly conserved residues (Figure 1 B-C). The three-dimensional structure of the ectodomain has been characterized for years, but the structure of the cytoplasmic domain has only recently been determined. The C-terminus is formed by two elements: a cysteine-rich region that serves as an anchor to the cell membrane, and a 200-residue long region that has been denominated as "cytoplasmic ballast" (Hattori and Gouaux 2012; Karasawa and Kawate 2016; McCarthy et al. 2019). Once activated, the P2X7R channel undergoes structural changes and adopts an open conformation, allowing the flow of positive ions (Habermacher et al., 2016) (Figure 1 B).

A distinct feature of P2X7R is the fact that it responds to much higher concentrations of ATP, with an EC50 of 100 µM, compared to the other members of the P2X family, whose EC50 ranges lie between 0.07 and 12 µM (Khakh & North, 2012). However, P2X7R has a higher sensitivity than any other member of the P2X family for the ATP analogue 2',3'-O-(benzoyl-4-benzoyl)-ATP (BzATP), which is commonly employed as a P2X7R agonist (Donnelly-Roberts, Namovic, Han, et al., 2009). Moreover, P2X7R possesses a long intracellular C-terminus domain, which is around 240 amino acids longer than those of other P2X receptors. This region of the protein has been linked to the ability of P2X7R to produce large pores in the cell membrane, which allows the trafficking of larger molecules, up to 8.5 Å (Di Virgilio et al., 2018; Riedel et al., 2007; Surprenant et al., 1996).

P2X7R promotes several physiological functions in the CNS, including neurotransmitter release, intercellular communication, cell proliferation and cell growth (Fellin et al., 2006; Suadicani et al., 2006; Tewari & Seth, 2015; Volonte et al., 2012). However, the most studied function of P2X7R is its role in the innate and adaptive immune responses. P2X7R is considered as the gatekeeper of the immune response in the brain, which is consistent with its comparably low sensitivity to ATP within the P2X family.

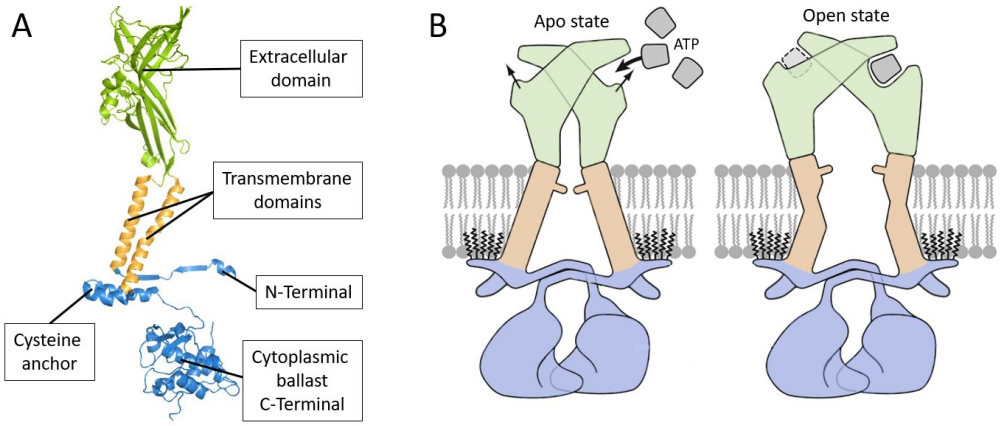

C

```
Human      MPACCSCSDVFQYETNKVTRIQSMNYGTIKWFFHVIIFSYVCFALVSDKLYQRKEPVISS     60
Mouse      MPACCSWNDVLQYETNKVTRIQSTNYGTVKWVLHMIVFSYISFALVSDKLYQRKEPVISS     60
           ****** .**:************ ****:**.:*:*:***:.****************

Human      VHTKVKGIAEVKEEIVENGVKKLVHSVFDTADYTFPLQGNSFFVMTNFLKTEGQEQRLCP     120
Mouse      VHTKVKGIAEVTENVTEGGVTKLGHSIFDTADYTFPLQGNSFFVMTNYVKSEGQVQTLCP     120
           ***********.*::.*.**.** **:*********************::*:*** * ***

Human      EYPTRRTLCSSDRGCKKGWMDPQSKGIQTGRCVVYEGNQKTCEVSAWCPIEAVEEAPRPA     180
Mouse      EYPRRGAQCSSDRRCKKGWMDPQSKGIQTGRCVPYDKTRKTCEVSAWCPTEEEKEAPRPA     180
           *** * : ***** ****************** *: .:********** *  :******

Human      LLNSAENFTVLIKNNIDFPGHNYTTRNILPGLNITCTFHKTQNPQCPIFRLGDIFRETGD     240
Mouse      LLRSAENFTVLIKNNIHFPGHNYTTRNILPTMNGSCTFHKTWDPQCSIFRLGDIFQEAGE     240
           **.*************.************* :* :****** :*** ********:*:*:

Human      NFSDVAIQGGIMGIEIYWDCNLDRWFHHCRPKYSFRRLDDKTTNVSLYPGYNFRYAKYYK     300
Mouse      NFTEVAVQGGIMGIEIYWDCNLDSWSHHCRPRYSFRRLDDKNTDESFVPGYNFRYAKYYK     300
           **::**:***************** * *****:*********.*: *:  ************

Human      ENNVEKRTLIKVFGIRFDILVFGTGGKFDIIQLVVYIGSTLSYFGLAAVFIDFLIDTYSS     360
Mouse      ENNVEKRTLIKAFGIRFDILVFGTGGKFDIIQLVVYIGSTLSYFGLATVCIDLLINTYSS     360
           ***********.************************************:* **:**:****

Human      NCCRSHIYPWCKCCQPCVVNEYYYRKKCESIVEPKPTLKYVSFVDESHIRMVNQQLLGRS     420
Mouse      AFCRSGVYPYCKCCEPCTVNEYYYRKKCESIMEPKPTLKYVSFVDEPHIRMVDQQLLGKS     420
             *** :**:****:**.*************:************** *****:*****:*

Human      LQDVKGQEVPRPAMDFTDLSRLPLALHDTPPIPGQPEEIQLLRKEATPRSRDSPVWCQCG     480
Mouse      LQVVKGQEVPRPQMDFSDLSRLSLSLHDSPLTPGQSEEIQLLHEEVAPKSGDSPSWCQCG     480
           ** ********* ***:***** *:***:*  *** ******::*.:*:* *** *****

Human      SCLPSQLPESHRCLEELCCRKKPGACITTSELFRKLVLSRHVLQFLLLYQEPLLALDVDS     540
Mouse      NCLPSRLPEQRRALEELCCRRKPGRCITTSKLFHKLVLSRDTLQLLLLYQDPLLVLGEEA     540
           .****:***.:*.*******:*** ***** :**:******..**:*****:***.*. ::

Human      TNSRLRHCAYRCYATWRFGSQDMADFAILPSCCRWRIRKEFPKSEGQYSGFKSPY         595
Mouse      TNSRLRHRAYRCYATWRFGSQDMADFAILPSCCRWRIRKEFPKTEGQYSGFKYPY         595
           ******* ************************************.******** **
```

Figure 1. Three-dimensional structure of P2X7R and analogy with the sequence. Depicted in colors are the ectodomain (green), transmembrane regions (orange) and cytoplasmic region (blue). (A) Three-dimensional structure of one subunit of P2X7R (PDB: 6U9V). Structure edited with Swiss-PDB Viewer (http://www.expasy.org/spdbv/). (B) Scheme depicting the interactions between two subunits of P2X7R and the conformational change occurring in P2X7R upon ATP binding. modified from McCarthy et al., 2019 with permission. (C) Sequence alignment of the human and murine P2X7R. The highly conserved ATP binding residues are K66, T189, L191, I214, I228, N292, R294, K311 (in bold). The residues involved in the cysteine-rich membrane anchor are S360, C362, C363, C374, C371, C363, C377 (in bold). Alignment produced with Clustal Omega, "*" indicates perfect alignment; ":" indicates group with strong similarity; "." indicates group with weak similarity; " " indicates no similarity.

Under physiological conditions, the levels of ATP in the extracellular space (ECS) are relatively low. Cell trauma leads to cell lysis, which elevates the levels of extracellular ATP (eATP). Although ATP is mostly known for its role in cell metabolism in the intracellular compartment, it also has a key role as a messenger in the ECS (Burnstock, 2006). This eATP binds to P2X7R expressed in the microglial cell membrane and elicits a conformational change to an open state, where the channel allows the flow of positive ions (Figure 1 B). This leads to sodium and calcium influx and potassium efflux. The latter is believed to be the key step to activate the assembly of the inflammasome (NLRP3/ASC/Procaspase-1) and the cleavage and activation of Caspase-1, which promotes the processing of pro-IL-1β to IL-1β and its secretion into the ECS (Figure 2). This process will potentiate the innate immune response by inducing proliferation, recruitment and activation of macrophages, microglia and lymphocytes as well as production of other inflammatory cytokines such as TNF-α or Interleukin 6 (IL-6) (Colonna & Butovsky, 2017; Dubyak, 2012). In fact, it was observed that inhibition of IL-1β led to impaired activation and proliferation of microglia, which stresses the significance of this cytokine in the microglia-mediated immune response (Monif et al., 2016).

Sustained activation of P2X7R can lead to formation of a large pore in the cell membrane that allows the trafficking of larger hydrophilic molecules. However, continued opening of this pore will lead to apoptosis and cell death, which will further potentiate the P2X7R response by releasing more ATP into the ECS (Mackenzie et al. 2005; Savio et al. 2018; Di Virgilio et al. 2018; Young et al. 2015).

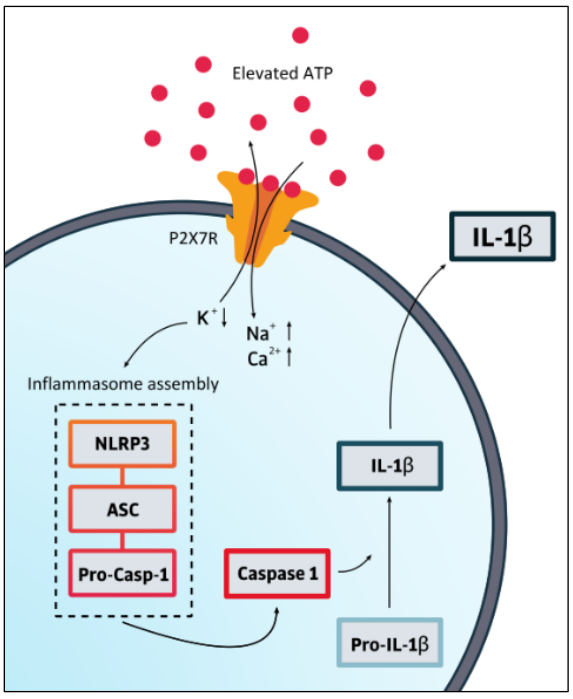

Figure 2. P2X7R-induced IL-1β release from microglia upon ATP stimulation. Elevated eATP binds to P2X7R, which adopts an open conformation and allows the passage of positive ions. The decrease of intracellular potassium leads to the assembly of the inflammasome and the cleaving and activation of Caspase 1. This enzyme catalyzes the transformation of Pro-IL-1β into IL-1β, which is then released into the ECS. Illustration created by Alba Sáenz de la Cuesta Martínez.

3.3.2 *Human and mouse P2X7R*

There are specific differences between the mouse and the human P2X7R. In terms of function, the human receptor has higher affinity for BzATP and ATP (EC50 20 µM and 100 µM respectively) compared to the murine receptor (EC50 295 µM and 850 µM respectively) (Khakh & North, 2012; Moore & MacKenzie, 2008). Its affinity for other compounds such as pharmacological agonists or inhibitors has also been shown to vary between different mammalian P2X7Rs (Donnelly-Roberts, Namovic, et al., 2009). Additionally, the human receptor has a higher deactivation speed, an effect that seems to be dependent on the C-terminal region of the protein (Bartlett et al. 2014). Both the human and murine receptors undergo post-translational modifications, including N-linked glycosylation and palmitoylation. However, due to the lack of specific ADP-ribosyl transferases (2.1 and 2.2), only the murine P2X7R is subject to ADP ribosylation in the residue R125, which is located in close vicinity to the ATP binding region. This process leads to the ATP-independent activation of the receptor in the presence of NAD^+ (Sluyter, 2017).

Table 1. Comparison of human and mouse P2X7 receptors

	Human P2X7R	**Mouse P2X7R**
ATP EC50	100 µM	850 µM
BzATP EC50	20 µM	295 µM
Chromosomal location	12q24.31	5 F
Gene localization (Genome Reference Consortium)	121,570,622-121,625,835 GRCh37	122,781,974-122,829,495 GRCm39
Splice variants	13	5
Size of main variant (including UTRs)	5113 bp (595 aa)	4936 bp (595 aa)

Although the regions where the P2X7R gene is located, as well as the P2X7R sequence itself, are highly conserved between mouse and human (Figure 1 C), certain disparities are observable between the murine and the human receptors at the genetic level. The P2X7R gene can undergo alternative splicing and produces 13 different splice variants in humans (P2X7R-A - K, P2X7-V3 and nfP2X7) and 5 in mice (P2X7R-A, B, C, D, and K) (Pegoraro et al., 2021), being P2X7R-A the main, functional variant in both species (Figure 3). Studies in mice have shown that some of these alternative variants, P2X7R-K and P2X7R-C in particular, can

produce functional channels and could be involved in processes such as cell growth, cell death and inflammation (Adinolfi et al., 2010; Cheewatrakoolpong et al., 2005; Feng et al., 2006; Sluyter & Stokes, 2011).

The murine sequences of P2X7R-A and P2X7R-K differ in the cytosolic N-terminal and first transmembrane domains (Figure 3). P2X7R-K shows increased sensitivity to BzATP, slower deactivation and increased ability to produce macropores in comparison to P2X7R-A (Nicke et al., 2009). Moreover, the expression patterns of these two variants are distinct. While P2X7R-A has an increased expression in tissues such as macrophages and skeletal muscle, P2X7R-K is more highly expressed in regulatory T cells (Schwarz et al., 2012). It is relevant to note that P2X7R-K is much more sensitive to ADP-ribosylation than P2X7R-A, which implies a differential activation potential, either ATP- or NAD-mediated, depending on the predominant isoform expressed in each cell type (Schwarz et al., 2012). As for the P2X7R-C variant, it is a C-terminal truncated version of P2X7R-A (Figure 3). It is known to be expressed in brain, salivary gland, and spleen. Although its membrane trafficking is less efficient than that of the main variant, a study proved that P2X7R-C presents functionality upon stimulation, albeit lower than the main variant (Masin et al., 2012).

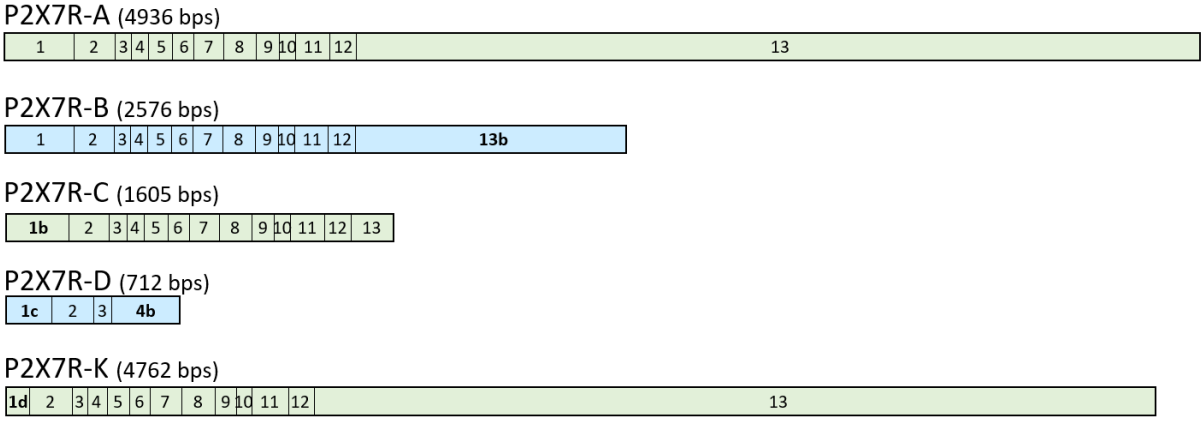

Figure 3. All known murine P2X7R splice variants (mRNA). The size of the depicted transcripts is proportional to their real size. The numbers indicate individual exons. The size of the transcripts is specified in brackets. The regions that vary from the main variant P2X7R-A are marked in bold and named with letters. In green (P2X7R-A, C, K) the variants that are functional, in blue (P2X7R-B, D) the ones that have not been proven to be functional. Modified from Metzger, 2016. Ensembl variant codes are the following: P2X7R-A: ENSMUST00000100737.10; P2X7R-B: ENSMUST00000121489.8; P2X7R-C: ENSMUST00000031425.15; P2X7R-D: ENSMUST00000086247.6; P2X7R-K: ENSMUST00000199281.2.

3.4 *Mouse lines targeting P2X7R*

In order to elucidate the role of P2X7R in physiological and pathological conditions *in vivo*, several transgenic mouse lines have been produced.

3.4.1 *Constitutive P2X7R KO mouse lines*

Three different P2X7R-KO mice were created by the companies Pfizer, Glaxo Smith Kline (GSK) and Lexicon Genetics to analyze the consequences of the lack of P2X7R gene expression. The Pfizer mouse contains a neomycin selection cassette that disrupts exon 13, which corresponds to the C-terminal region of the protein (Solle et al., 2001). The mouse from GSK was produced by inserting a LacZ-neomycin reporter cassette in exon 1 resulting in a fusion transcript comprised of partial exon 1 and LacZ (Chessell et al., 2005). Finally, the transgenic mouse from Lexicon Genetics was created by substituting exons 2 and 3 with a LacZ – neomycin cassette, producing a fusion transcript formed by exon 1-LacZ-neomycin (Basso et al., 2009) (Figure 4)

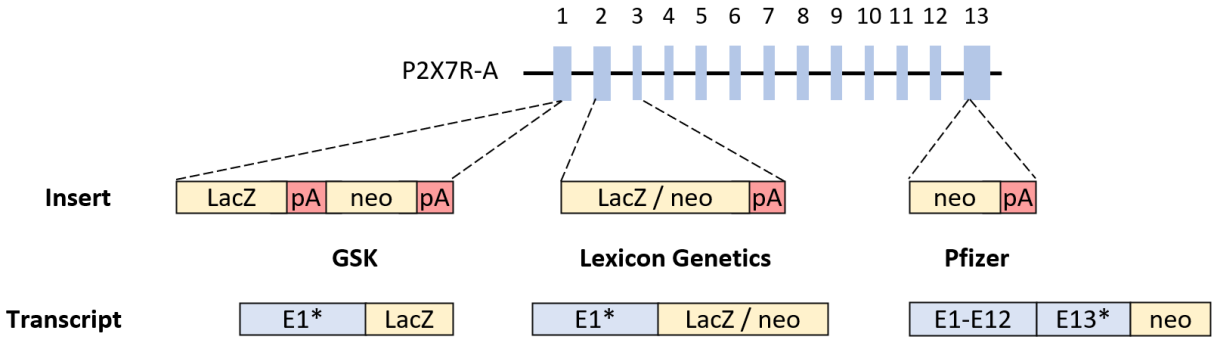

Figure 4. Schematic representation of constitutive P2X7R-KO mouse lines. GSK mouse: contains a LacZ-neomycin (neo) cassette in exon 1, which results in an exon 1-LacZ fusion transcript. Lexicon Genetics: contains a LacZ - neo cassette replacing exons 2 and 3, which results in an exon 1-LacZ-neo fusion transcript. Pfizer mouse: contains a neo cassette in exon 13, which truncates the transcript in the C-terminal region. "pA": Poly A signal. "*": truncated P2X7R exon. The dashed lines point to the insertion site of the construct.

In these studies, they analyzed the gene and protein expression of P2X7R, but they also confirmed that the production and release of IL-1β and the pore formation capability of peritoneal macrophages were reduced in KO animals *in vitro* and *in vivo*. They could also observe an increase in inflammatory hypersensitivity in the KO animals. Therefore, the functional effects in these transgenic mouse lines are consistent with the lack of P2X7R expression.

3.4.2 *Humanized and conditional KOs*

Although a constitutive knockout mouse provides valuable information about the physiology of the murine P2X7R, there are several instances which would benefit from studying the human receptor *in vivo*, such as pharmacological affinity studies or single-nucleotide polymorphism (SNP) analysis. To respond to these needs, the humanized P2X7R mouse model (hP2X7R) was generated.

This mouse line ($P2rx7^{tm1.1(P2RX7)Jde}$) is a knockin of the human P2X7R cDNA fragment (exons 2 to 13), which is followed by a poly A signal replacing exon 2 of the murine locus on chromosome 5 (Figure 5). This way, the humanized protein presents the same expression pattern as the native murine protein in wildtype (WT) mice. When comparing the activity of P2X7R after stimulation with BzATP, a 10-fold higher sensitivity to ATP of the humanized receptor was observed (Metzger et al., 2017), which is consistent with the previously described EC50 values of the human and murine receptors (Khakh & North, 2012; Moore & MacKenzie, 2008). This mouse line was also modified to introduce the polymorphism Q460R that had previously been linked with MDD. This allowed to produce and analyze homozygote and heterozygote mice for both the risk and the WT alleles (Metzger et al., 2017).

Another trait of the hP2X7R mouse line is that it is susceptible to conditional inactivation. The human cDNA fragment is flanked by two loxP sites and thus can be removed by Cre-mediated recombination. This results in a truncated murine gene, which lacks the ability to produce a functional receptor (Figure 5, Metzger et al., 2017). Therefore, crossing these mice with a mouse line expressing Cre recombinase fused with a modified ligand binding domain of the estrogen receptor protein (ERT2) results in a tamoxifen-inducible cell-type specific knockout mouse line. In contrast to constitutive KO mouse lines, this has the added benefit that P2X7R can be inactivated once the animals are adults, therefore minimizing the potential effects caused by the absence of the receptor during development. Furthermore, cell type-specific inactivation avoids the pleiotropic effects consequent from a full P2X7R inactivation. The lack of hP2X7R in the knockout mice was tested functionally, by assessing the capability of peritoneal macrophages to produce IL-1β, as well as by the lack of calcium influx after stimulation with BzATP. The absence of the known P2X7R splice variants was also tested demonstrating the absence of any functional transcripts (Metzger et al., 2017).

P2X7R wildtype locus (WT)

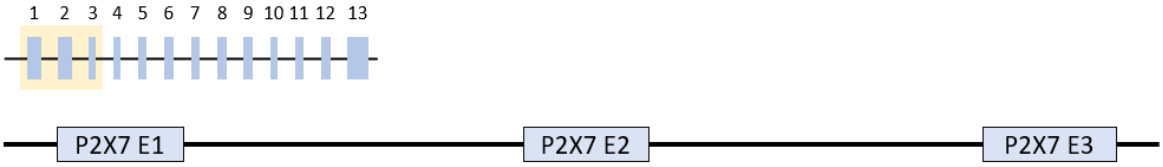

P2X7R humanized locus (hWT)

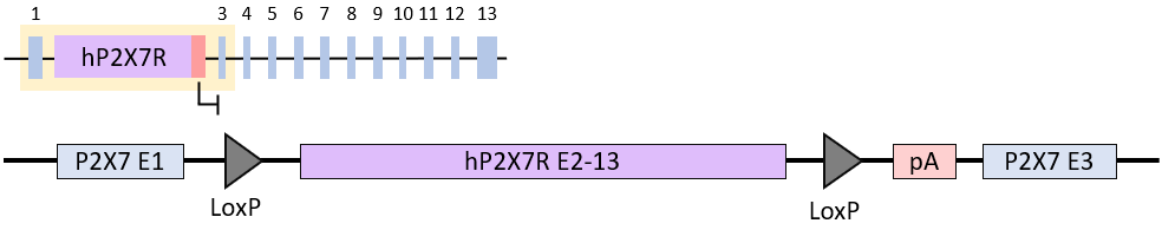

P2X7R knockout locus (hKO)

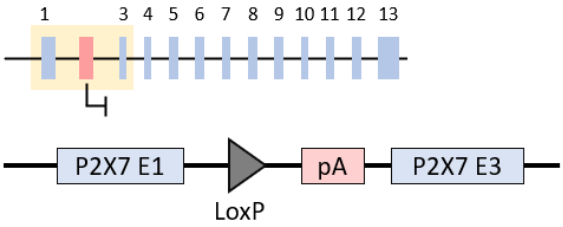

P2X7-EGFP BAC construct

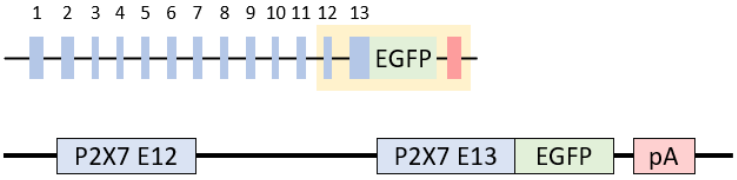

sEGFP BAC construct

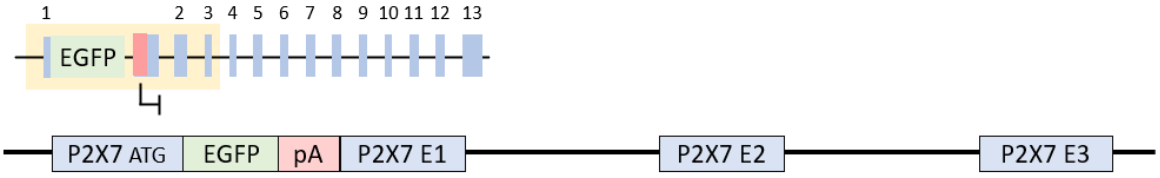

P2X7R knockin locus (P2X7-CreERT2)

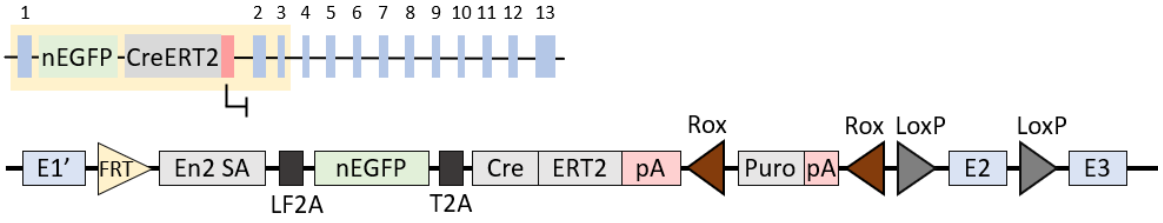

Figure legend on the next page

Figure 5. Schematic representation of all P2X7R transgenic mouse lines employed in this project. WT: original wildtype locus. **hWT**: humanized locus. It contains the human sequence from exon 2 to exon 13 downstream of the murine exon 1. This sequence is flanked by two LoxP sites. Upon Cre recombinase activity, this cDNA fragment is deleted, and produces the **hKO** line, which is lacking exon 2 and does not allow the transcription of functional variants of P2X7R. **P2X7-EGFP**: it harbors an EGFP downstream of the P2X7R coding sequence in exon 13, which creates a P2X7-EGFP fusion transcript. **sEGFP**: it contains an EGFP cassette downstream the ATG of P2X7R in exon 1, theoretically blocking the transcription of the remainder of the gene through its poly A signal. **P2X7-CreERT2** (Before tamoxifen induction): It contains an engrailed 2 splice acceptor (En2 SA), a LF2A sequence and a nuclear EGFP cassette, followed by a T2A sequence and a CreERT2 fusion protein. Downstream, a puromycin (Puro) selection cassette flanked by two Rox sites can be found, followed by P2X7R exon 2 flanked by loxP sites. "pA"/red box: poly A signal, which terminates transcription as indicated with a symbol below the construct. In yellow, the area that is detailed underneath.

3.4.3 *Reporter mouse lines*

There has been a significant advance in the detection and biological targeting of P2X7R, with the recent development of a specific P2X7R nanobody, which will be further discussed in this dissertation (Kaczmarek-Hajek et al., 2018). However, the currently available commercial antibodies that target P2X7R show deficits in functionality and specificity (Anderson & Nedergaard, 2006; Illes et al., 2017). As a consequence, detecting P2X7R in the CNS has been a challenge, which has been circumvented by creating transgenic mouse lines that express enhanced green fluorescent protein (EGFP) as a reporter of P2X7R expression.

a) EGFP tagged P2X7R (P2X7-EGFP) expressing mice

The P2X7-EGFP mouse line (Tg(RP24-114E20P2X7451P-Strep-His-EGFP)17Ani) is a BAC transgenic mouse line, generated by adding an EGFP sequence at the C-terminus of the P2X7R, which is translated as a P2X7R-EGFP fusion protein (Figure 5). This resulting construct was tested for functionality as well as for its expression pattern. It was demonstrated that there was no significant difference in physiological responses between the native and the fusion protein, thus concluding that the EGFP tag has no influence on the functionality of P2X7R. However, Southern blot analysis showed that several copies had integrated into the genome of these mice, which means that this mouse line is not only reporting P2X7R expression but also overexpressing the receptor (Kaczmarek-Hajek et al., 2018).

b) Soluble EGFP (sEGFP) expressing mice

The sEGFP mouse line (Tg(P2rx7-EGFP)FY174Gsat) is a BAC transgenic line which was generated by inserting an EGFP cassette followed by a polyA signal downstream of exon 1 of the P2X7R gene (Figure 5). Therefore, when the P2X7R promoter is active, there will be production of soluble EGFP confined to P2X7R expressing cells. Differently from the P2X7-EGFP mouse line, one cannot detect the receptor directly. Instead, EGFP expression reflects only the level of the P2X7R promoter activity (Gong et al., 2003). It was produced by the Gene Expression Nervous System Atlas project (GENSAT). This mouse line has recently been characterized and it was discovered that it unexpectedly overexpresses P2X7R and P2X4R. Moreover, it also presented an aberrant spatial expression pattern compared to the endogenous P2X7R in terms of cell type and brain region (Ramírez-Fernández et al., 2020)

c) P2X7R-EGFP-T2A-CreERT2 (P2X7-CreERT2)

The P2X7-CreERT2 mouse line ($P2rx7^{tm1(EGFP/Cre/ERT2)wtsi}$) is a knockin line which contains a nuclear EGFP (nEGFP) reporter cassette driven by the P2X7R promoter. At the same time, it is linked via a T2A site to a CreERT2, which allows for the Tamoxifen-induced Cre-mediated recombination in P2X7R-expressing cells (Figure 5). This line has not yet been fully characterized and was studied during this project. It was produced by the EUCOMMTOOLS (EUCOMM: Tools for Functional Annotation of the Mouse Genome) project which is part of the International Knockout Mouse Consortium (IKMC).

3.5 *P2X7R Expression Pattern in the CNS*

The pattern of P2X7R expression in the brain has been widely studied. However, because of the lack of reliable antibodies that detect P2X7R in a consistent manner, there is still a debate about which are the cell types in the CNS that are actually expressing it.

There is extensive proof that P2X7R is being expressed in microglial cells in the CNS. It has been observed that P2X7R is expressed in human and mouse-derived primary microglia and it is believed that its activation upon trauma has a neuroprotective function (Liu et al., 2017; Masuch et al., 2016). In addition, P2X7R was found responsible for mediating the changes in morphology and the increased cell death upon BzATP stimulation of primary microglial cultures, since these effects could be reversed through blockade of the receptor. Furthermore, inactivation or pharmacological inhibition of P2X7R led to a decrease in the release of IL-1β,

which directly depends on the receptor's activation cascade (He et al., 2017). Besides, mRNA analysis proved that inactivation of microglia-specific P2X7R leads to a significant reduction of overall P2X7R levels in certain regions of the brain, thus proving microglial mRNA expression of the receptor (Metzger et al., 2017). By employing the P2X7-EGFP mouse, it was also observed that the EGFP reporter was colocalizing with microglial markers *in vivo* (Ramírez-Fernández et al., 2020). In summary, P2X7R is known to be expressed in microglia and its activation upon pro-inflammatory stimulation is a crucial step in the initiation of the immune response (Bartlett et al., 2013; He et al., 2017).

P2X7R mRNA as well as protein expression has been previously confirmed in astrocytes. In fact, activation of astrocytic P2X7R through ATP and BzATP leads to a release of signaling molecules, which are believed to have an impact on neurons in close proximity (Illes et al., 2012; Metzger et al., 2017). Additionally, employing the P2X7-EGFP mouse line, colocalization of the P2X7R reporter with astrocytic markers in cortex and hippocampal regions could be observed (Kaczmarek-Hajek et al., 2018). As for oligodendrocytes, P2X7R mRNA as well as protein expression has been detected in these cell types as well as in NG2 glia *in vitro* and *in vivo* (Kaczmarek-Hajek et al., 2018; Metzger et al., 2017; Ramírez-Fernández et al., 2020). In fact, stimulation of P2X7R with BzATP leads to permeabilization of oligodendrocytes and cell death *in vitro*, which was reversed upon blockade of the receptor with the inhibitor Coomassie Brilliant Blue G (BBG) (Matute et al., 2007). We can conclude that P2X7R is in fact expressed in astrocytes, oligodendrocytes and microglia and can act as mediator of immunogenic pathways in response to cellular damage (Zhao et al., 2021).

Neuronal expression of P2X7R has been highly debated in the purinergic field. There are studies in rodent tissue *in vivo* and *in vitro* which found an electrophysiological response to pharmacological P2X7R stimulation, which was reverted by exposure to a receptor antagonist (Cho et al., 2010; Xia et al., 2012). However, it has been theorized that the observed effects in neuronal cells could be caused by the indirect influence of nearby glial P2X7R (Zhao et al., 2021). Although it has been stated that P2X7R mRNA can be found in neuronal populations *in vivo* (Metzger et al., 2017), it has not been possible to directly detect the protein in neurons. Several studies that employed the sEGFP mouse line stated having found neuronal expression of P2X7R (Martínez-Frailes et al., 2019; Miras-Portugal et al., 2017). However, a thorough comparison between the sEGFP and the P2X7-EGFP mouse lines revealed that the sEGFP mice are not reliable reporters and present, not only overexpression of P2X7R and P2X4R, but also

what is believed to be ectopic EGFP reporter gene expression. In fact, in the P2X7-EGFP mouse line neuronal expression could not be detected (Ramírez-Fernández et al., 2020). Therefore, although glial P2X7R expression can have an influence in neuronal physiology, and although P2X7R mRNA has been previously detected in hippocampal regions *in vivo*, there is no consistent proof that P2X7R protein is being expressed in neurons (Zhao et al., 2021).

3.6 *P2X7R and MDD*

3.6.1 *Human genetics*

The activation of P2X7R, the consequent inflammatory response in the CNS and its association with mood disorders has been broadly investigated. In fact, dysregulation of P2X7R gene expression has been associated with treatment-resistant MDD and disease severity (Iacob et al., 2013; Zhang et al., 2011). Furthermore, the region of chromosome 12 in which P2X7R is found (12q24) has been previously linked with psychiatric disorders, namely MDD and bipolar disorder (BD) (Abkevich et al., 2003; Curtis et al., 2003; Degn et al., 2001; McGuffin et al., 2005; Shink et al., 2005). In particular, a SNP in the P2X7R gene has been associated with mood disorders. That is rs2230912, which is caused by the non-synonymous transition 1405 A > G that translates as Gln460Arg in the C-terminal region of the protein (Barden et al., 2006; Lucae et al., 2006). Although clinical cohorts could not always show a linkage between the incidence of mood disorders and this polymorphism (Green et al., 2009; Grigoroiu-Serbanescu et al., 2009; Viikki et al., 2011), the SNP seems to influence the severity of these disorders. In particular, the patients carrying the G allele show longer disease time and higher symptom severity (Hejjas et al. 2009; Nagy et al. 2008; Soronen et al. 2011). Another study witnessed alterations in sleep patterns of the patients that carried both alleles, suggesting a heterozygote disadvantage (Metzger et al., 2017). Although a meta-analysis from 2014 could not detect an association between this SNP and mood disorders (Feng et al., 2014), a more recent study presented a significant association of the rs2230912 polymorphism with MDD (Czamara et al. 2018). In contrast, recent genome-wide association analyses identified 44 risk variants for MDD and 30 for BD, none of which were within the P2X7R gene (Stahl et al., 2019; Wray et al., 2018).

The lack of consistency between studies could be explained by the fact that MDD is a polygenic disorder where many low-impact loci interact with each other and the environment to

promote disease development (Peterson et al., 2018). Therefore, studying the impact of a single SNP will most likely not be sufficient to understand the complex reality of the genetics behind MDD. Haplotype studies go one step further and examine not only the link between MDD and a specific SNP, but also consider other polymorphisms found in the same region. Specifically, the combination of rs2230912 and rs1718119 (Ala348Thr), leads to a gain-of-function variant of P2X7R. Immune cells carrying these two SNPs show an increased production of IL-1β in response to ATP (Stokes et al., 2010). Given the evidence that the pathophysiology of MDD might be influenced by a heightened immune response, it is logical to consider the possibility that these SNPs could be involved in depression. Confirming this idea, it has been observed that the combination of rs2230912 and rs1718119 leads to a higher severity of depression (Vereczkei et al., 2019).

In conclusion, human studies provide evidence that P2X7R can be a contributing factor in the appearance, severity, and treatment responsiveness of MDD. Therefore, further animal studies are needed to elucidate the physiology as well as pathophysiological role of P2X7R in this disorder.

3.6.2 *Animal studies*

To shine some light into the mechanisms by which the receptor might be involved in MDD, many animal studies have been performed. By employing the humanized transgenic mouse line, we could see how genetic changes in the human protein can impact depression- and anxiety-related behaviors in this animal model. Particularly, when the rs2230912 polymorphism was introduced in these animals, it was observed that primary mixed cultures derived from hippocampus of heterozygote animals showed impaired calcium uptake after BzATP stimulation when compared to homozygous littermates carrying only the wildtype or disease-associated variant. Although clear depressive-like or anxious behaviors could not be observed in these mice, it was detected that heterozygous mice suffered from impaired sleep quality, which was consistent with the findings in human studies. In addition, heterozygous mice presented a stronger response to chronic social defeat stress (CSDS) than homozygous mice. These findings point out that even though the polymorphism might not be enough to cause depressive-like behavior, it can influence factors that are deeply related to MDD, as is sleep quality and stress responsiveness (Metzger et al., 2017)

Studies on the murine P2X7R have been carried out to analyze to what extent the receptor can influence the appearance of depressive-like endophenotypes in animal models. Experiments on the constitutive P2X7R-KO mouse lines showed that genetic inactivation, as well as pharmacological inhibition of P2X7R leads to a decrease of anxiety- and depressive-like behaviors. However, the results are not fully consistent from study to study. Certain experiments result in reduced depressive-like behaviors in the KO mice under baseline conditions (Basso et al., 2009; Csölle, Andó, et al., 2013), while others observed this reduction only under stress conditions (Boucher et al., 2011; Csölle, Baranyi, et al., 2013 Yue et al., 2017). In addition, a P2X7R-KO mouse produced by CRISPR-Cas9 inactivation showed that deletion of the gene in young, female mice (2 months old) causes depressive-like behavior as opposed to adult and aged mice (10 and 18 months old respectively), which present anti-depressant-like phenotypes following P2X7R disruption (Gao et al., 2018). Other publications reported an impact of P2X7R inactivation on depressive phenotypes by employing alternative behavioral readouts such as coat status, nesting abilities or failed escapes in a learned helplessness test (Farooq et al., 2018; Otrokocsi et al., 2017; Troubat et al., 2021). As for anxiety phenotypes, there is also a discordance, with some studies presenting a decrease of anxiety in P2X7R-KO mice under baseline conditions (Boucher et al., 2011; Yue et al., 2017) while other studies could not witness a significant difference between genotypes (Basso et al., 2009; Csölle, Andó, et al., 2013).

Targeted pharmacological inhibition of P2X7R is another widely used tool to study anxiety- and depression-like behavior in the mouse. The trend that has been observed when treating rodents with P2X7R inhibitors is a decrease of depressive-like symptoms. Mice exposed to acute stress by intraperitoneal lipopolysaccharide (LPS) injection, that were also pretreated with P2X7R inhibitors, namely BBG, showed an increase in sucrose preference compared to mice treated with vehicle. Moreover, BBG treatment led to decreased immobility time in the tail suspension test and the forced swim test after LPS injection (Csölle, Baranyi, et al., 2013; Ma et al., 2014). A similar pattern is detected in rats which are exposed to chronic unpredictable stress (CUS). When these animals were treated with BBG, they showed reduced stress and depressive-like behaviors in a dose-dependent manner in the open field, sucrose preference and forced swim test (Aricioglu et al., 2019; Yue et al., 2017). A more specific P2X7R inhibitor, A-804598 (Donnelly-Roberts et al. 2009), has also been employed to assess the role of the receptor. Treatment with this compound reduced the release of inflammatory cytokines

and rescued the depressive-like and anxious phenotype in rats subjected to CUS (Iwata et al., 2016). Moreover, in a genetically selected rat depression model, Flinders Sensitive Line, chronic treatment with this P2X7R inhibitor produced anti-depressant, but not anxiolytic phenotypes (Ribeiro et al., 2019).

It is relevant to note that further analysis of the KO models has proved that certain P2X7R splice variants are able to escape the gene deletion, namely variants B, C and D in the Pfizer mouse; and variants C, D and K in the GSK mouse (Masin et al., 2012; Nicke et al., 2009). Therefore, the phenotypes that were observed in the aforementioned constitutive KO mouse lines do not correspond to a full P2X7R-KO but rather to a partial P2X7R deletion. Finally, it is pertinent to mention that the inhibitors that are employed to block P2X7R are not always specific. Consequently, the results obtained depend on the selectivity and poly-pharmacology of each particular compound (Savio et al., 2018). For instance, BBG, which has been widely employed as a P2X7R inhibitor, also blocks P2X1R and P2X4R (Greve et al., 2017). These facts make apparent a need for a reassessment of anxiety and depressive-like behaviors in a validated full P2X7R-KO mouse line.

3.7 *The influence of P2X7R in MDD*

Despite great advances in the last decades, the exact pathophysiology of MDD has not been fully characterized. It is known to be a highly complex disease, in which several biological systems have a contributing role on its appearance, development and treatment outcome. The most studied mechanisms involved in MDD are abnormal neurotransmission, namely of monoamines, glutamate and GABA (Berton & Nestler, 2006; Fogaça & Duman, 2019; Y. Liu et al., 2018); altered regulation of the hypothalamic-pituitary-adrenal axis (HPA axis) (De Kloet et al., 2005; Keller et al., 2017); decreased neurogenesis and neural connectivity (Castrén, 2013; Castrén & Rantamäki, 2010; Santarelli, 2003; Taliaz et al., 2010), and elevated inflammation (Amodeo et al., 2018; Dowlati et al., 2010; Felger & Lotrich, 2013). Even though not all MDD patients necessarily present alterations in all these systems simultaneously, they are known to interact and have an impact on the appearance and evolution of the disorder (Dean & Keshavan, 2017) (Figure 6).

3.7.1 *Neuroinflammation*

Inflammatory diseases such as rheumatoid arthritis or lupus have a high comorbidity with depression (Margaretten et al., 2011; Lijuan Zhang et al., 2017). These studies are consistent with the fact that inflammatory inductors, such as interferon alpha, can cause depressive symptoms in up to 50% of the treated patients (Capuron and Miller 2004; Raison et al. 2006). Moreover, depressed patients present elevated levels of inflammatory markers in plasma (Dowlati et al., 2010; Miller et al., 2002; Thomas et al., 2005). This increase of inflammation can lead to a lack of antidepressant treatment effectivity and persistence of MDD symptoms, an effect that can be reversed with anti-inflammatory agents (Köhler et al., 2014; Köhler, Krogh, Mors, & Benros, 2016; Lee & Giuliani, 2019). Furthermore, post-mortem brains from MDD patients show signs of increased neuroinflammation and microglial activation (Steiner et al., 2008). All these studies point out that the inflammatory response is influencing not only the appearance and development of MDD, but also the severity of the symptoms as well as the response to the treatment (Liu et al. 2019; Raison et al. 2013).

Upon psychological stress, neurons produce glutamate, a mediator that stimulates astrocytes to release ATP into the ECS (Iwata et al., 2016). The increase of eATP will lead to a P2X7R-mediated release of inflammatory cytokines into the ECS, and the subsequent promotion of the immune response. Although this process is essential for the maintenance of homeostasis upon physiological stress, sustained activation of P2X7R due to chronically high eATP levels leads to pore formation. As a consequence, there is an efflux of intracellular components, which will, in turn, maintain elevated ATP levels in the ECS. This will extend P2X7R activation in the area and will eventually lead to cell death (Di Virgilio et al., 2018; Mackenzie et al., 2005a; Savio et al., 2018; Surprenant et al., 1996). Furthermore, if this inflammatory response is prolonged, it can directly cause tissue damage through production of neurotoxic compounds (Hewinson & MacKenzie, 2007; Mead et al., 2012). The role of P2X7R in the promotion of the immune response and potential subsequent damage in the CNS upon psychological stress, makes this receptor a key mediator in inflammatory pathways, which can influence the appearance and development of MDD.

3.7.2 *HPA axis hyperactivation*

Although hyperactivation of the HPA axis is only found in a subset of MDD patients, it is deeply involved in the appearance of this disorder (Stetler & Miller, 2011). Activation of the HPA axis

leads to an adaptive response: an increase in glucocorticoid levels, which enable the organism to produce a response to stressful stimuli. However, sustained elevated levels of glucocorticoids lead to a reduction of neuronal functionality in areas that are relevant to depression, namely prefrontal cortex and hippocampus (Duman et al., 2016; Magariños and McEwen, 1995; Liu and Aghajanian, 2008). The HPA axis activity is closely related to the immune response. In fact, release of cytokines such as IL-1β, TNF-α and IL-6, activates the HPA axis and can produce resistance to glucocorticoids in the organism, which impedes the negative feedback loop that regulates their production, thus facilitating the appearance of MDD (Pace and Miller, 2007; Chrousos, 1995; Dunn, 2006).

3.7.3 *Excitotoxicity*

Clinical studies have found alterations in glutamatergic metabolism in limbic and cortical areas in patients suffering from depression. In particular, they observe an increase of glutamate in MDD patients, which can be decreased with antidepressant therapy (Sanacora, Treccani and Popoli, 2012). It has been hypothesized that the activation of neuronal P2X7R promotes the efflux of glutamate into the ECS, while the decrease of calcium in the ECS is simultaneously preventing the reuptake of this mediator, thus maintaining elevated levels of glutamate within the synapse (Barros-Barbosa et al., 2015; Barros-Barbosa et al., 2018). Other studies postulate that the activation of P2X7R in astrocytes residing in close proximity to the synapse can lead to the release of ATP and glutamate from neurons, as well as from other astrocytes. This process maintains high levels of ATP and glutamate in the synapse, consequently stimulating post-synaptic neurons (Csölle, Baranyi, et al., 2013; M. T. Khan et al., 2018; Wei et al., 2018). Even though glutamate is one of the most abundant neurotransmitters, excessively high levels can lead to neuronal excitotoxicity in mood-related areas, promoting the appearance of MDD (Dong et al., 2009). Additionally, microglia are also known to be involved in glutamate-mediated excitotoxicity, as IL-1β and TNF-α can increase the levels of glutamate in the ECS, further contributing to the astrocyte-mediated neurotoxicity (Fogal & Hewett, 2008; Ye et al., 2013).

3.7.4 *Monoamine transmission interference*

Although the mechanism by which monoamine transmission contributes to MDD is still being elucidated, it has been the main focus for antidepressant treatment for decades. The monoamine hypothesis of depression describes that depletion of monoamines in specific

areas of the brain can lead to MDD (Mulinari, 2012). P2X7R knockout mice present differential serotonin and noradrenaline levels in basal conditions, meaning that even in the absence of stress, P2X7R can have an influence on the metabolism of monoamines (Csölle et al., 2013). Both pharmacological and genetic blockade of P2X7R reduces the release of serotonin in the hippocampus (Gölöncsér et al., 2017). Furthermore, inflammatory cytokines such as IL-1β and TNF-α can induce the expression of monoamine reuptake channels, reducing the extracellular levels of monoamines, a process that has often been associated with MDD (Zhu et al., 2006).

3.7.5 *Inhibition of neuronal morphology and neurogenesis*

Studies have shown that an alteration in neuronal plasticity, survival and neurogenesis in emotion-related areas can lead to depressive symptoms (Jin et al., 2019). In fact, certain antidepressants are known to boost neurogenesis and neuronal plasticity (Duman et al., 2016; Malberg and Duman, 2003; Santarelli, 2003). A relevant player in these processes is the brain-derived neurotrophic factor (BDNF). BDNF promotes neurogenesis and neuroplasticity and is essential for neuronal maintenance and survival. It has relevance in mood disorders, as it is known to be decreased in MDD patients, an effect that can be reverted with antidepressant therapy (Sen, Duman and Sanacora, 2008; Van der Meij et al., 2014). Even though physiological levels of glutamate induce BDNF signaling, it is hypothesized that stress-mediated, sustained release of glutamate leads to the activation of extra-synaptic glutamate receptors that inhibit BDNF signaling (Csölle, Baranyi, et al., 2013). IL-1β production can also lead to an interference of the BDNF signaling pathway and to the decline of adult neurogenesis in the hippocampus (Guadagno et al., 2015; Tong et al., 2012). In fact, sustained production of this cytokine leads to apoptosis in neuronal progenitor cells. Additionally, the antiproliferative effect of stress in the rodent brain can be reduced by inhibiting the IL-1β receptor, which also correlates with a reduction of anhedonic behavior (Wook Koo & Duman, 2008).

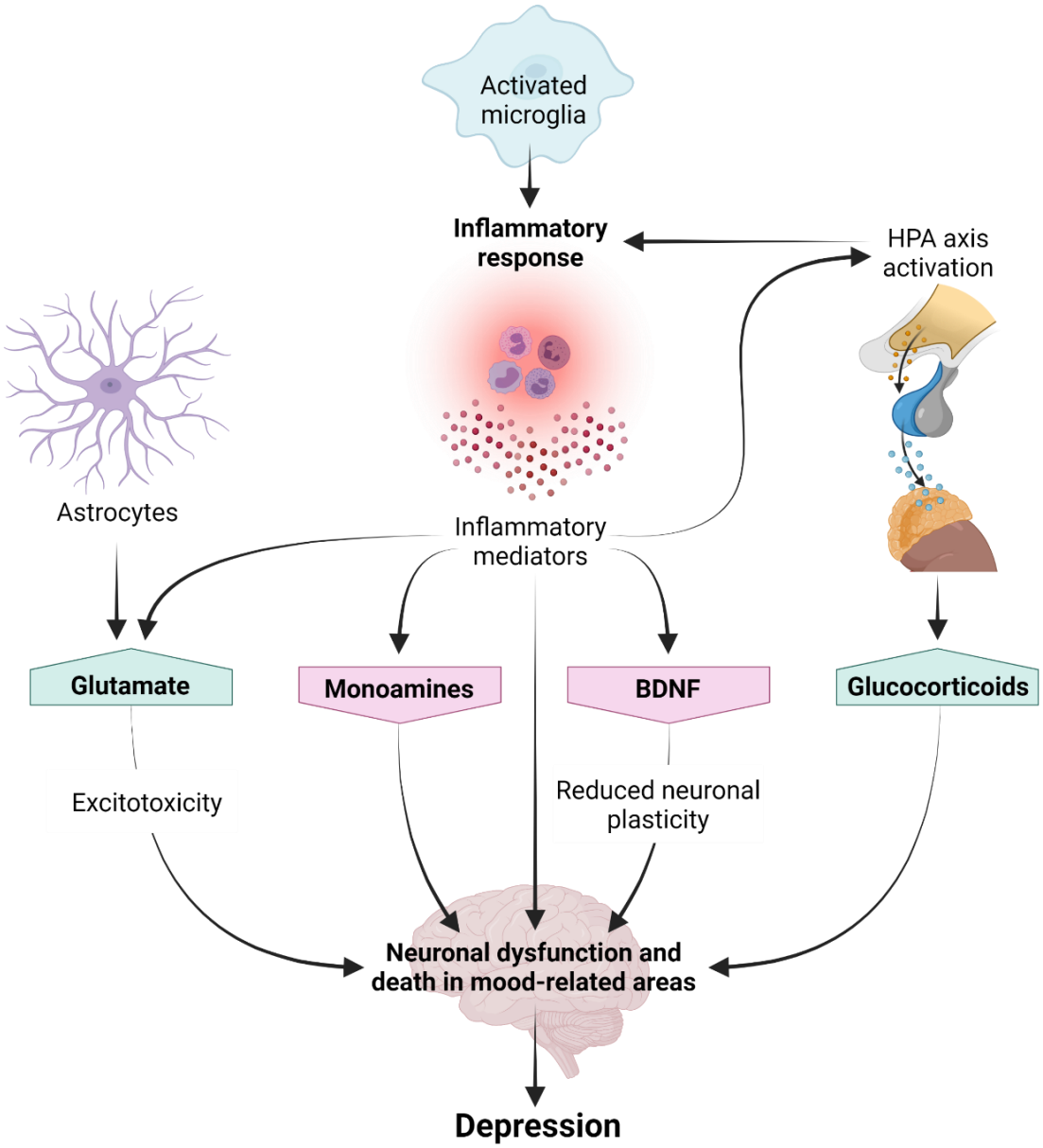

Figure 6. The impact of P2X7R and neuroinflammatory processes on systems involved in depression. The activation of microglial P2X7R promotes an inflammatory response. The subsequent release of inflammatory mediators has been linked to a decrease of monoamines in the synaptic cleft, a decrease of BDNF, the activation of the HPA axis, and the release of glutamate to the ECS, also mediated by astrocytic P2X7R activation. These events can lead to neuronal dysfunction and cell death in mood-related brain areas, which can affect the appearance and development of depression. Created with Biorender.com.

In conclusion, P2X7R activity is clearly not the sole initiator of MDD, but it is a relevant factor in several physiological and pathophysiological processes that are deeply connected with the development of MDD (Figure 6).

3.8 *Novel compounds to target P2X7R*

There is clear evidence for the importance of P2X7R in the context of CNS disorders. To further deepen our knowledge in the physiology and pathophysiology of the receptor, it is highly relevant to develop compounds that can target and modify the activity of P2X7R specifically and efficaciously.

3.8.1 *Pharmacological compounds*

There are currently two types of pharmacological compounds that block P2X7R: competitive inhibitors that bind to the ATP binding sites and non-competitive inhibitors that change the conformation of the receptor reducing ligand binding affinity (Young and Górecki 2018)**.** There are a number of pharmacological compounds that are used as P2X7R inhibitors in animal models. However, as a consequence of their lack of selectivity for P2X7R, their elevated toxicity or their lack of permeability to the brain, they cannot be used in human studies.

In response to this, several compounds have been developed that are effective, specific, and permeable to the brain. The ones that have been found to have the best overall functionality for human studies are the following: JNJ47965567, an irreversible P2X7R inhibitor, shows a high activity and specificity, but did not produce a change in the immobility time of rats in the forced swim test under baseline conditions (Bhattacharya et al., 2013). On the other hand, oral dosing of a reversible inhibitor: JNJ55308942, leads to an increase of sucrose preference in rat models of depression after chronic or acute stress (Bhattacharya et al., 2018). In fact, this compound is currently in a phase I clinical trial in healthy volunteers to assess its safety and tolerability. The most advanced compound in the search for a treatment of MDD is JNJ54175446 (Chrovian et al., 2018). Phase I trials have been finalized, which show that an oral dose permeates to the brain, doesn't show toxicity and reduces peripheral IL-1β levels in blood (Timmers et al., 2018). Moreover, LPS-primed, BzATP-dependent IL-1β release in blood has been blocked with a single oral dose of JNJ54175446 of 10 mg or higher (Timmers et al., 2018). PET studies have also shown that this dose permeates to the brain and binds specifically to P2X7R (Bhattacharya & Ceusters, 2020). This compound is currently undergoing a phase II trial in depressed patients to assess its antidepressant effect (http://www.isrctn.com/ISRCTN44411633).

3.8.2 *Biological compounds*

The niche for molecules that specifically target P2X7R is still being explored. Antibodies are good candidates as they can target a molecule with high selectivity. However, nanobodies, which are single domain antibodies, due to their relatively small size compared to regular antibodies (15 and 150 kDa respectively), show higher solubility while retaining the same specificity. For the same reason, they can position themselves in specific functional regions of target proteins, such as active sites, and potentially act as activity modulators (Koch-Nolte et al., 2019; Muyldermans, 2013). In addition, nanobodies can be modified to make them permeable to the blood-brain barrier, so they could theoretically be delivered peripherally to treat brain disorders (Farrington et al., 2014; Li et al., 2012).

The lack of good-quality antibodies on the market that specifically target the active variants of P2X7R has created a challenge for the study of this receptor (Anderson and Nedergaard 2006; Illes et al. 2017). By fusing a P2X7R-specific nanobody to a rabbit-IgG domain, a novel mechanism to detect the receptor has been created. Staining of brain tissue with this nanobody achieves the same expression pattern as the EGFP fusion protein from the P2X7-EGFP mouse line. Moreover, knocking out P2X7R leads to lack of signal, therefore proving its specificity for P2X7R (Danquah et al., 2016; Kaczmarek-Hajek et al., 2018).

4. Aims of the project

The overall goal of this project was to deepen our knowledge on P2X7R physiology and its connection with MDD. Several transgenic mouse lines were employed and analyses at the genetic, molecular, cellular, and organismic levels were carried out. The specific aims are detailed below.

4.1 *Understanding the involvement of P2X7R in anxiety- and depression-related endophenotypes*

I validated a microglia-specific P2X7R-KO mouse line through primary microglia cell culture assays and immunohistochemical analysis of brain tissue. I carried out behavioral assays to evaluate the impact of constitutive or conditional microglia-specific P2X7R inactivation on behavioral phenotypes related to depression under baseline, acute and chronic stress conditions.

4.2 *Validating P2X7R reporter mouse lines and understanding the behavioral consequences of P2X7R overexpression*

I analyzed the expression pattern and expression levels of P2X7R, EGFP and P2X4R, as well as P2X7R splice variants in the brain of different P2X7R transgenic reporter mouse lines. I also collected behavioral readouts related to depression and anxiety under baseline conditions to evaluate the consequences of P2X7R overexpression.

4.3 *Analyzing an inducible P2X7R-specific Cre driver mouse line*

In the P2X7-CreERT2 mouse line, I analyzed the CreERT2 expression pattern based on its co-expression of an EGFP reporter and through Cre-dependent reporter gene activation using immunohistochemistry of brain tissue. Successively, I studied the insertion site of the transgenic construct in the P2X7R locus through PCR and sequencing to uncover potential causes for the aberrant expression.

5. Materials

5.1 *Genotyping*

Table 2. Primers employed for genotyping

Primer	Sequence	Size
hP2RX7-mIntron1-for	5'-AGA CTG TCA CCA GCA GCA GCT C-3'	hWT: 933 bp hKO: 613 bp
hP2RX7-hExon6–7-rev	5'-CAG GAT GTT TCT CGT GGT GTA G-3'	
hP2RX7-mIntron2-rev	5'-GCC AAG CAT TCT ACC AGT TGA GC-3'	
hP2RX7-KO-for	5'-GCA-GTC-TCT-CTT-TGC-CTC-GT-3'	hKO: 186 bp
hP2RX7-KO-rev	5'-CGT-CGA-CTG-TCT-TCT-GGT-CA-3'	
hP2X7R-cDNA-for	5'-CAC CAT GCC GGC CTG CTG CAG CTG CAG TGA TGT TTT-3'	1,789 bp
hP2X7R-cDNA-rev	5'-GTA AGG ACT CTT GAA GCC ACT GTA CTG CCC TTC ACT-3'	
Cx3cr1-cre-for	5'-CTC CCC CTG AAC CTG AAA C-3'	WT: 500 bp Cre: 410 bp
Cx3cr1-cre-rev	5'-CCC AGA CAC TCG TTG TCC TT-3'	
Cx3cr1-cre-rev '	5'-GTC TTC ACG TTC GGT CTG GT-3'	
Ribotag-for	5'-GGG ACG CTT GCT GGA TAT-3'	WT: 260 bp RTag: 290 bp
Ribotag-rev	5'-TTT CCA GAC ACA GGC TAA GTA CAC-3'	
P2X7R-B-for (Ex12)	5'-CGT TGA AGT ATG TGT CCT TTG TC-3'	1,224 bp
P2X7R-B-rev (Ex13)	5'-TTC TTA AAT AAA TGA ATT GAA ATC AAG-3'	
P2X7R-B-NES-for (Ex12)	5'-GCA TGG TGG ACC AGC AGC TGC-3'	1,062 bp
P2X7R-B-NES-rev (Ex13)	5'-CAG TCG TCC AGG AAG TCA GCC G-3'	
P2X7R-D-for (Ex1)	5'-CAC ATG ATC GTC TTT TCC TAC-3'	455 bp
P2X7R-D-rev (Ex4)	5'-TGA CCA TTC TCC TGG CTG AC-3'	
P2X7R-D-NES-for (Ex2)	5'-TGG TGA GCG ATA AGC TGT AC-3'	397 bp
P2X7R-D-NES-rev (Ex4)	5'-CAA GTA TCT CC TCC CTT TTG AGC-3'	
P2X7Cre-long5'-for	5'-CAG CTC TGC TCC CTG TAA ACT TAT CCT TTG-3'	1,781 bp
P2X7Cre-long5'-rev	5'-CCG TTC ACG TCG CCA TCC AGT TCC-3'	
P2X7Cre-long3'-for	5'-GAA ACG AGA TGG CGC AAC GCA ATT AAT G-3'	4,822 bp
P2X7Cre-long3'-rev	5'-CAT CCT TCT GAG GCC TGA GGA ATG TAG-3'	

Table 3. Reagents employed for genotyping

Reagent	Brand
Dream-Taq Buffer	Thermo Scientific
Deoxyribonucleotides (dNTPs)	Thermo Scientific
Taq Polymerase	Thermo Scientific
Agarose powder	Thermo Scientific
Ethidium Bromide	Roth
1 Kb plus Ladder	Invitrogen
Long Amp Taq PCR Kit	New England Biolabs

Solutions

1 x Tris acetate EDTA (TAE) buffer

- 4.84 g TRIS
- 1.142 ml acetic acid
- 20 ml 0.05 M EDTA, pH 8.0
- 800 ml ddH2O
- pH adjusted to 8.3 with acetic acid
- Adjust to 1 l with ddH2O

Agarose gel (2%)

- 450 ml TAE buffer
- 10 g agarose
- 0.1 µg/ml Ethidium Bromide

6 x DNA loading buffer

- 1 g orange G
- 10 ml 2M TRIS/HCl, pH 7.5
- 150 ml glycerol
- Adjust to 1 l with ddH2O

5.2 *RT-qPCR*

Table 4. Primers employed for RT-qPCR

Primer	Sequence	Exon
mP2X4R-for	5'-TAT GTG GTC CCA GCT CAG GA-3‘	1
mP2X4R-rev	5'-TCA CAG ACG CGT TGA ATG GA-3‘	4
mP2X7R-for	5'-ACT GGC AGG TGT GTT CCA TA-3‘	5
mP2X7R-rev	5'-TTG GCA AGA TGT TTC TCG TG-3‘	7
mP2X7R-A-for	5'-GCA CAT GAT CGT CTT TTC CTA C-3‘	1
mP2X7R-K-for	5'-TAT GGA TCG GGA CGC TGA AG-3‘	1
mP2X7R-A/K-rev	5'-CCC TCT GTG ACA TTC TCC G-3‘	2
mP2X7R-ABC-for	5'-CCC AAG CCG ACG TTG AAG TA-3‘	11-12
mP2X7R-A-rev	5'-TCG TGG AGA GAT AGG GAC AG-3‘	13
mP2X7R-C-rev	5'-GCG CAT ACA TAC ATG CAG GC-3‘	13
hP2X7R-for	5'-CCT AAT GTG GGA TTC ACT CAC A-3‘	7
hP2X7R-rev	5'-AAC TGC TGT CGC TCC CAT ATT-3‘	8
Cx3cr1-for	5’-CCT TCC CAT CTG CTC AGG A-3’	1
Cx3cr1-rev	5'-CAA AGG CCA CAA TGT CGC C-3	2
GFAP-for	5'-GCT GGA GGG CGA AGA AAA C-3‘	6
GFAP-rev	5'-GAG AGG TCT TGT GAC TTT TTG G-3‘	9
Synapsin-for	5'-TAG TCA TCA GCA AGA TGA ACC AG-3‘	10
Synapsin-rev	5'-GGA GGG GTC TTG CTG GAG-3‘	11
HPRT-for	5'-TGG GCT TAC CTC ACT GCT TTC C-3‘	1
HPRT-rev	5'-CCT GGT TCA TCA TCG CTA ATC ACG-3‘	2

All primer pairs were designed to have a melting temperature of 60°C and to produce an amplicon of 80-120 bp.

Table 5. Reagents employed for RT-qPCR

Reagent	Brand
Trizol	Invitrogen
RNeasy Mini Kit	Qiagen
Superscript III First strand system	Invitrogen
Oligo (dT) 12-18 Primers	Thermo Scientific

Dithiothreitol (DTT)	Roche
RNAse inhibitor	Sigma Aldrich
Light cycler FastStart DNA Master SYBR Green	Roche
96 Well PCR Microplate (White)	Invitrogen
Sealing tape (Optically clear)	Sarstedt AG

5.3 *In situ hybridization*

Table 6. Primers employed to generate riboprobes

Primer	Sequence
P2X4R-for	5‘-ACA ATG GAT TTC TGG TGT GC-3‘
P2X4R-rev	5‘-GAA GAG GAC TTA TGC CGC TG-3‘
P2X7R-A-for	5'-CAG ATG GAC TTC TCC GAC CT-3'
P2X7R-A-rev	5'-CTT CAC CAC CTC CGC AAT G-3
P2X7R-AB-for	5'-CGT TGA AGT ATG TGT CCT TTG TC-3'
P2X7R-AB-rev	5'-TTC TTA AAT AAA TGA ATT GAA ATC AAG-3'
P2X7R-C-for	5'-GTC AAA GGC CAA GAA GTT CCA-3'
P2X7R-C-rev	5'- GGC TGA ATG GTT ACG ACC ACT -3'
TOPO-Sp6	5’-CCA AGC TAT TTA GGT GAC ACT ATA GAA TAC T-3’
TOPO-T7	5’-GAA TTG TAA TAC GAC TCA CTA TAG GGC GAA TTG-3’

Table 7. Identity of the probes employed for ISH

Probe	Identity
P2X7R	1199–1620 of GenBank accession no. NM_011027
P2X4R	1004–1910 of GenBank accession no. NM_011026
EGFP	907–1698 of GenBank accession no. LC311024
P2X7R-A	1444-2220 of GenBank accession no. NM_011027
P2X7R-AB	1337-2560 of GenBank accession no. NM_011027
P2X7R-C	1302-1610 of GenBank accession no. NM_001038845.3

Table 8. Reagents employed for ISH

Reagent	Brand
Bacto-tryptone	BD Biosciences
Bacto-yeast extract	BD Biosciences
SuperFrost slides	Menzel
QIAquick Gel Extraction Kit	Qiagen
NEB Turbo Electrocompetent *E. coli*	New England Biolabs
NEB Growth medium	New England Biolabs
TOPO PCR Cloning Kit	Thermo Scientific
Miniprep Kit	Qiagen
PCR Extraction Kit	Qiagen
RNAse inhibitor	Sigma Aldrich
10x Transcription buffer	Roche
NTP-mix	Roche
Diethyl pyrocarbonate (DEPC)	RPI
Dithiothreitol (DTT)	Roche
Sulfur-labeled UTP (^{35}S-UTP)	PerkinElmer
Sp6 Polymerase	Roche
T7 Polymerase	Roche
RNase-free DNase	Sigma Aldrich
RNeasy Mini Kit	Qiagen
Scintillation cocktail	Zinsser Analytic
Paraformaldehyde (PFA)	Sigma
tRNA	Roche
RNase A	Thermo Scientific
Autoradiography film	Kodak
Photo emulsion solution	Kodak
Developer solution	Kodak
Fixation solution	Kodak
DPX mounting solution	VWR International

Solutions

LB medium

- 1% bacto-tryptone
- 0.5% bacto-yeast extract
- 1.5% NaCl
- Adjust pH to 7.4
- For LB agar plates add 1.5% Bacto agar

10x PBS

- 1.37 M NaCl
- 27 mM KCl
- 200 mM Na_2HPO_4 x 12 H_2O
- 20 mM KH_2PO_4
- Adjust volume to 1 l with ddH_2O
- Adjust pH to 7.4

DEPC-H_2O

- 1 l dd H2O
- 1 ml DEPC
- Incubate o/n and autoclave twice

20% PFA

- 1000 g PFA
- Adjust to 5l with 1xPBS-DEPC
- Adjust pH to 7.4

10x TEA

- 1M TEA
- Adjust volume to 1l with ddH2O
- Adjust pH to 8.0
- 1 ml DEPC
- Incubate o/n and autoclave twice

20x SSC

- 3M NaCl
- 300mM sodium citrate
- Adjust volume to 1l with ddH_2O
- Adjust pH to 7.4
- 1 ml DEPC

5x NTE

- 146.1 g NaCl
- 50 ml 1M TRIS/HCl, pH 8.0
- 50 ml 0.5M EDTA, pH 8.0
- Adjust volume to 1 l with ddH_2O
- Adjust pH to 7.4
- 1 ml DEPC

Hybridization mix

- 50 ml formamide
- 1 ml 2M TRIS/HCl, pH 8.0
- 1.775 g NaCl
- 1 ml 0.5M EDTA, pH 8.0
- 10 g dextran sulphate
- 0.02 g ficoll 400
- 0.02 g polyvinylpyrrolidone 40
- 0.02 g bovine serum albumin
- 5 ml tRNA (10 mg/ml)
- 1 ml carrier DNA (salmon sperm, 10 mg/ml)
- 4 ml 5M DTT

Hybridization chamber fluid

- 250 ml formamide
- 50 ml 20x SSC
- 200 ml ddH_2O

- 5M DTT/DEPC
- 7.715 g DTT
- 4 ml H_2O-DEPC
- Shake until solution is clear
- Adjust volume to 10 l with H_2O-DEPC

5.4 *Cell culture*

Table 9. Reagents employed for cell culture

Reagent	**Brand**
(Z)-4-Hydroxytamoxifen (OH-TAM)	Sigma
Lipopolysaccharide (LPS)	Sigma
2'(3')-O-(4-Benzoylbenzoyl) adenosin-5'-triphosphat -triethylammonium (BzATP)	Sigma
Mouse IL-1 beta ELISA kit	Abcam
Poly-D-Lysine (PDL)	Sigma
DMEM/F-12, Glutamax supplement	Thermo Scientific
DPBS	Gibco
Fetal Bovine Serum (FBS)	Thermo Scientific
Penicillin/Streptomycin (P/S)	Thermo Scientific
Non-essential amino acids (NEAA)	Merck
Sodium Pyruvate (NaPyr)	Gibco

Media

Dissection medium:

- DMEM/F12 - Glutamax
- 1% P/S

Growth medium:

- DMEM/F12 - Glutamax
- 10% FBS
- 1% P/S
- 1% NEAA
- 1% NaPyr

5.5 *Immunostainings*

Table 10. Antibodies employed for immunostainings

Antibody	Brand	Dilution
Rabbit anti IBA1	Wako Chemicals	1:1000
Rat anti GFAP	Thermo Scientific	1:1000
Rabbit anti S100B	Abcam	1:1000
Chicken anti GFP	Thermo Scientific	1:1000
Rabbit anti HA-Tag	Cell Signaling Technology	1:1000
Goat anti rabbit Alexa 488	Invitrogen	1:1000
Goat anti rabbit Alexa 594	Invitrogen	1:1000
Goat anti chicken Alexa 488	Invitrogen	1:1000
Goat anti-rat Alexa 488	Invitrogen	1:1000

Table 11. Reagents employed for immunostainings

Reagent	Brand
Isoflurane	Abbot
Paraformaldehyde (PFA)	Sigma
Triton X-100	Sigma
Normal Goat Serum (NGS)	Thermo Scientific
DAPI mounting medium (Fluoromount)	Invitrogen

Solutions

Blocking solution (in 1x PBS)

- 5% NGS
- 0.1% Triton 100x

Cryoprotectant solution

- 125 ml Ethylene glycol
- 125 ml Glycerol
- 250 ml 1x PBS

6. Methods

6.1 *Animals*

6.1.1 *Housing conditions*

The animals were kept on a 12-hour light-dark cycle with *ad libitum* food and water in the following conditions: Temperature 21°C, humidity 50%. All animal experiments were conducted in accordance with the Guide for the Care and Use of Laboratory Animals of the Government of Upper Bavaria, Germany, as well as with the Animal Care and Use Committee of the Max Planck Institute of Psychiatry (Munich, Germany).

6.1.2 *Mouse lines*

Table 12. Mouse lines employed throughout the project

Mouse line	Characteristics	References
hP2X7R (hWT)	Expresses humanized P2X7R	Metzger et al., 2017
hKO	Conditional, full P2X7R-KO	
Microglia KO	Conditional, microglia P2X7R-KO	
Cx3cr1-CreERT2	Expresses TdTomato in microglia upon Tamoxifen stimulation	Parkhurst et al., 2013
Glast-CreERT2	Expresses TdTomato in astrocytes upon Tamoxifen stimulation	Mori et al., 2006
sEGFP	Expresses EGFP under the P2X7R promotor	GENSAT project Rockefeller University, USA
P2X7-EGFP	Overexpresses a P2X7-EGFP fusion protein	Kaczmarek-Hajek et al., 2018
P2X7-CreERT2	Expresses nuclear EGFP upon Tamoxifen stimulation	EUCOMM program. International Knockout Mouse Consortium.

All mouse lines were backcrossed for <5 generations to a C57BL/6N background.

6.1.3 *Tamoxifen treatment*

Tamoxifen was administered to the inducible Cre mice in the form of tamoxifen food (GENOdiet CreActive, T400, Genobios, LAVAL cedex 9) for two weeks. In the case of the P2X7R-

KO mouse lines, to guarantee the degradation of the previously expressed P2X7R, at least one more week passed before the start of the experiments. Tamoxifen treatment in the P2X7-CreERT2, Glast-CreERT2 and Cx3cr1-CreERT2 mouse lines consisted of intraperitoneal injections (100 mg/kg) on three consecutive days.

6.2 *Genotyping*

The tail tissue was collected after weaning or at the end of an experiment, shortly after sacrifice. It was lysed in 100 µl of NaOH (50 mM) at 90°C for 30 minutes. The sample was neutralized with 30 µl of Tris-HCl (1M, pH 7.0). Samples were stored at 4°C until analysis. 1-2 µl of the sample were added to the following mix:

- 18 µl milliQ H_2O
- 2 µl 10x Taq buffer
- 0.4 µl dNTPs
- 0.04 µl forward primer
- 0.04 µl reverse primer
- 0.1 µl Taq polymerase

The samples were processed in a Thermal Cycler (Bio-Rad) with a standard program which follows. The annealing temperature as well as the elongation time were calculated depending on the size of the amplified sequence as well as the melting temperature of the primers employed. The primers are summarized in Table 2.

- Preincubation: 95°C; 1 min
- Amplification (35 cycles):
    - Denaturation 95°C; 30 sec
    - Annealing X°C; 30 sec
    - Elongation 72°C; X min
- Elongation: 72°C; 5 min
- Cooling: 4°C; hold

2% agarose gels were prepared by adding 10 g of powdered agarose to 450 ml of 1x TAE buffer. The mix was heated for 5-8 minutes, until it had a clear appearance. Then, 0.1 µg/ml ethidium bromide was added to the solution, which was mixed and poured into an electrophoresis

chamber (PeqLab) already prepared with the dams and combs. After solidification of the gel, the combs and dams were removed, and 1x TAE buffer was poured until filling the chamber to the required volume. 20 µl of loading buffer were added to each sample, and then 20-40 µl of sample were loaded into each well. A 1 Kb Plus DNA Ladder was employed as a size marker. The gel was run at 160 V, 300 A for 1 to 1.5 hours. For imaging of the gel, a Quantum ST5 system (Analis) was used.

6.3 *RT-qPCR*

Adult brain tissue was homogenized with Trizol (1ml per 50 mg of tissue) and incubated for 5 minutes at room temperature (RT). After that, chloroform (200 ul per 50 mg of tissue) was added, and the tube was inverted several times until the sample was homogeneous. This mix was incubated for 3 minutes at RT. The tubes were then centrifuged (13000 rpm, 4°C, 15 min) and the supernatant was collected in a new tube. RNA was isolated with the RNeasy Minikit. The samples were kept at -80°C until further use. The RNA was reverse transcribed into cDNA by using the SuperScript III First-Strand Synthesis System. The following components were added to a nuclease-free microcentrifuge tube:

- 1 ul Oligo (dT) 12-18 primers (50 µM)
- 1-2 ul of template RNA
- 1 ul dNTP mix (10 mM)
- Distilled H_2O to a total of 13 µl.

The mixture was heated to 65°C for 5 minutes and subsequently incubated on ice for 1 minute. The following components were added:

- 4 µl 5x First Strand Buffer
- 1 µl DTT (0.1M)
- 1 µl RNase inhibitor
- 1 µl Superscript III retro transcriptase

This mix was incubated at 50°C for 45 minutes and at 70°C for 15 minutes afterwards. The samples were kept at -20 °C until qPCR analysis.

For the qPCR experiment, the following volumes were added to the reaction. Every sample was added to a 96-well plate in triplicate and the whole plate was sealed with a clear plastic film.

- 10 µl SYBR Green Mastermix
- 0.2 µl forward primer
- 0.2 µl reverse primer
- 8.6 µl sterile water
- 1 µl cDNA template (1:10)

The plate was shortly centrifuged to collect the contents at the bottom of the well and it was placed in a Light cycler 96 system (Roche). The protocol was set to the following parameters:

- 95°C; 600 seconds
- 40 cycles
    - 95°C; 10 seconds
    - 55°C; 45 seconds
- 95°C; 60 seconds
- 50°C; 16 minutes

Crossing points (Ct) were automatically calculated by the software Light cycler 96 (Roche), and the results were normalized with the ΔΔCt method to the housekeeping gene and to the reference samples (Livak & Schmittgen, 2001). The primers employed in this experiment are summarized in Table 4. Primers employed for RT-qPCR

6.4 *In situ hybridization*

Mice were sacrificed by an overdose of isoflurane. They were decapitated and the brains were extracted and snap frozen on dry ice. Brains were stored at -80°C until further use. For *in situ* hybridization (ISH), brains were cut at the cryostat (HM 560 M, Microm, Thermo Fisher Scientific) at a 20 µm thickness and mounted on Super Frost slides in a series of 6. The samples were stored at -20°C until analysis. Riboprobes of interest were generated by PCR (primers obtained from Allen Brain Atlas and summarized in Table 6). The PCR product was extracted from the gel by employing a DNA gel purification kit. The TOPO cloning kit was utilized to insert the fragment of interest to the pCRII vector.

For transformation of the ligation product, electrocompetent *E. coli* cells were thawed on ice and 1 µl of vector DNA (1:4) was added to 25 µl of *E. Coli* in an electroporation cuvette. The cells were electroporated at 2100 kV, 100 Ω, 24 µF, 2.6 ms and 975 µl of growth medium were added to the cuvette. After resuspending twice, the sample was transferred to a 2 ml Eppendorf tube with holes pierced on the lid. The cells were placed in a shaker at 37°C for 1 hour (250 rpm). Finally, the cells were seeded and grown overnight (14h) at 37°C on LB-agar plates with Ampicillin.

Four individual colonies were selected from each plate with a pipette tip, placed momentarily into the PCR master mix to confirm the presence of the insert in our vector, then regrown on a new agar plate with ampicillin. Finally, the tip was dropped in a tube with 5 ml of LB medium with ampicillin. The plates and the tubes were incubated overnight at 37°C. The next morning, the tubes with the samples that had been confirmed to contain the vector were centrifuged at 4000 rpm for 8 minutes and the supernatant was discarded. The DNA was then extracted from the bacterial pellet with a Miniprep kit according to the manufacturer's protocol. The DNA concentration was tested with a nanophotometer (P330, Implen).

A standard PCR with the Sp6 and T7 primers was carried out on the plasmid to amplify the fragment of interest. This amplified DNA was purified with the PCR extraction kit and an electrophoresis was run to confirm the amplification of the fragment. The DNA was employed as a template for the reverse-transcription of the riboprobe. The mix prepared was the following:

- 1.5 µg of PCR product
- 13 µl RNase-free water
- 3 µl 10x transcription buffer
- 3 µl NTP-mix
- 1 µl 0.5M DTT
- 1 µl RNAse inhibitor
- 6 µl ^{35}S-UTP (12.5 mCi/ml)
- 1.5 µl Sp6 or T7 RNA polymerase

The sample was incubated at 37°C for two hours. Then another 0.5 µl of polymerase was added to the tube and it was incubated for another hour. To destroy the DNA template, 2 µl

of RNase-free DNase was added and it was incubated for 15 min at 37°C. To purify the RNA, the RNeasy Mini kit was employed, and the samples were eluted in a final volume of 100 µl in RNase free water. 1 µl of the product was added to a tube with 2 ml scintillation cocktail and the radioactivity was measured in a beta counter (LS6000, Beckmann Counter).

The slides with the samples of interest were placed in container wells to be treated in the manner described next:

- 4% PFA in PBS, 10 min on ice
- 3x PBS/DEPC, 5 min
- 0.1 M TEA (pH 8.0) + 0.3% acetic anhydride, 10 min on stirring
- 2x SSC/DEPC, 5 min
- 60% Ethanol/DEPC, 1 min
- 75% Ethanol/DEPC, 1 min
- 95% Ethanol/DEPC, 1 min
- 100% Ethanol/DEPC, 1 min
- 100% Chloroform, 1 min
- 100% Ethanol/DEPC, 1 min
- Air dry in a dust-free area

The hybmix buffer was mixed with the tagged riboprobe until getting a concentration of 100.000 cpm/µl. The solution was incubated at 90°C for 2 minutes and then 100 µl were loaded on each slide and coverslips were placed on top avoiding bubbles. The samples were placed into a humidified hybridization chamber and incubated overnight at 55°C. The next day the coverslips were removed, and the samples were treated following the next protocol.

- 3x SSC (4x), 5 min
- NTE + 20 µg/ml RNase A, 20 min 37°C
- 2x SSC (2x) + 1 mM DTT, 5 min
- SSC (1x) + 1 mM DTT, 10 min
- SSC (0.5x) + 1 mM DTT, 10 min
- 2x SSC (0.1x) + 1mM DTT, 30 min 64°C
- SSC (0.1x), 10 min

- 60% Ethanol/DEPC, 1 min
- 75% Ethanol/DEPC, 1 min
- 95% Ethanol/DEPC, 1 min
- 2x 100% Ethanol/DEPC, 1 min
- Air dry in a dust-free area

The slides were taped down in a light-proof photo cassette and a light-sensitive X-ray film was placed on top of it in a dark room. The samples were left exposing for 5-9 days. The film was developed and fixed in a medical film processor (SRX-101A, Konica Minolta). To do thorough microscope analysis the slides were dipped in photo-emulsion at 37°C for a few seconds and stored at 4°C in the dark for 2-4 weeks depending on the expected intensity of the signal. The slices were developed with the next protocol:

- Developer solution, 3 min
- Distilled water, 2 min
- Fixation solution, 5 min
- Distilled water, 30 sec
- Air dry overnight
- Add 100 ul of DPX mounting solution and coverslip

For data analysis, the signal intensities of 12 representative areas throughout the brain were measured on three mice per group using ImageJ. The background noise was subtracted, and the resulting values were normalized with the control animals from each group. An example of this analysis on three sections is shown in Figure 7.

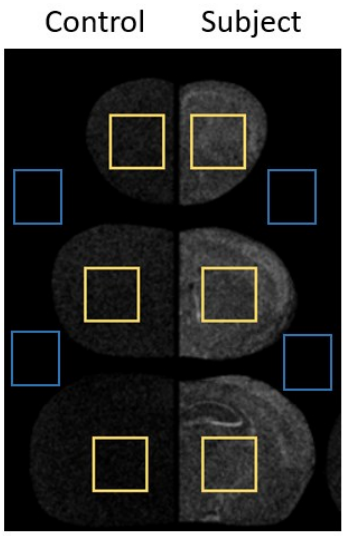

Figure 7. Example of ISH analysis areas. The intensity of equivalent areas was measured throughout the brain in three mice per group. In yellow are shown examples of the areas measured. In blue is depicted the measurement of background noise. Areas with orifices or localized high intensity were circumvented to avoid bias.

6.5 *Cell culture*

6.5.1 *Microglial culture*

T75 flasks were coated with 1x PDL for at least 2 h at 37°C before washing with water and adding the growth culture medium. Mouse pups were decapitated at P1-P3, and their heads were kept in ice cold dissection medium. The brains were extracted, and the meninges were removed. The cortical tissue was isolated and dissociated mechanically. First with spring scissors and subsequently with a P1000 pipette and a glass Pasteur pipette. The cells were centrifuged for 5 min at 900 rpm, and then resuspended in 1 ml growth medium. The cells were seeded in the flasks at a rate of 1-2 flasks per brain. The medium was changed 24 h later and then every 3 days until confluence was reached (around day 14). The genotype of the pups employed was elucidated through PCR. The cells from each individual were evaluated separately.

To enrich the microglial cell culture, the plates were tapped for 5 minutes, and the supernatant was collected. 50.000-100.000 cells per well were seeded on 24-well plates, containing a PDL-coated round, glass slide. The medium was changed on the next day and the experiments were carried out from the day after and on.

6.5.2 *Peritoneal macrophage culture*

Mice were sacrificed by an overdose of isoflurane. The skin from the abdomen was cut until the peritoneal lining could be seen. With a 5 ml syringe with a 27 g needle, 5 ml of ice-cold PBS (3% FBS) was injected into the peritoneal cavity. The abdomen was gently massaged to allow cell detachment from the tissues into the PBS. Afterwards, the same syringe with a 25 g needle was employed to collect as much fluid as possible, trying to avoid puncturing organs or getting the needle clogged with tissue. This step could be repeated when necessary. When the collected PBS was contaminated with blood, the sample had to be discarded. The cells were centrifuged for 5 min at 900 rpm and the pellet was resuspended with growth medium. These cells were seeded at 50.000 cells per well in PDL-coated 24 well plates containing round, glass slides.

6.5.3 *Drug treatment*

After confluence was reached in the T75 flasks, the expression of Cre recombinase was induced with OH-TAM 1 µM for 7 days. The cells were challenged with LPS 100 ng/ml 24h and stimulated with BzATP triethylammonium salt 300 µM 30 min - 1 h. After the treatments, the supernatant was collected, and the wells were washed with 1x DPBS and fixed with 4% PFA for 15 minutes. The samples immediately underwent immunocytochemistry analysis. IL-1β production was measured from the supernatant samples by employing an ELISA kit.

6.6 ***Behavioral experiments***

The mice were habituated to a single-housed environment under standard laboratory conditions for at least 2 weeks prior to the start of the experiments. They were maintained on a 12-hour light-dark cycle with *ad libitum* food and water. Male littermates aged 12-16 weeks were employed in all tests. The baseline behavioral testing was carried out in the morning, during the light phase, in non-consecutive days. The order of the tests was the following: open field test (OFT), elevated plus maze (EPM), light-dark box (LDB), novelty-suppressed feeding (NSF), forced swim test (FST), sucrose preference test (SPT) and home cage locomotion test (HCL), after which the mice were sacrificed (figure 8).

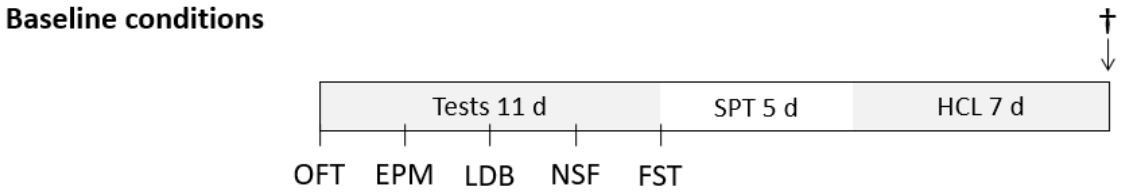

Figure 8. Schematic of the behavioral experiments carried out under baseline conditions. In non-consecutive days the mice underwent OFT, EPM, LDB, NSF and FST. After this, an SPT experiment was performed for 5 days. Following this, a HCL was carried out after which the animals were sacrificed (†).

6.6.1 *Open field test*

Locomotion and anxiety-related behaviors were measured in a PVC open field arena (50 x 50 x 45 cm) with an even illumination of 10-15 lux. An inner area was determined in the center of the arena (25 x 25 cm). The animals were always placed facing the upper left corner and their movement was tracked for a period of 30 minutes. The parameters measured were overall locomotion throughout the entire 30 minutes, as well as distance ratio, time, and number of entries to the inner area during the first 10 minutes of test.

6.6.2 *Elevated plus maze*

Anxiety-related behavior was assessed in a PVC elevated plus maze arena with an even illumination of 10-15 lux. The arena consists of four intersecting arms that join in a central zone (5 x 5 cm). Each pair of opposing arms is either open (30 x 5 x 0.25 cm) or enclosed (30 x 5 x 15 cm) and the whole apparatus is elevated 50 cm above ground level. The animals were placed facing the upper closed arm and their movement was tracked for a period of 10 minutes. The parameters measured include distance ratio, time, and number of entries to the open arms.

6.6.3 *Light-dark box*

Further anxiety testing was carried out in the light-dark box. It consists of two PVC arenas, one black with no lighting (15 x 20 x 25 cm) and one white with even 700 lux illumination (30 x 20 x 25 cm), connected by a gate (4 x 7 x 10 cm). The animals were placed facing the upper right corner in the dark compartment and their motion was captured for a period of 10 minutes. The parameters measured include latency to the first exit to the lit side, as well as time and number of entries to this area.

6.6.4 *Forced swim test*

Stress coping behavior was measured with the forced swim test. The setup consisted of a glass beaker (12 cm diameter, 25 cm height) filled with 1.4 liters of water (23-25°C). The mice were gently placed in the water and recorded for 6 minutes. The behaviors measured were struggling (forelegs are crossing the surface, body is vertical, highly energetic swimming), swimming (forelegs are not crossing the surface, body is horizontal, goal-directed movement) and floating (immobility except for small, steering movements). The time spent in each of these behaviors was scored manually.

6.6.5 *Sucrose preference test*

To assess anhedonic behavior the mice were subjected to the sucrose preference test. In a home cage, two bottles were presented to the single caged animals. During the first 3 days, the bottles contained drinking water. After the habituation period, one of the bottles, with its location randomly chosen, was filled with 2% sucrose. Every consecutive day during the period of 5 days, the weight of both bottles was measured to evaluate how much each animal had drunk from each bottle. A percentage of sucrose preference over water was calculated for

every animal. In the CSDS paradigm, the same animals went through the test before and after the stress paradigm. Under baseline conditions, the subject mice were compared to a control group. Mice with a clear side preference were removed from the analysis.

6.6.6 *Home cage locomotion test*

The home cage activity was measured with the Mouse-E-Motion infrared-detecting devices (Infra-e-motion, Germany). Mice were single housed in fresh cages, and a food grid with a plexiglass panel was employed. The base bedding was kept, but extra nesting material or other elements that could conceal the animal were removed. The device was placed on the plexiglass tray and the sensor was activated. The readout lasted 5-7 days during which time the animals were not disturbed. Locomotor activity was detected in 4-minute increments and averaged by the hour. The final analysis applied to 3-4 full days, which began at least 24 hours after the beginning of the testing to avoid the hyperactive period that occurs after a cage change.

6.6.7 *Acute restraint stress*

Acute restraint stress was induced by placing the mice inside falcon tubes for 30 minutes. The tubes had a longitudinal, 0.5 cm cut to facilitate ventilation without allowing extra mobility of the animals. After this, the animals, including the control group, were let rest for 20 minutes in a home cage before starting the behavioral assessment. The tests were carried out in three consecutive days and happened in the following order: OFT, EPM and FST (Figure 9). Given the stressful nature of the forced swim test, we only applied restraint stress on days 1 and 2.

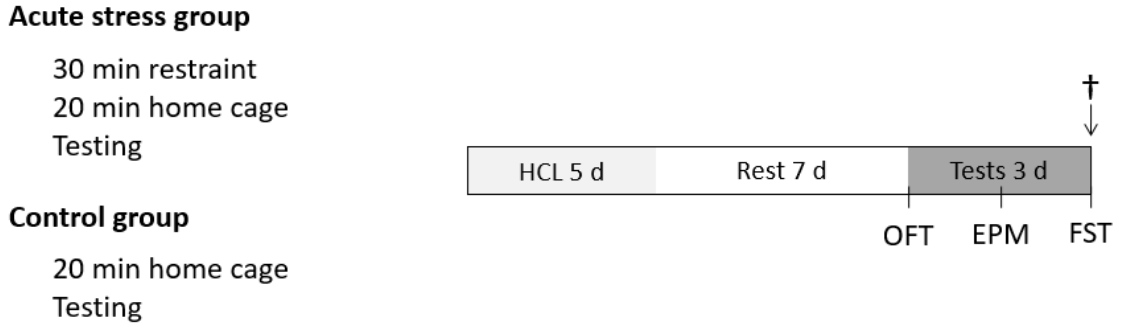

Figure 9. Schematic of the behavioral experiments carried out in acute stress conditions. The animals in the stress group were kept under restraint for 30 minutes. After this, both the control and the stress group were kept in a home cage for 20 minutes, after which the testing was performed. The OFT, EPM and FST were carried out in consecutive days, after which the animals were sacrificed (†).

6.6.8 *Chronic social defeat stress*

Aggressive CD1 mice were trained to become socially hostile for a week. Following this, the experimental mice were exposed to a different aggressive mouse every day for 21 days. After the CD1 mice attacked and the testing mouse showed signs of social defeat (immobility with exposed abdomen lying down or standing on the hind legs) the two mice were separated with a clear, perforated, plexiglass barrier that divided the home cage longitudinally. This barrier prevented physical access but enabled sensory contact. The experiments were carried out in four non-consecutive days in the following order: OFT, EPM, social avoidance test (SAT), FST. To prevent the effects of acute stress on the experiments, the CSDS paradigm was carried out after the behavioral assessment on testing days. The control group was kept single caged in standard conditions throughout the experimental period. The SPT was carried out before and after the CSDS paradigm. After the testing was finished, the animals were sacrificed, and the adrenal glands were dissected and weighted to assess the effectivity of the chronic stress paradigm (Figure 10).

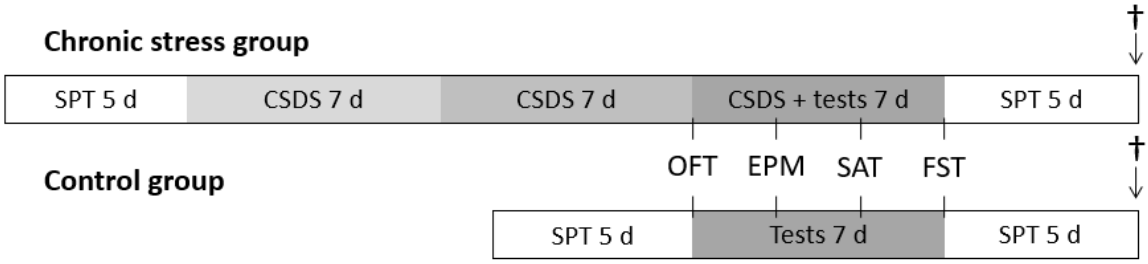

Figure 10. Schematic of the behavioral experiments carried out under chronic stress conditions. After 14 days of CSDS for the stress group, the OFT, EPM, SAT and FST were carried out in non-consecutive days. The SPT was performed before and after the CSDS for the stress group and before and after the behavioral tests in the control group. After this, the animals were sacrificed (†).

6.6.9 *Social avoidance test*

To assess the effect of the CSDS paradigm, the social avoidance test was carried out. An open field apparatus with an even illumination of 10-15 lux is set up with an upside-down wire mesh cup (10 cm diameter) placed adjacent to the center of the right edge of the arena. The mouse was allowed to explore this environment for 5 minutes. After this, a novel mouse was introduced into the cup and the test mouse was tracked for another 5 minutes. The arena was divided in 3 areas: the corners on the opposite side to the cup (10 x 10 cm), the interaction

area around the cup (12 cm diameter) and the rest of the area. The time spent in the far corners, as well as interacting with the empty cup and novel mouse were recorded, and a ratio was calculated between the habituation and the test phases.

6.6.10 *Data processing*

Automatic tracking was performed with the software ANY-maze (Stoelting, USA). All manual scoring was performed by a researcher blinded to the genotypes and conditions.

6.7 *Immunostainings*

6.7.1 *Immunohistochemistry*

The mice were sacrificed by an overdose of Isoflurane and perfused trans-cardially with 4% PFA. The brains were extracted and kept in PFA overnight (4°C). They were then transferred to 30% sucrose and left at 4°C for 3-5 days. The brains were cryo-sliced in series of 6 at 50 µm and kept in antifreeze solution at -20°C until analyzed. The sections were washed with PBS and blocked in PBS, 0.1% Triton X-100, 5% NGS. Then, they were incubated with primary antibodies in blocking solution overnight (4°C) with gentle shaking. Following washes with PBS, they were incubated with the secondary antibodies (2h RT) in PBS. After washing, the sections were mounted on microscope slides and cover slipped with DAPI mounting medium. Image acquisition was carried out with a confocal microscope (Zeiss). Automatized colocalization analysis was carried out with the software Strataquest (Tissuegnostics). Manual colocalization analysis was carried out with the software Fiji (ImageJ).

6.7.2 *Immunocytochemistry*

After fixation with 4% PFA for 15 minutes and three washes with PBS, the samples were processed following the same protocol as for immunohistochemistry. Coverslips were placed on microscope slides with mounting medium containing DAPI and left at 4°C overnight to solidify. Three areas of the cell culture were randomly selected to analyze each replicate. Microglia presenting fusiform processes was considered “inactive” while amoeboid cells were considered “active”. The researcher was blinded to the genotype and treatment of the samples. Pictures were obtained in a binocular fluorescent microscope with the software Axiovision (Zeiss). Manual counting was carried out with Fiji (ImageJ).

6.8 *Statistical analysis*

Statistical analyses were carried out with GraphPad Prism version 8.0 (La Jolla). Outlier analysis was carried out for all results ($p<0.01$). The data was compared with a Student's T-test (one variable) or with a two-way ANOVA with a Bonferroni post-test (two variables). The level of significance was set at $p<0.05$.

7. Results

7.1 *Behavioral analysis of humanized P2X7R knockout mice*

Behavioral studies in mice previously revealed that full genetic inactivation or pharmacological inhibition of P2X7R leads to increased active coping and decreased overall anxiety phenotypes (Basso et al., 2009; Boucher et al., 2011; Csölle, Andó, et al., 2013; Csölle, Baranyi, et al., 2013; Yue et al., 2017). Along these lines, it was decided to analyze these phenotypes in the hP2X7R mouse line, comparing humanized wildtype (hWT) mice with constitutive knockout (hKO) littermates derived from the conditional humanized allele. Previous unpublished data from our laboratory showed no alteration in anxiety- nor depressive-like phenotypes upon full inactivation of human P2X7R (Metzger, 2016). Home cage locomotion was also unaltered during both the day and the night cycle (Figure 11). Therefore, it was hypothesized that the lack of P2X7R might have a more prominent role in anxiety- and depressive-like behavior when the animals were subjected to an environmental challenge. To that end, humanized knockout mice were subjected to an acute and a chronic stress paradigm.

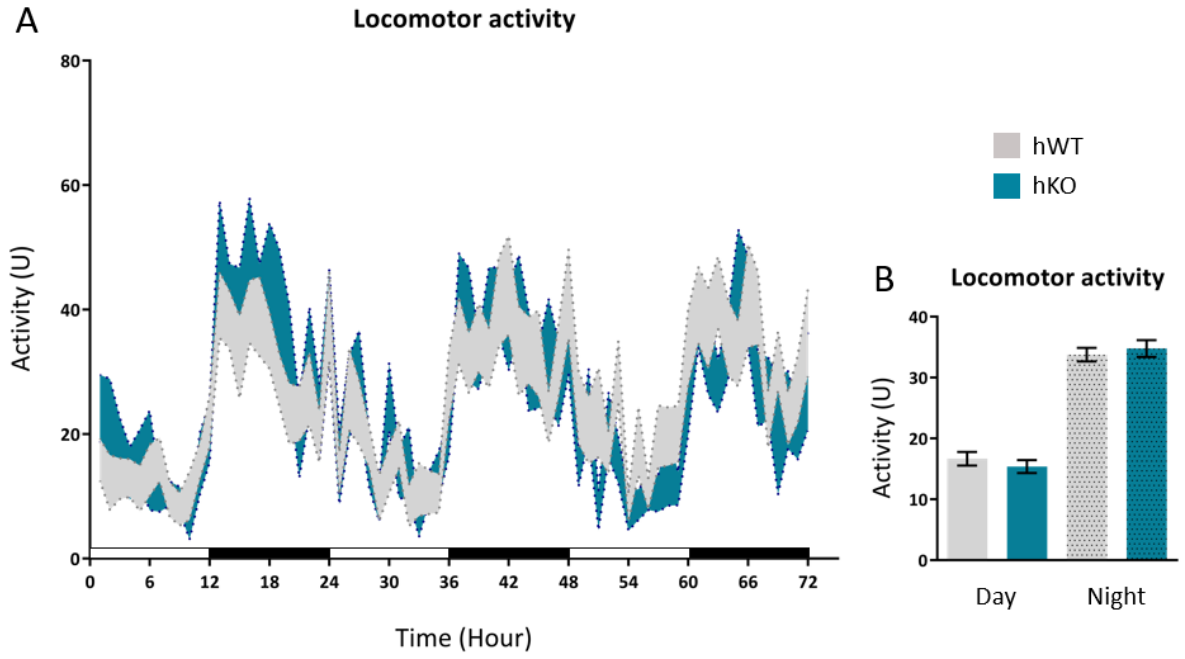

Figure 11. Home cage locomotor activity of hP2X7R knockout mice. (A) Representation of the hourly locomotor activity throughout 72 hours. White and black bars at the bottom represent day and night hours respectively. (B) Average activity during the day and night cycles. Data is represented as mean ± SEM (n_{hWT}:9, n_{hKO}:11).

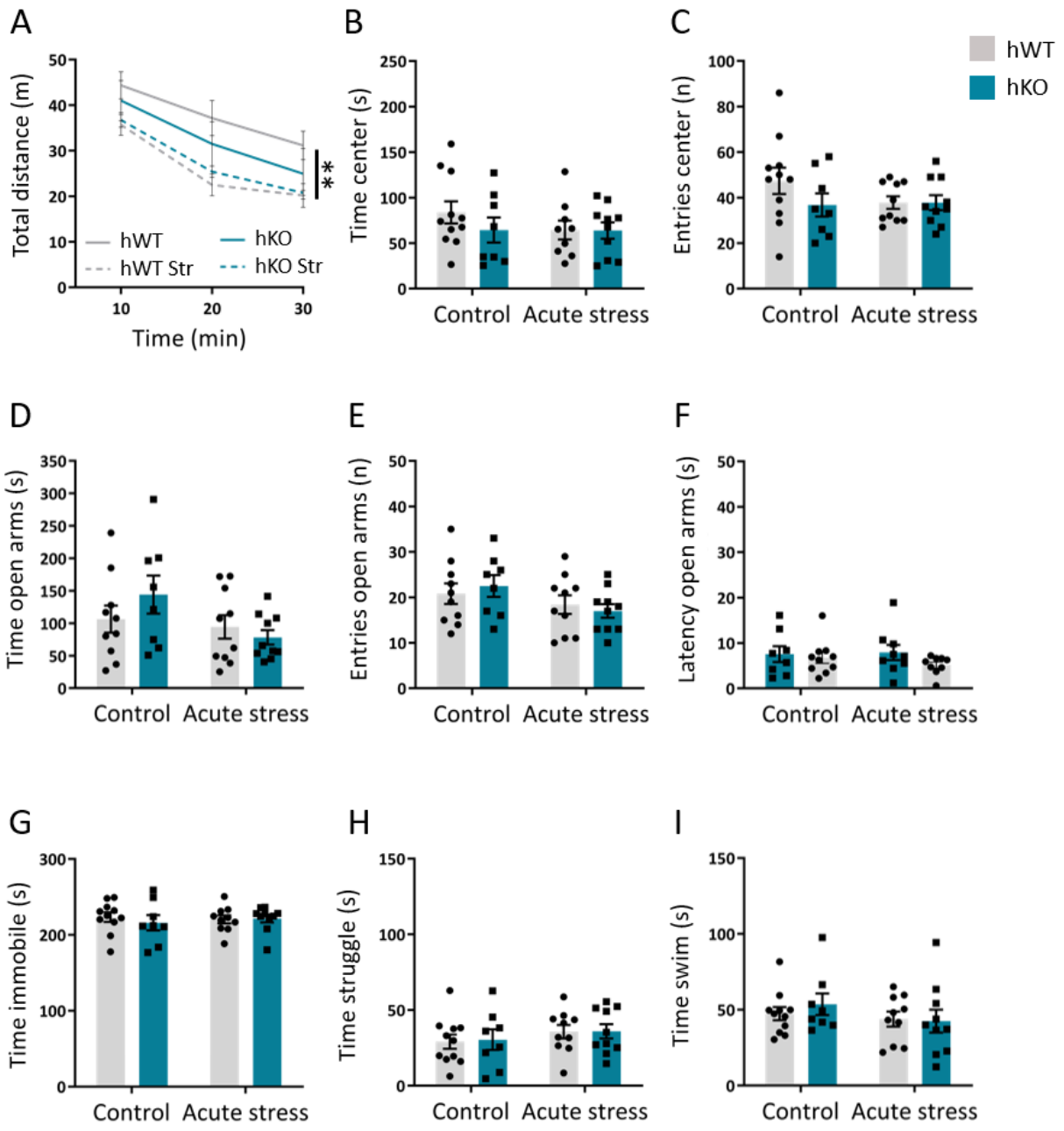

Figure 12 Anxiety- and depressive-like behavior assessment of hP2X7R knockout mice subjected to acute stress conditions. (A) Overall distance covered throughout 30 minutes in 10-minute increments, (B) time spent in the center in the first 10 minutes, and (C) entries to the center in the first 10 minutes of OFT. (D) Time spent in the open arms, (E) entries to the open arms, and (F) latency to the first entry to an open arm in the EPM. Time spent (G) floating, (H) struggling, and (I) swimming in the FST. Data is represented as mean ± SEM. Two-way ANOVA (n:10). Stress effect **: $p<0.01$.

Comparison of control mice with acutely stressed animals revealed that acute restraint stress resulted in a significant decrease of the distance covered throughout the OFT compared to unstressed animals (Two-way ANOVA, stress $F(1, 37) = 8.88$; $p=0.0051$) (Figure 12 A). However, this stress paradigm had no impact on anxiety parameters measured in the OFT and

EPM, as indicated by the time spent in the center (Figure 12 B), the number of entries to the center (Figure 12 C), the time spent in the open arms (Figure 12 D), the number of entries to these areas (Figure 12 E) and the latency to the first exit (Figure 12 F). Similarly, no significant impact of the restraint stress was observed on stress-coping behavior, as reflected by comparable immobility times in the FST (Figure 12 G), as well as time spent struggling (Figure 12 H) and time spent swimming (Figure 12 I). Furthermore, acute stress effects were independent of the genotype as hWT and hKO animals were statistically indistinguishable in all parameters measured (Figure 12 A-I).

To validate the efficacy of the CSDS paradigm, the adrenal glands of the animals were weighted upon sacrifice. There was a significant gain of adrenal weight in the mice that were subjected to the CSDS paradigm (Two-Way ANOVA, stress F (1, 37) = 10.83; p=0.0022) (Figure 13 A). In addition, a SAT was carried out to assess whether the animals that underwent CSDS had a higher avoidance to socialization with novel mice than control animals. There was a significant reduction in interaction ratio in the stress group (Two-Way ANOVA, stress F (1, 38) = 4.696; p=0.0176) (Figure 13 B), as well as an increase in the time spent in the far corners, away from the novel mouse (Two-Way ANOVA, stress F (1, 38) = 4.696; p=0.0366) (Figure 13 C). These measures proved the efficacy of the CSDS, albeit hWT and hKO mice responded to a comparable extent to this paradigm.

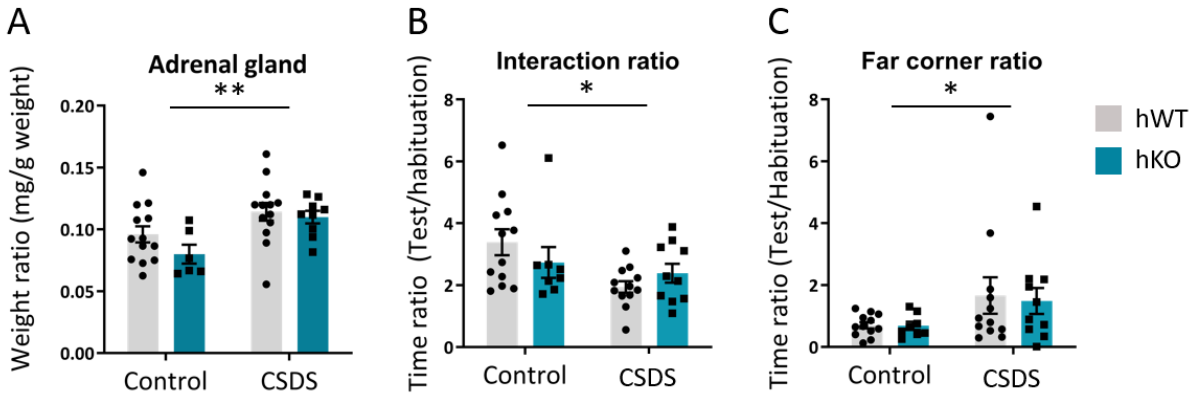

Figure 13. Validation of the CSDS in hP2X7R knockout mice. (A) Weight ratio of the adrenal glands under baseline and CSDS conditions, normalized to the body weight of each animal. (B) Ratio of the interaction time with a novel mouse in the SAT. (C) Ratio of the time spent in the far corner, away from the interaction area in the SAT. Ratios in the SAT were calculated by dividing the time spent in the field of interest during the test phase by the same value during the habituation phase for each individual. Data is represented as mean ± SEM. Two-way ANOVA (n_{hWT}:9, n_{hKO}:11). Stress effect *: p<0.05; **: p<0.01.

Chronic stress had a significant impact on several behavioral readouts. Chronically stressed animals showed a significant decrease of the distance covered in the OFT throughout the 30 minutes of test (Two-way ANOVA, stress F (3, 39) = 7.66; p=0.0004) (Figure 14 A), as well as reduced number of entries to the center area (Two-way ANOVA, stress F (1, 39) = 13.92; p=0.006) (Figure 14 C). Similarly, animals which underwent the CSDS paradigm showed decreased time in the open arms in the EPM (Two-way ANOVA, stress F (1, 39) = 26.16; p<0.0001) (Figure 14 D), as well as reduced number of entries to the open arms (Two-way ANOVA, stress F (1, 37) = 18.48; p=0.0001) (Figure 14 E). Furthermore, the FST revealed that animals that underwent CSDS presented a higher immobility time (Two-way ANOVA, stress F (1, 38) = 11.71; p=0.0015) (Figure 14 G) and lower swimming time (Two-way ANOVA, stress F (1, 37) = 5.63; p=0.0228) (Figure 14 I), while no stress effects were observed in the time struggling (Figure 14 H). Finally, sucrose preference was significantly increased after the chronic stress paradigm (Two-way ANOVA, stress F (3, 32) = 3.55; p=0.0252) (Figure 14 J-K), although it is relevant to note that eight of the animals, which carried out the test without incidences before the CSDS, had to be removed from the analysis due to strong side preference after the CSDS.

In terms of genotype effects, under baseline conditions, hKO mice showed a higher locomotion in the first 10 minutes of the OFT in comparison with the hWT littermates, which was not observed in the CSDS group (Two-way ANOVA, stress x genotype F (6,78) = 3.18; p=0.0076; genotype F (3, 39) = 7.664; p=0.0004; Bonferroni post hoc test p<0.05) (Figure 14 A). Furthermore, there was a significant increase of the time spent in center in the OFT (Two-way ANOVA, stress x genotype F (1, 39) = 4.932; p=0.0322; Bonferroni post hoc test p<0.01) (Figure 14 B), but also an increase of the latency to the first open arm entry in the EPM (Two-way ANOVA, stress x genotype F (1, 36) = 4.402; p=0.043; genotype F (1,36) = 5.198; p=0.0286; Bonferroni post hoc test p<0.01) (Figure 14 F), which was not observed in the control group. Taken together, fully inactivating the expression of the humanized P2X7R resulted in limited effects on anxiety phenotypes, and no measurable effects on depressive-like behaviors under baseline as well as under acute or chronic stress conditions.

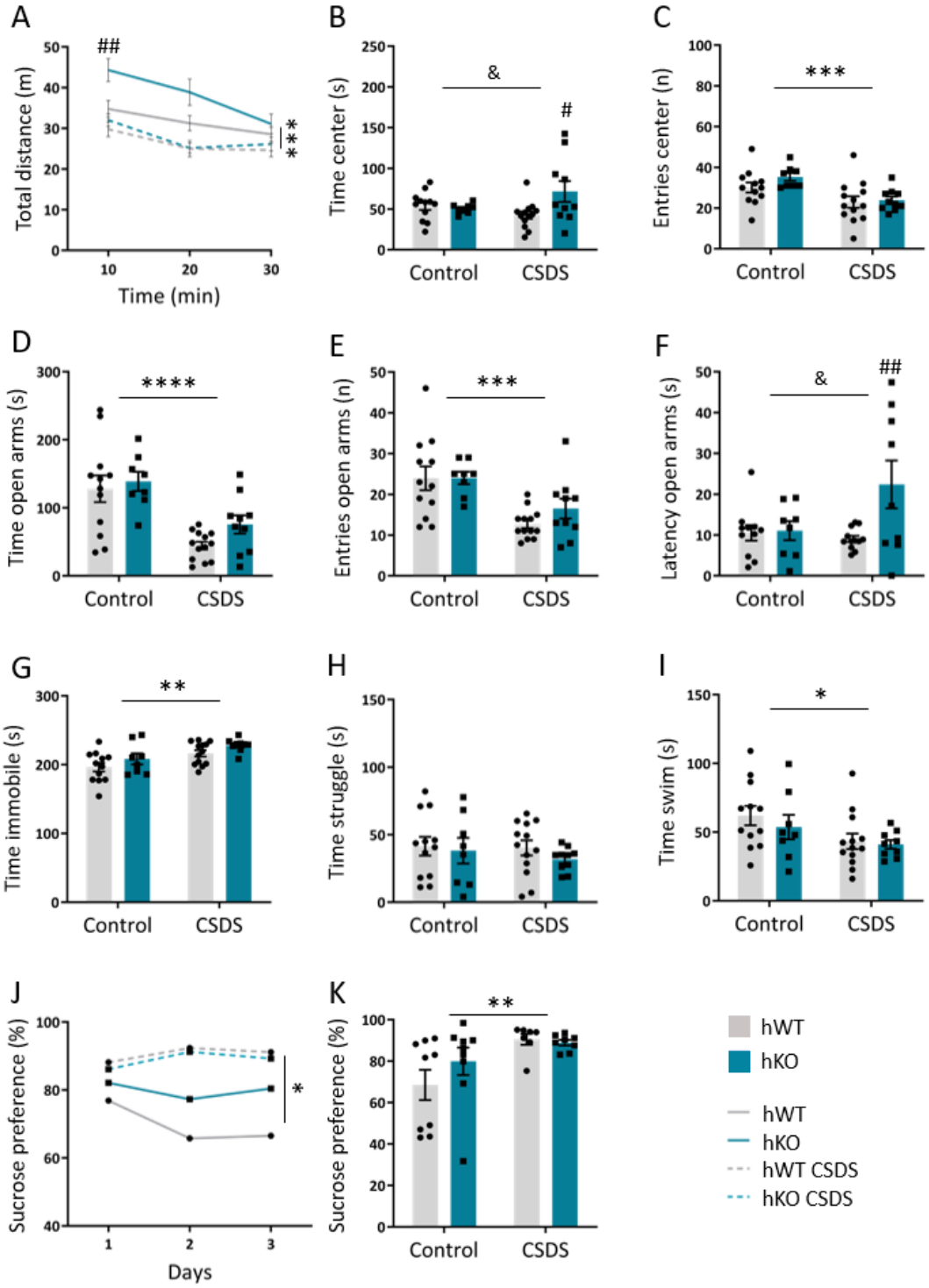

Figure 14. **Assessment of anxiety- and depressive-like behavior in hP2X7R knockout mice following CSDS.** (A) Overall distance covered throughout the 30 minutes in 10-minute increments (CSDS values shown in dashed lines), (B) time spent in center in the first 10 minutes, and (C) entries to the center in the first 10 minutes of OFT. (D) Time spent in the open arms, (E) entries to the open arms, and (F) latency to the first entry to an open arm of the EPM. Time spent (G) floating, (H) struggling, and (I) swimming in the FST. (J) Daily sucrose preference during the 3 days of SPT. CSDS values shown in dashed lines. (K) Average sucrose preference throughout the SPT. Data is represented as mean ± SEM. Two-way ANOVA with Bonferroni post hoc test (n_{hWT}=9, n_{hKO}=11). Stress effect *: p<0.05; **: p<0.01; ***: p<0.001; ****: p<0.0001. Genotype effect #: p<0.05; ##: p<0.01. Stress x genotype effect &: p<0.05.

7.2 *Validation and characterization of the microglia-specific hKO mouse line*

There is a strong connection between neuroinflammation and the development of depression. Therefore, the next objective was to analyze whether the previously published decrease in depressive-like phenotypes in the P2X7R-KO mice was specifically connected to P2X7R function in microglia. To this end, a conditional microglia-specific P2X7R-KO mouse line was established (Figure 15).

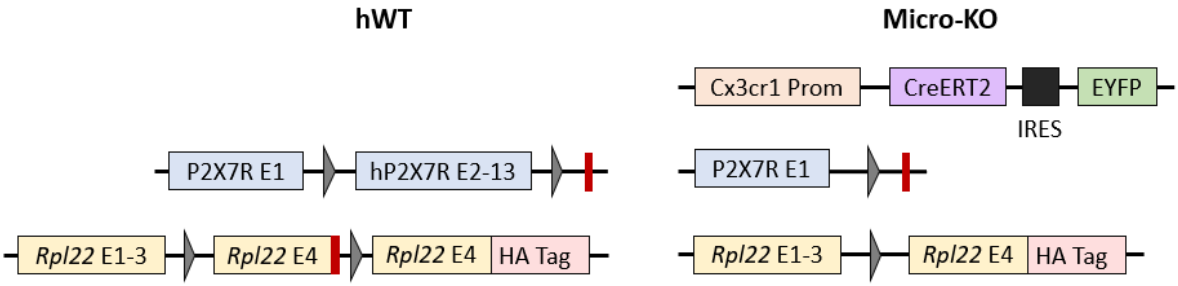

Figure 15. Scheme illustrating the transgenes carried by microglia-specific hP2X7R knockout mice. Control mice (hWT) carry the loxP-flanked (grey arrowheads) hP2X7R sequence (exon 2-13), as well as a modified allele of the ribosomal protein RPL22, in which exon 4 is flanked by loxP sites followed by an alternative exon 4 carrying an HA-tag. Besides these constructs, the microglia-specific knockout littermates (micro-KO) also harbor a CreERT2-IRES-EYFP expressed under the control of a microglia specific promoter (Cx3cr1). Upon tamoxifen treatment, Cre will induce inactivation of the hP2X7R allele specifically in microglia. Simultaneously, it will replace the endogenous exon 4 by the alternative exon 4 resulting in a HA-tagged RPL22 protein. Sites of transcriptional termination are marked in red.

7.2.1 *Validating a microglia-specific Cre driver*

To assess the functionality and specificity of the CreERT2 driver employed for the generation of the conditional microglia-specific hP2RX7 KO mouse line, two Cre driver lines were analyzed. The microglia-specific driver expresses CreERT2 under the control of the Cx3cr1 promoter. For comparison an astrocyte-specific driver was analyzed in which CreERT2 is driven by the Glast promoter. Both lines were bred to a Cre-dependent TdTomato reporter line enabling monitoring of Cre activity by expression of this reporter. To confirm the penetrance of the tamoxifen treatment, as well as to assess its specificity, immunohistochemistry was carried out using cell type-specific markers GFAP and S100β for astrocytes, and Iba1 for microglia. The analysis revealed full colocalization throughout the brain of the activated reporter with microglial and astrocytic markers respectively (Figure 16 A-B). This result confirmed full penetrance of the two-week, oral tamoxifen treatment, as well as microglia-

specificity of Cre-dependent activation, which validates the tamoxifen-inducible CreERT2 line as suitable for the establishment of a conditional microglia-specific hP2RX7 KO mouse line.

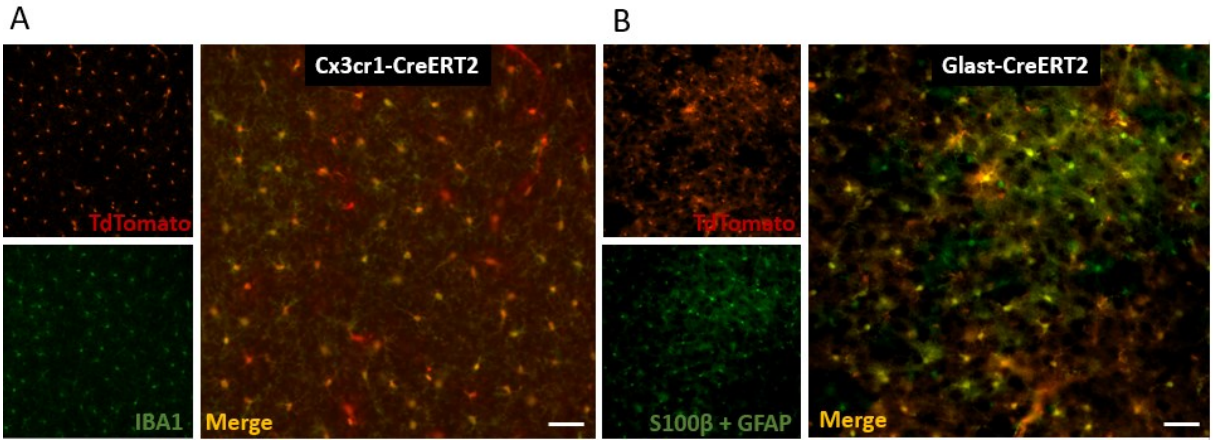

Figure 16. Colocalization of cell type-specific markers with Cre-dependent reporter gene activation. Representative image corresponding to the prefrontal cortex showing colocalization of the Cre-dependent reporter TdTomato (red) with cell type-specific markers (green) after tamoxifen treatment. (A) Microglia-specific marker IBA1 was targeted in the Cx3cr1-CreERT2 line. (B) Astrocyte-specific markers S100β and GFAP were targeted in the Glast-CreERT2 line. Merged images displayed larger on the right. The scale bar corresponds to 100 µm.

7.2.2 *Microglial physiological changes upon P2X7R inactivation in vitro*

In humanized mice, the effect of P2X7R inactivation in immune cells had been previously assessed in peritoneal macrophages. However, functional readouts in primary microglial cell culture were still to be confirmed. To corroborate that the specific inactivation of the P2X7R gene had a clear effect on the physiology of these cells, primary microglial cultures were produced from P1-P3 mice. These mice were homozygous for the humanized P2X7R allele and either negative (hWT) or positive for Cx3cr1-CreERT2 (micro-KO). After induction of Cre with OH-TAM, the culture was exposed to BzATP, either with or without prior LPS priming. Penetrance and effectiveness of the OH-TAM treatment was assessed through immunohistochemical detection of the HA-Tag (Figure 15), which proved that Cre activation was present in virtually all microglial cells (Data not shown).

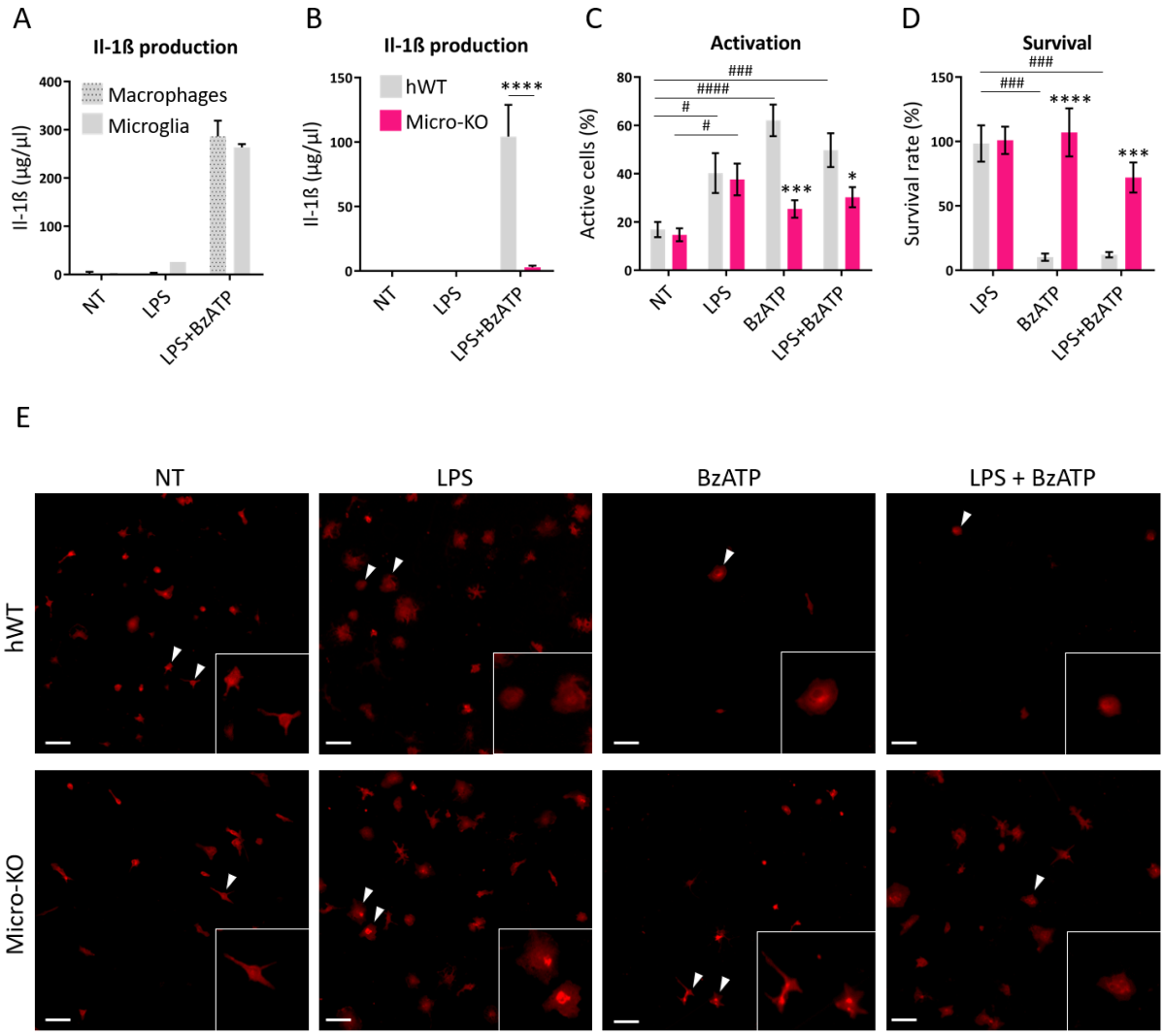

Figure 17. Response of primary microglial cell culture to P2X7R activation. (A) ELISA analysis of IL-1β release of macrophages and microglia following LPS (24h; 100 ng/ml) and BzATP (1h; 300 µM) treatment. (B) ELISA analysis of IL-1β release of hWT and P2X7R-KO microglia following LPS and BzATP treatment. (C) Morphological and (D) survival analysis of hWT and P2X7R-KO microglia following LPS, BzATP and combined treatment. (E) Primary microglia culture stained for the microglial marker Iba1. Marked with white arrow heads representative individual microglia that are shown at higher magnification. The scale bar corresponds to 100 µm. Bars represent mean ± SEM. Two-way ANOVA (n:3-6). Treatment effect: #: $p<0.05$; ###: $p<0.001$; ####: $p<0.0001$. Genotype effect: *: $p<0.05$; ***: $p<0.001$; ****: $p<0.0001$.

The results of the ELISA assay showed that BzATP stimulation caused a significant increase in IL-1β production, both in microglia and in macrophages, which could not be observed in non-treated (NT) or only LPS-treated samples (Two-way ANOVA, treatment $F(2, 8) = 715.2$; $p<0.0001$) (Figure 17 A). As expected, induction of microglia-specific P2X7R-KO led to a lack of IL-1β production upon BzATP stimulation (Two-way ANOVA, genotype $F(2, 15) = 11.76$, $p=0.0037$; Bonferroni post hoc test $p<0.0001$) (Figure 17 B). Furthermore, stimulation of

microglia led to changes in morphology, from a generally fusiform shape to a larger, amoeboid structure. This effect was observed in both hWT and hKO microglia upon priming with LPS (Two-way ANOVA, treatment F (3, 69) = 9,821; p<0.0001; Bonferroni post hoc test: hWT $_{NT-LPS}$ p<0.05; micro-KO $_{NT-LPS}$ p<0.05). However, only hWT microglia, and not P2X7R-deficient microglia, presented significant activation, when treated with BzATP alone or in combination with LPS (Two-way ANOVA, treatment F (3, 69) = 9,821, p<0.0001; Bonferroni post hoc test: hWT $_{NT-BzATP}$ p<0.0001; hWT $_{NT-LPS+BzATP}$ p<0.001. Genotype F (1, 69) = 15.02, p=0.0002; Bonferroni post hoc test BzATP $_{hWT-MicroKO}$ p<0.001; LPS+BzATP $_{hWT-MicroKO}$ p<0.05) (Figure **17** C, E). Additionally, there was a drastic decrease of hWT microglia survival after treatment with BzATP, alone or in combination with LPS, which was not detected in the micro-KO group (Two-way ANOVA, treatment F (2, 54) = 11.68, p<0.0001; Bonferroni post hoc test: hWT $_{LPS-BzATP}$ p<0.005; hWT $_{LPS-LPS+BzATP}$ p<0.005. Genotype F (1, 54) = 29.21, p<0.0001; Bonferroni post hoc test BzATP $_{hWT-MicroKO}$ p<0.0001; LPS+BzATP $_{hWT-MicroKO}$ p<0.005) (Figure 17 D, E). We confirmed with these analyses that conditional inactivation of P2X7R in micro-KO mice causes alterations in microglia function, which can be measured *in vitro*.

7.2.3 *Confirmation of Cre recombinase activity in microglia in vivo*

The micro-KO mouse line was treated with tamoxifen to induce the P2X7R inactivation. This mouse line expresses simultaneously with the CreERT2 an enhanced yellow fluorescent protein (EYFP) in all microglial cells, as well as HA-tagged RPL22 upon Cre activation (Figure 15). To assess the penetrance of the Cre activation immunohistochemistry was carried out on brain sections. There was full co-expression of the HA-tag and EYFP throughout the brain. In addition, there was total co-expression of EYFP with the microglial marker Iba1. It is inferred from this data that tamoxifen treatment induces Cre activity in every microglial cell, and therefore that the mouse is, as expected, a microglia-specific P2X7R-KO (Figure 18).

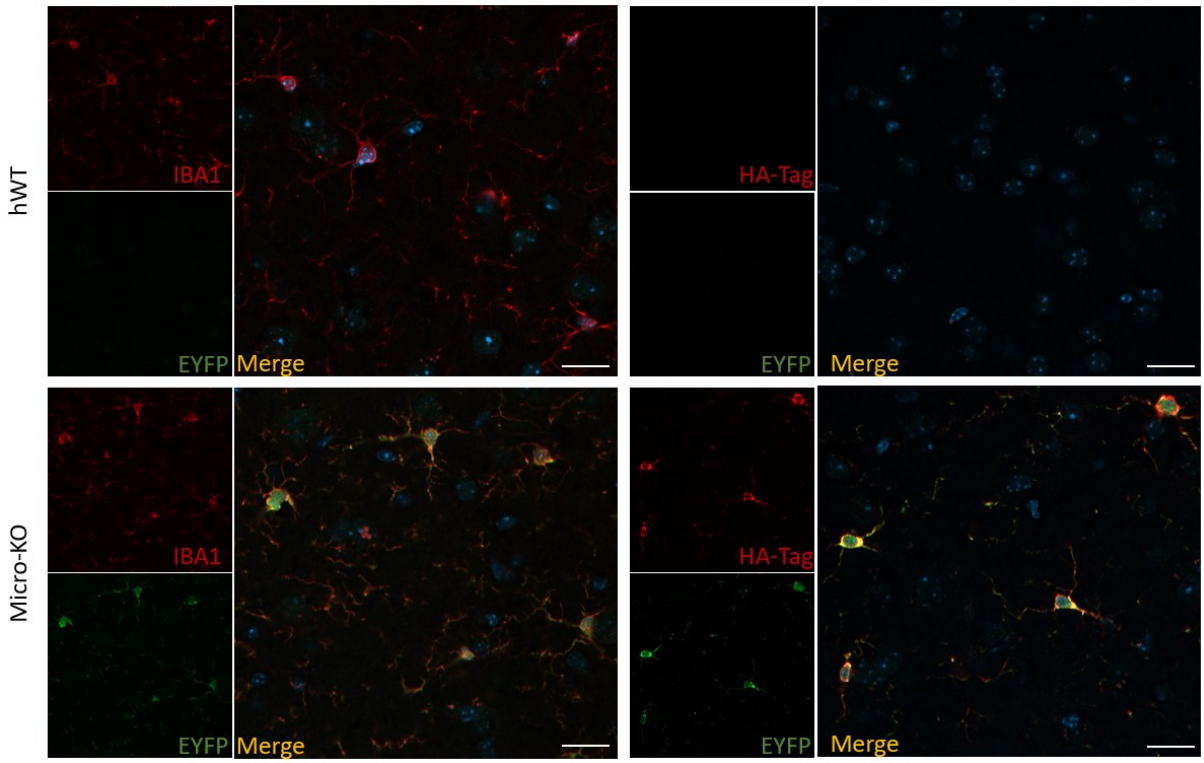

Figure 18. Colocalization of microglia-specific marker with Cre-activated reporter gene expression. Representative immunostaining corresponding to the cortex. Microglial marker Iba1 (red) and EYFP (green), as well as HA-Tag (red) and EYFP (green) revealed coexpression in the micro-KO mice, while no EYFP or HA-Tag signal could be detected in hWT mice. Nuclei were stained with DAPI (blue). Scale bar corresponds to 20 µm.

7.2.4 *Behavioral characterization of micro-KO mice under baseline and chronic stress conditions*

Once the micro-KO mouse model was validated, the next step was to assess anxiety- and depressive-like behaviors under baseline conditions. Home cage locomotion analysis revealed that micro-KO animals presented a significantly higher locomotion than hWT during both the day and night cycles (Two-way ANOVA, genotype $F(1, 25) = 4.51$; $p=0.0438$; One-way ANOVA, $p<0.0001$; Bonferroni post hoc test Day $_{\text{hWT-MicroKO}}$ $p<0.0001$; Night $_{\text{hWT-MicroKO}}$ $p<0.0001$) (Figure 19).

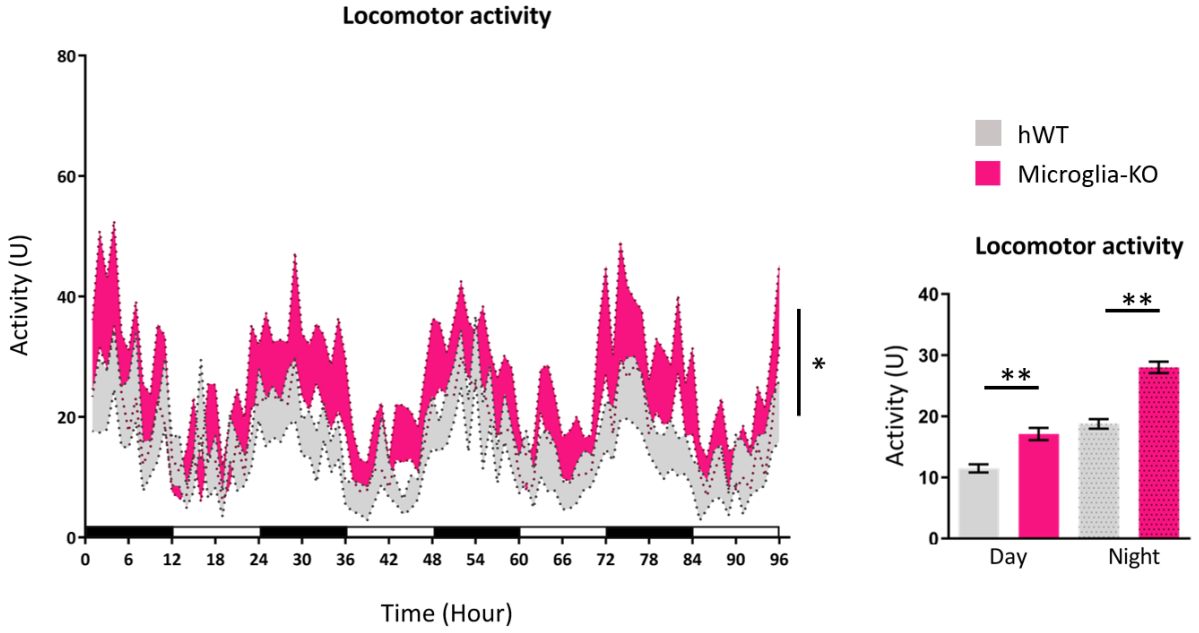

Figure 19 Home cage locomotor activity of hWT and micro-KO mice. (A) Representation of the hourly locomotor activity throughout 72 hours. White and black bars at the bottom represent day and night hours respectively. (B) Average activity during the day and night cycles. Data is represented as mean ± SEM. Two-way/One-way ANOVA with Bonferroni post hoc test (n_{hWT}:14, $n_{micro\text{-}KO}$:13). Genotype effect ****: $p<0.0001$; *: $p<0.05$.

On the other hand, inactivation of P2X7R in microglial cells did not lead to a significant variation with respect to anxiety-related phenotypes, namely the total distance covered (Figure 20 A), the time spent in the center area (Figure 20 B), and the number of entries to the center in the OFT (Figure 20 C); the time spent in the open arms (Figure 20 D), the number of entries to the open arms (Figure 20 E), and the latency to the first entry to an open arm in the EPM (Figure 20 F); and the time spent in the lit compartment (Figure 20 G), the latency to the first entry to this area (Figure 20 H), and the number of entries to the lit box in the LDB (Figure 20 I). Additionally, micro-KO animals did not present differential values in anhedonic behaviors, as observed in the latency to the first eating event (Figure 20 J), time spent eating (Figure 20 K), and number of eating events in the NSF (Figure 20 L); as well as in the sucrose preference index measured in the SPT (Figure 20 M-N). Finally, coping behavior was analyzed in the FST, but no significant difference between hWT and micro-KO animals could be detected neither in the immobility time (Figure 20 O), the time spent struggling (Figure 20 P) nor the time spent swimming (Figure 20 Q).

In conclusion, under baseline conditions, microglia-specific genetic inactivation of P2X7R had an impact on home cage locomotion, but not on the anxiety and depressive-like phenotypes measured.

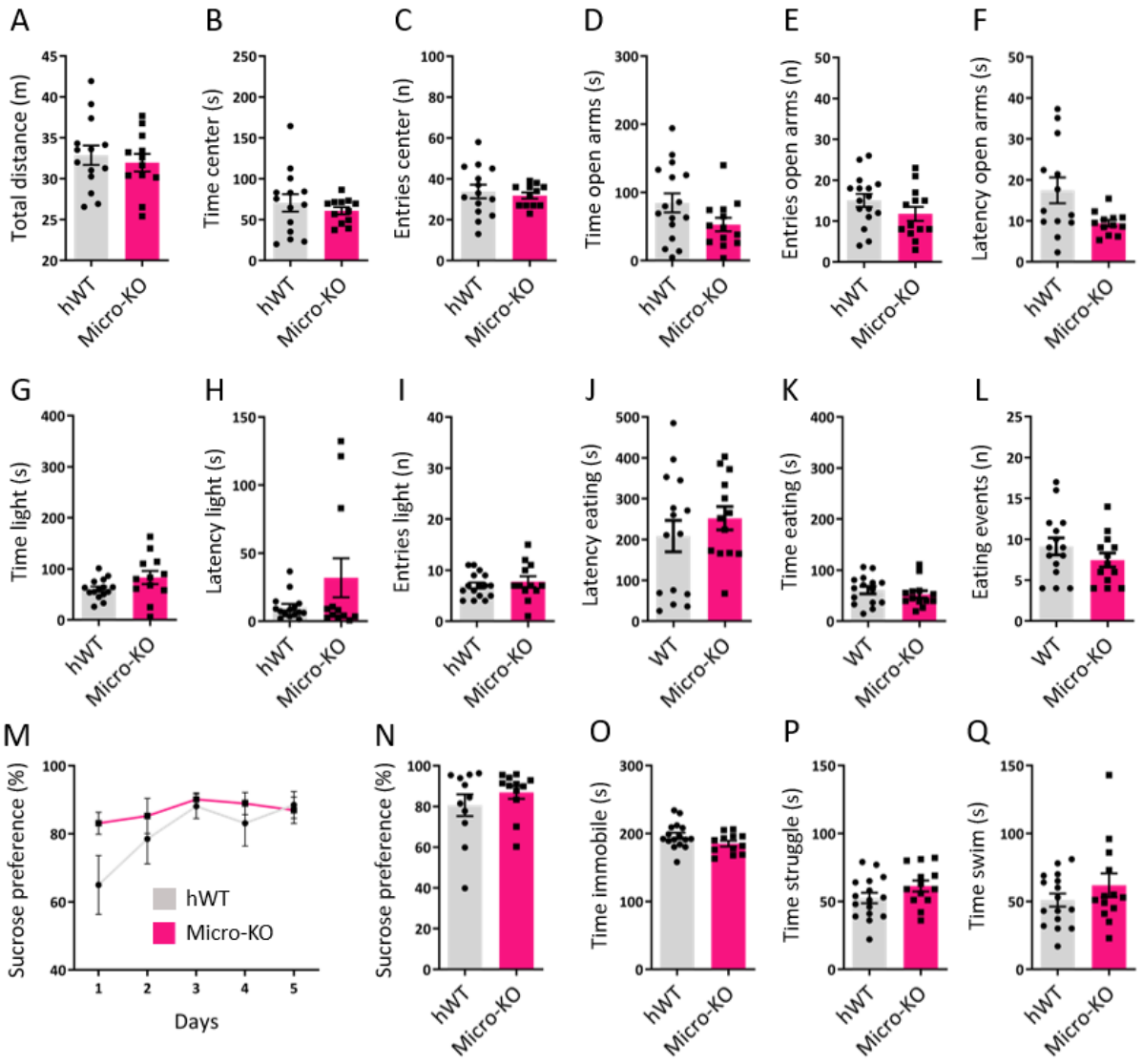

Figure 20. Anxiety- and depressive-like behavior assessment of the hWT and micro-KO under baseline conditions. (A) Total distance covered, (B) time spent in center, and (C) entries to the center in the first 10 minutes of OFT. (D) Time spent in the open arms, (E) entries to the open arms, and (F) latency to the first entry to an open arm in the EPM. (G) Time spent in the lit compartment, (H) latency to the first entry to the lit compartment, and (I) number of entries to the lit compartment in the LDB. (J) Latency to the first eating event, (K) time spent eating, and (L) number of eating events in the NSF. (M) Daily sucrose preference during the 5 days of SPT. (N) Average sucrose preference throughout the SPT. Time spent (O) floating, (P) struggling, and (Q) swimming in the FST. Data is represented as mean ± SEM. (n_{hWT}=14, n_{hKO}=13).

To evaluate the potential influence of P2X7R on anxiety- and depressive-like behavior under stress conditions, the animals were subjected to a CSDS paradigm. It was carried out as previously described and validated by weighting the adrenal glands and carrying out a SAT to assess the levels of social avoidance after stress. The animals that underwent CSDS presented a significantly higher adrenal weight ratio (Two-way ANOVA, stress F (1, 34) = 49.55; p<0.0001) (Figure 21 A). However, the interaction ratio and the far corner ratio in the SAT did not show a significant reduction of social behavior in the CSDS group (Figure 21 B-C).

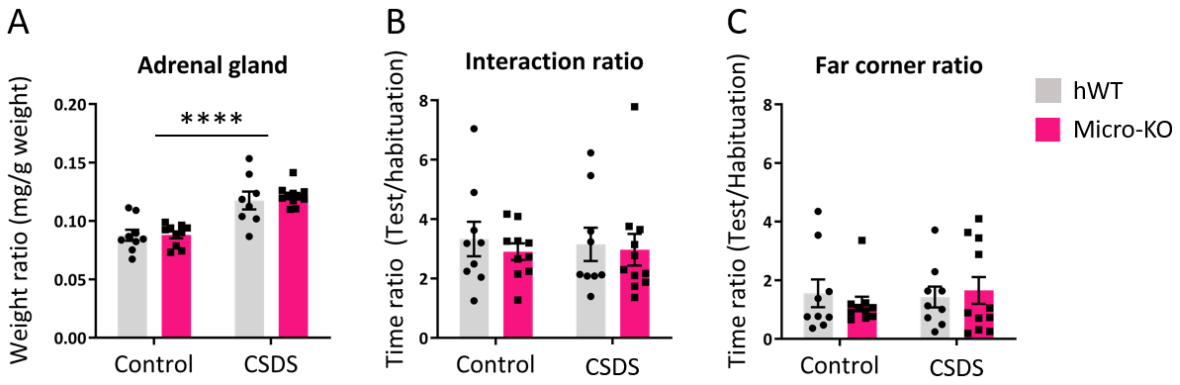

Figure 21. Validation of the CSDS in hWT and micro-KO mice. (A) Weight ratio of the adrenal glands under baseline and CSDS conditions. This value was normalized with the body weight of each animal. (B) Ratio of the interaction time with a novel mouse in the SAT. (C) Ratio of the time spent in the far corner, away from the interaction area in the SAT. Ratios in the SAT were calculated dividing the time spent in the field of interest during the test phase by the same value during the habituation phase for each individual. Data is represented as mean ± SEM. Two-way ANOVA (nhWT:8, nhKO:11). Stress effect ****: p<0.0001.

The CSDS paradigm had a significant effect on anxiety parameters, specifically the total distance covered (Two-way ANOVA, stress F (3, 35) = 6.26; p=0.0016) (Figure 22 A), the time in the center area (Two-way ANOVA, stress F (1, 35) = 29.67; p<0.0001) (Figure 22 B), and the number of entries to the center in the OFT (Two-way ANOVA, stress F (1, 35) = 46.02; p<0.0001) (Figure 22 C); as well as the time spent in the open arms (Two-way ANOVA, stress F (1, 35) = 4.92; p<0.0001) (Figure 22 D), and the number of entries to the open arms (Two-way ANOVA, stress F (1, 35) = 19.26; p=0.0001) (Figure 22 E), while the latency to visit the open arms in the EPM was unaffected (Figure 22 F). Furthermore, coping mechanisms were also affected by the CSDS, specifically the immobility time (Two-way ANOVA, stress F (1, 32) = 48.79; p<0.0001) (Figure 22 G), the time spent struggling (Two-way ANOVA, stress F (1, 34) = 4.93; p=0.0332) (Figure 22 H), and the time spent swimming in the FST (Two-way ANOVA, stress F (1, 34) = 10.57; p=0.0026) (Figure 22 I).

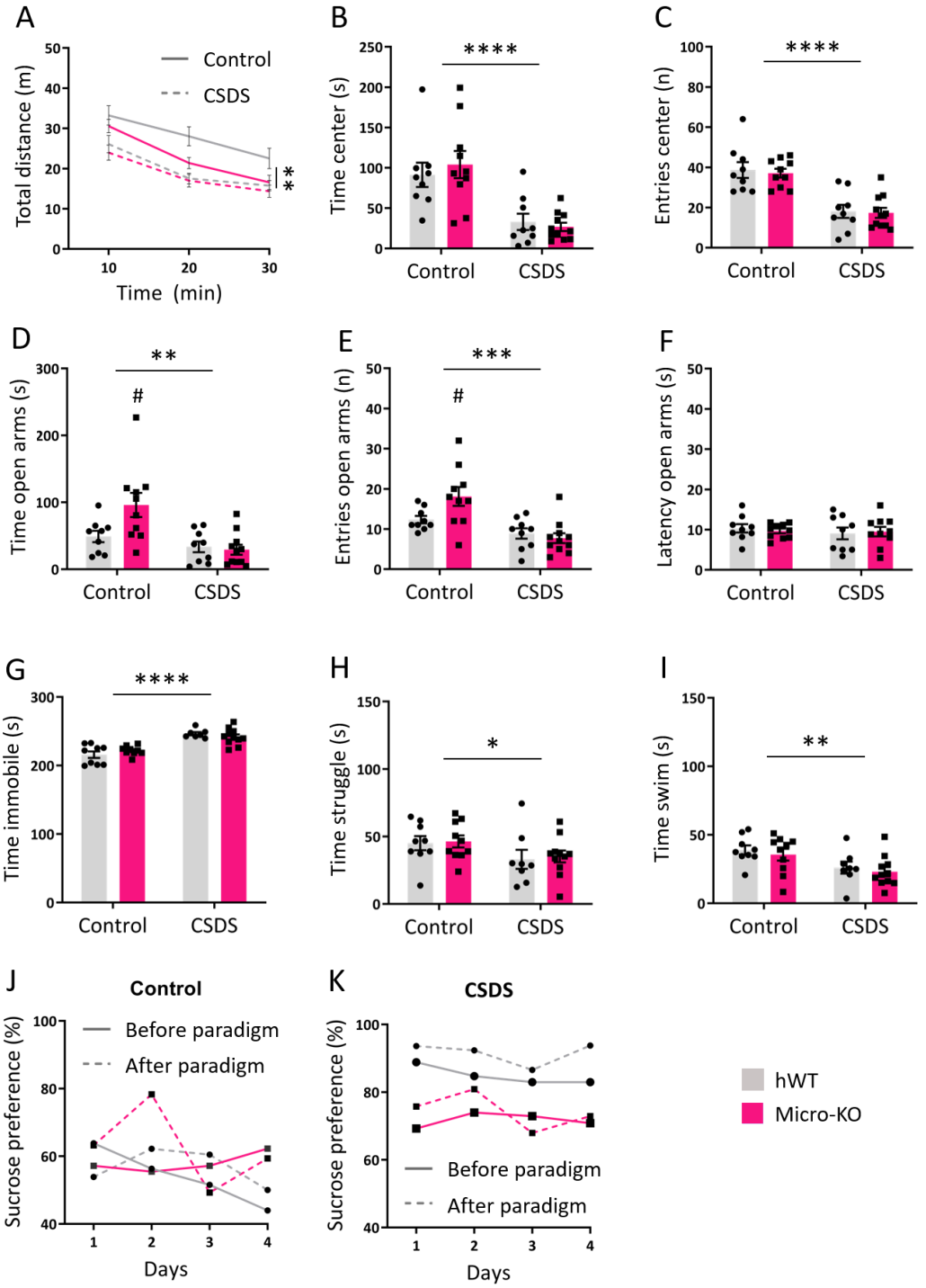

Figure 22. Behavioral assessment of hWT and micro-KO mice subjected to CSDS conditions. (A) Overall distance covered throughout the 30 minutes in 10-minute increments (CSDS values are indicated by dashed lines), (B) time spent in center in the first 10 minutes, and (C) entries to the center in the first 10 minutes of OFT. (D) Time spent in the open arms, (E) entries to the open arms, and (F) latency to the first entry to an open arm in the EPM. Time spent (G) floating, (H) struggling, and (I) swimming in the FST. (J) Daily sucrose preference during the 4 days of SPT in the control group before (full lines) and after (dashed lines) the behavioral assessment. (K) Daily sucrose preference during the 4 days of SPT in the CSDS group before (full lines) and after (dashed lines) the stress paradigm and behavioral assessment. Data is represented as mean ± SEM. Two-way ANOVA (n_{hWT}=8, $n_{micro\text{-}KO}$=11) Stress effect *: p<0.05; **: p<0.01; ***: p<0.001; ****: p<0.0001. Genotype effect #: p<0.05.

A SPT was carried out on the same mice before and after the behavioral assessment and stress paradigm. As expected, sucrose preference did not vary significantly in the control group before and after the testing (Figure 22 J). However, chronic stress did also not differentially affect the sucrose preference (Figure 22 K).

An effect of inactivating P2X7R in microglia on assessed behavioral readouts was only observed in the EPM under control conditions, where the micro-KO mice showed an increased time spent in the open arms (Two-way ANOVA, stress x genotype $F(1, 35) = 4.92$; $p=0.0332$; Bonferroni post hoc test $p<0.05$) (Figure 22 D), as well as an increased number of entries to the open arms (Two-way ANOVA, stress x genotype $F(1, 35) = 4.84$; $p=0.0345$; Bonferroni post hoc test $p<0.05$) (Figure 22 F). It is notable that this difference was not observed in the previous battery of behavioral experiments carried out on the micro-KO mice (Figure 20 C-D). From this data it was inferred that microglia-specific inactivation of P2X7R does not produce a significant change in the anxiety- and depressive-like parameters that were measured under CSDS conditions.

7.3 *Characterization of P2X7R overexpressing mouse lines - P2X7-EGFP and sEGFP*

7.3.1 *Analysis of mRNA expression in P2X7-EGFP and sEGFP mice*

The sEGFP mouse line has been employed for over a decade to study the expression pattern of P2X7R in the CNS. However, a comprehensive, thorough study to validate the correct functioning of this reporter mouse was never carried out. Given the nature of BAC transgenic mouse lines, they can present unexpected expression patterns depending on the genomic area covered by the BAC construct, the site of integration, and number of construct copies integrated. Before using a BAC transgenic line, it is fundamental to study the expression of the reporter in comparison to the endogenous expression pattern. Therefore, it was considered highly relevant to analyze the sEGFP mouse line in terms of expression of P2X7R, EGFP as well as P2X4R. P2X4R is the closest relative of P2X7R among the P2X family members. This fact is also reflected by their location in the immediate vicinity on mouse chromosome 5. Therefore, the BAC construct used to generate sEGFP mice also comprises P2X4R. It was decided to compare it to the more recently produced P2X7-EGFP mouse line, given the significant differences in expression pattern that had been observed in these models in previous studies (Kaczmarek-Hajek et al., 2018).

To compare the expression pattern and region-specific expression levels of EGFP, P2X7R, and P2X4R transcripts in the two transgenic lines, ISH analysis was performed. This assay revealed a clear EGFP signal and increased P2X7R mRNA levels throughout the brain of both the P2X7-EGFP (Unpaired T-test; P2X7R: p=0.038; EGFP: p=0.0062) and the sEGFP mice (Unpaired T-test; P2X7R: p=0.0445; EGFP: p=0.0137) in comparison to their respective WTs (Figure 23 A). EGFP expression was in full agreement with endogenous P2X7R expression in the P2X7-EGFP mice (Figure 23 B). In contrast, both the EGFP and P2X7R expression patterns in the sEGFP mouse line showed a very prominent signal in the lateral septum, dentate gyrus, and superior colliculus which deviated from the endogenous expression pattern in WT mice (Figure 23 B). Similarly, a strong overexpression of P2X4R transcripts was detected in these areas as well as throughout the brain in the sEGFP mice (Unpaired T-test; P2X4R: p=0.0052), which is not observed in WT or P2X7-EGFP mice (Figure 23 A).

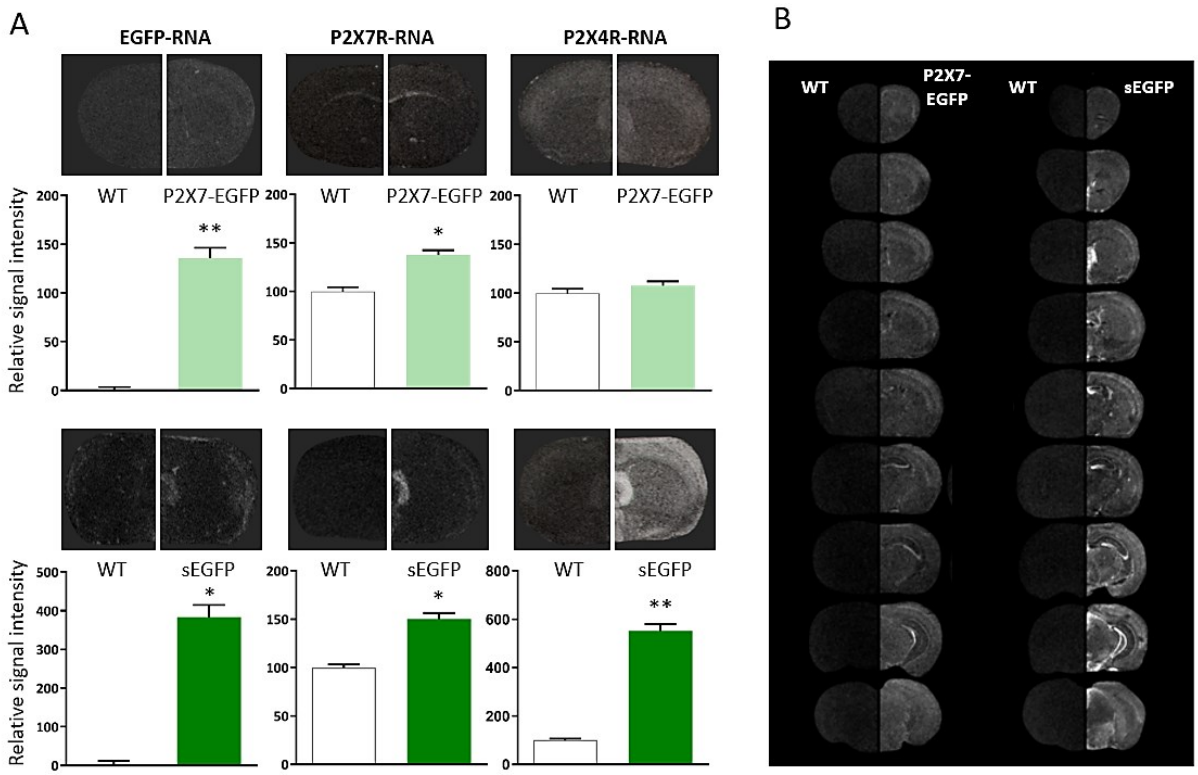

Figure 23. EGFP, P2X7R and P2X4R mRNA expression patterns in the sEGFP and P2X7-EGFP mouse lines. (A) Representative coronal brain sections (Bregma 0.62 approximately) showing the expression pattern of EGFP (left), P2X7R (middle) and P2X4R (right). Below each section, the average intensity measured in 12 representative sections throughout the brain of three animals per group. Background noise was subtracted, and resulting values were normalized with those of the WT animals for each group. Bars represent mean ± SEM. Unpaired T-test (n=3) *: p<0.05; **: p<0.01. (B) EGFP mRNA expression comparison between WT mice and the P2X7-EGFP (left) and sEGFP (right) mouse lines. Coronal sections correspond to Bregma 2.245, 1.345, 0.845, -0.48, -1.155, -2.055, -2.55, -3.88 approximately.

A more detailed analysis of P2X7R and P2X4R expression levels in different brain regions by region-specific RT-qPCR revealed upregulation of P2X7R and not P2X4R mRNA, as well as a relatively even distribution of P2X7R and P2X4R transcripts in all investigated brain regions of the P2X7-EGFP mouse (Figure 24 A). However, both P2X4R and P2X7R levels in the sEGFP mouse were upregulated and varied considerably between regions (P2X7R: two to tenfold, P2X4R: five to eleven-fold) with lowest expression of both genes in the thalamus and highest expression in the prefrontal cortex and cerebellum (Figure 24 A). To understand whether the P2X7R and EGFP expression patterns observed by ISH is translated into protein expression, an antibody staining against EGFP was performed. While the EGFP staining pattern was homogenous in P2X7-EGFP transgenic mice, staining of sections of the sEGFP mouse showed a clear signal in the lateral septum, as well as in cortical layers, confirming the mRNA expression pattern observed by ISH (Figure 24 B).

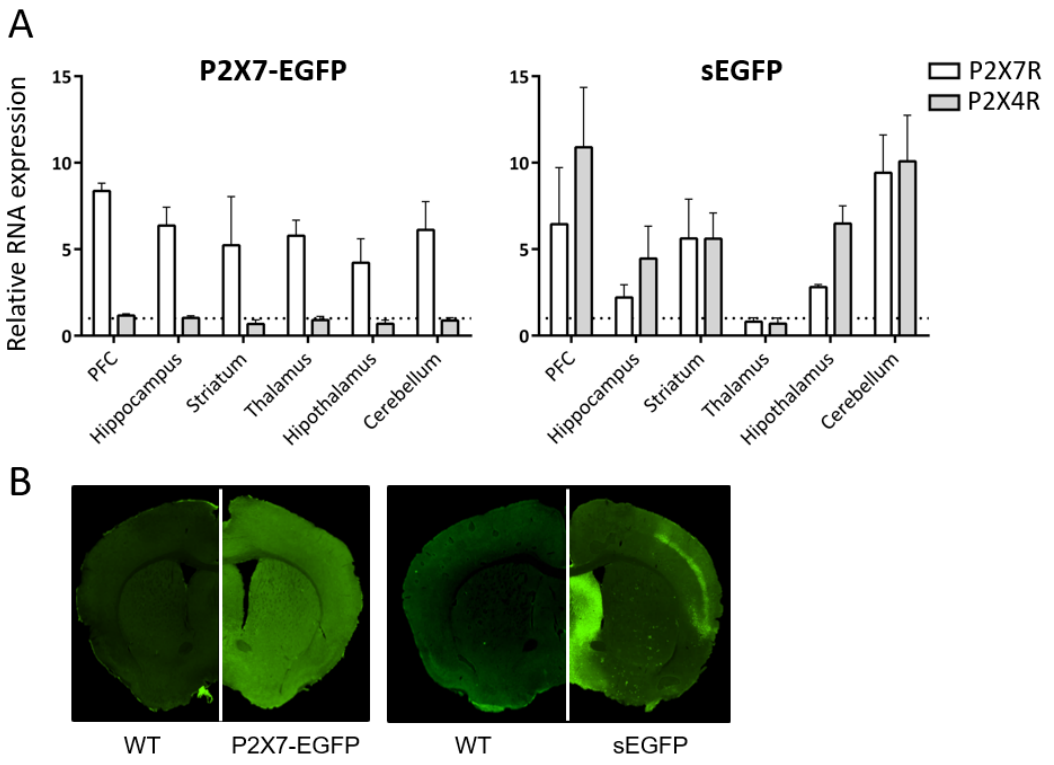

Figure 24. EGFP, P2X7R and P2X4R region-specific expression patterns in the sEGFP and P2X7-EGFP mouse lines. (A) RT-qPCR analysis of P2X7R and P2X4R levels in specific brain regions of the P2X7-EGFP (left) and sEGFP (right) mice. RNA levels were normalized to levels in WT animals as well as a housekeeping gene (HPRT) which corresponds to the dotted line. Bars represent mean ± SEM (n=3). (B) Immunofluorescence staining for EGFP in coronal sections (Bregma 0.62 approximately) from P2X7-EGFP (left) and the sEGFP (right) mice.

7.3.2 *Characterization of EGFP-expressing cells in sEGFP mice*

The expression pattern of P2X7R in the sEGFP mouse was further elucidated by analyzing brain sections, corresponding to the dentate gyrus, stained against EGFP and a cell type-specific marker: IBA1 for microglia, NeuN for neurons and Olig2 for oligodendrocytes. The confocal images were provided by the "Ion Channel Receptors" research group at the Walter Straub Institute of Pharmacology and Toxicology. Co-expression analysis was automatized with the software Strataquest (Tissuegnostics). It was observed that 83.43% of GFP positive cells are neurons, while virtually no microglia nor oligodendrocytes were expressing the reporter (Figure 25).

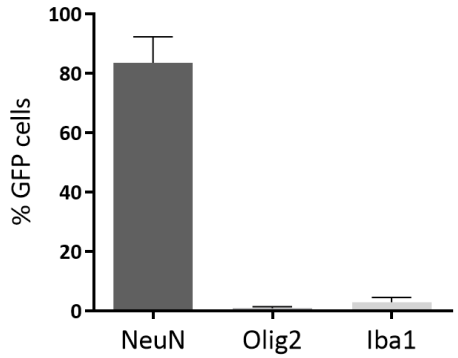

Figure 25. Automated coexpression analysis between cell-specific markers and EGFP in the sEGFP mouse line. Three representative sections from the dentate gyrus were automatically analyzed per animal. Bars represent mean ± SEM (n=3).

7.3.3 *Behavioral analysis of the P2X7-EGFP mouse line under baseline conditions*

There are many publications investigating the impact of P2X7R inactivation on anxiety- and depressive-like behaviors. However, the consequence of receptor overexpression has not been investigated in this context. To ascertain whether an elevated presence of the P2X7R can lead to behavioral changes under baseline conditions, the P2X7-EGFP mouse line was employed. This mouse line contains 15 copies of the P2X7-EGFP construct (Kaczmarek-Hajek et al., 2018) and, as previously confirmed, overexpresses the fusion protein in a homogeneous fashion throughout the brain, mirroring the P2X7R expression pattern that occurs in the WT animals (Figure 23).

A HCL test was carried out, which revealed that the P2X7-EGFP mice did not show a significant alteration in the activity patterns neither during the day nor the night cycle (Figure 26 A-B). To verify if overexpression of P2X7R could lead to any changes in anxiety- or depressive-like behaviors, the P2X7-EGFP mice were analyzed under baseline conditions. In the OFT, the P2X7-EGFP presented higher locomotion in the second fragment of the test (Two-Way ANOVA, genotype x time $F(1, 26) = 3.38$; $p=0.0418$; Bonferroni post hoc test $p<0.05$) (Figure

27 A) and a significantly higher number of entries to the center area (Unpaired T-test; p=0.0388) (Figure 27 C).

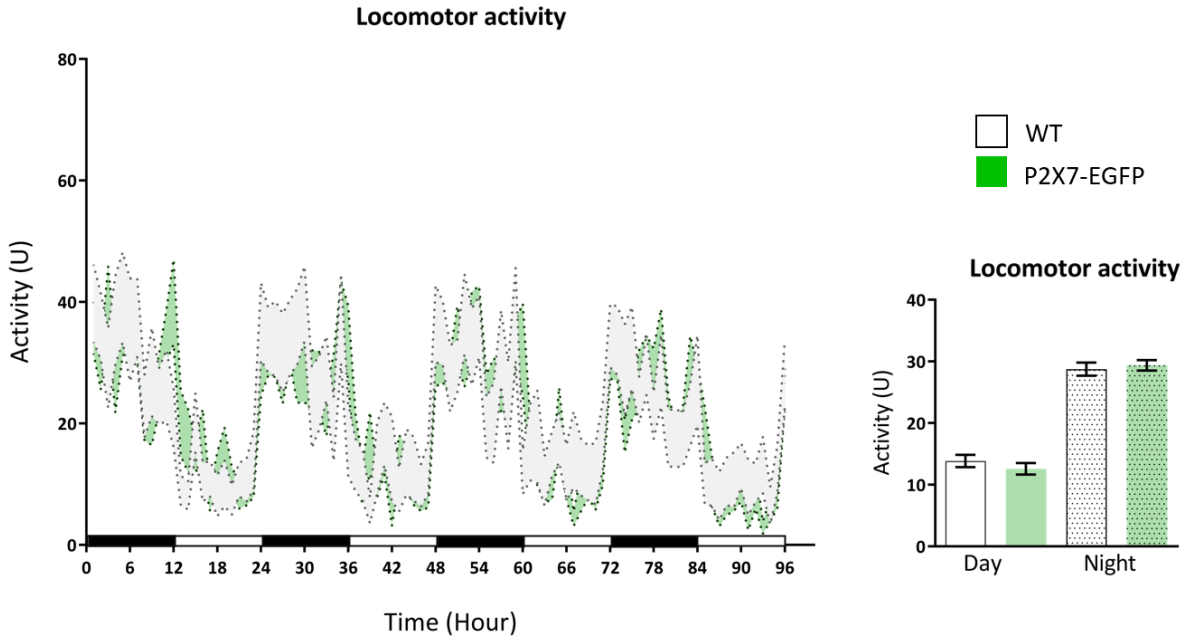

Figure 26. Home cage locomotor activity of the P2X7-EGFP mice. (A) Representation of the hourly locomotor activity throughout 72 hours. White and black bars at the bottom represent day and night hours respectively. (B) Average activity during the day and night cycles. Data is represented as mean ± SEM (n_{WT}:13, $n_{P2X7\text{-}EGFP}$:16).

However, these mice did not present a differential time spent in the center (Figure 27 B). Furthermore, overexpression of P2X7R did not have an impact on other anxiety parameters, such as the time spent in the open arms (Figure 27 D), the number of entries to the open arms (Figure 27 E) or the latency to the first open arm entry in the EPM (Figure 27 F); and neither on the time spent in the lit compartment (Figure 27 G), the latency to the first exit to this area (Figure 27 H) or the number of entries to the lit box in the LDB (Figure 27 I). Anhedonic behavior was also unaltered, as shown by the latency to the first eating event (Figure 27 J), the time spent eating (Figure 27 K) and the number of eating events in the NSF (Figure 27 L); along with the sucrose preference in the SPT (Figure 27 M-N). Finally, coping parameters were not significantly different in the P2X7-EGFP mice, as can be observed in the time spent in immobility (Figure 27 O), struggling (Figure 27 P), or swimming in the FST (Figure 27 Q).

It is inferred from this data, that overexpression of P2X7R in endogenous sites causes a limited effect on anxiety behavior, and no measurable effect on locomotion, anhedonia, and coping behaviors under baseline conditions.

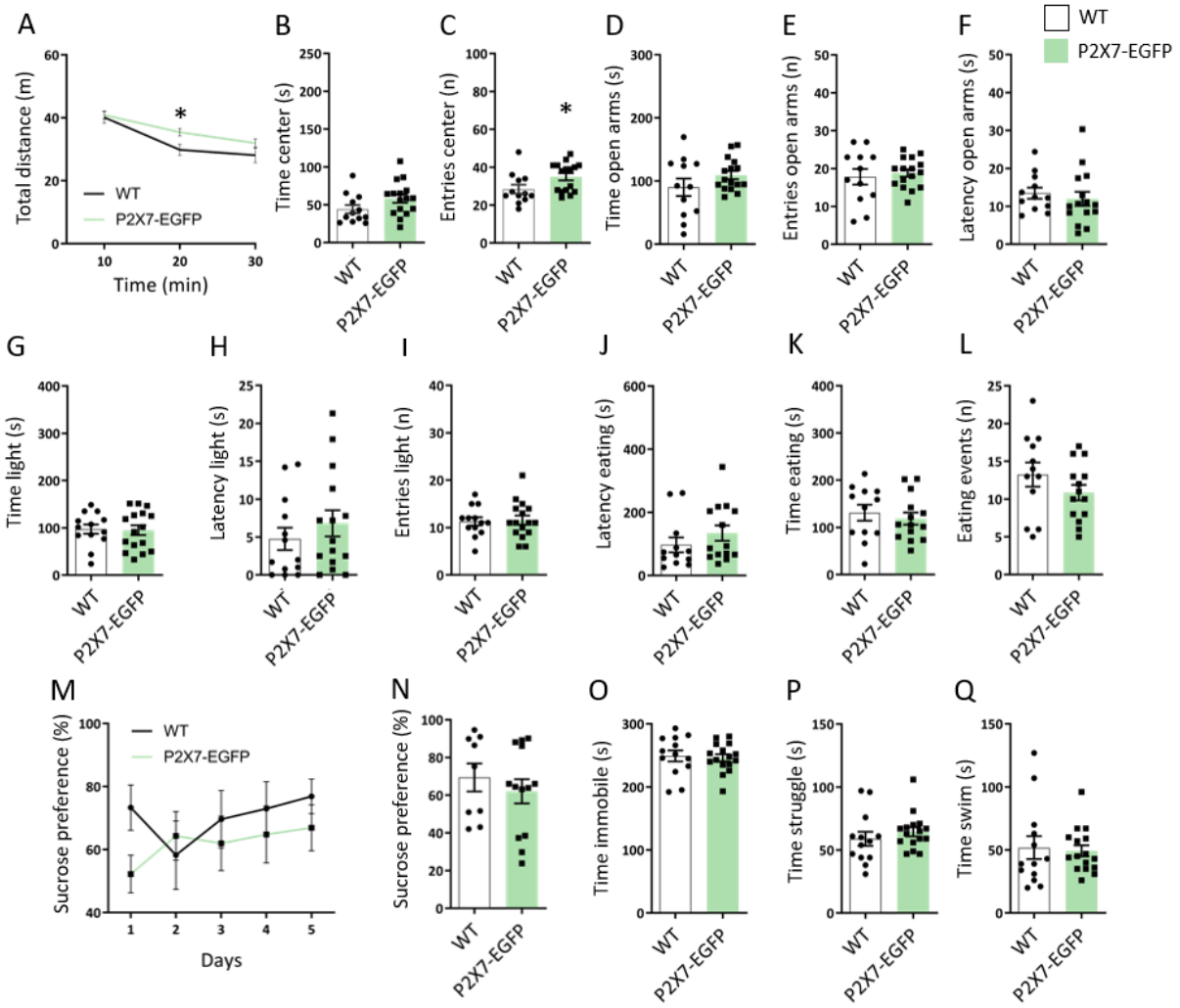

Figure 27. Assessment of anxiety- and depressive-like in P2X7-EGFP mice under baseline conditions. (A) Total distance covered throughout the 30 minutes in 10 min intervals, (B) time spent in center in the first 10 minutes, and (C) entries to the center in the first 10 minutes of OFT. (D) Time spent in the open arms, (E) entries to the open arms, and (F) latency to the first entry to an open arm in the EPM. (G) Time spent in the lit compartment, (H) latency to the first entry to the lit compartment, and (I) number of entries to the lit compartment in the LDB. (J) Latency to the first eating event, (K) time spent eating, and (L) number of eating events in the NSF. (M) Daily sucrose preference during the 5 days of SPT. (N) Average sucrose preference throughout the SPT. Time spent (O) floating, (P) struggling, and (Q) swimming in the FST. Data is represented as mean ± SEM. Two-way ANOVA (n_{WT}:13, $n_{P2X7\text{-}EGFP}$:16). Genotype *: $p<0.05$.

7.3.4 *Behavioral analysis of the sEGFP mouse line under baseline conditions*

Following the same direction as the P2X7-EGFP mouse line, it was decided to employ the sEGFP as an alternative P2X7R overexpression model to assess the effects of this phenomenon on anxiety- and depressive-like phenotypes. In this case, the sEGFP mouse is overexpressing P2X7R in an ectopic pattern compared to the WT animals, and simultaneously overexpresses P2X4R (Figure 23 B) (Ramírez-Fernández et al., 2020). The established set of behavioral tests was carried out in these mice under baseline conditions.

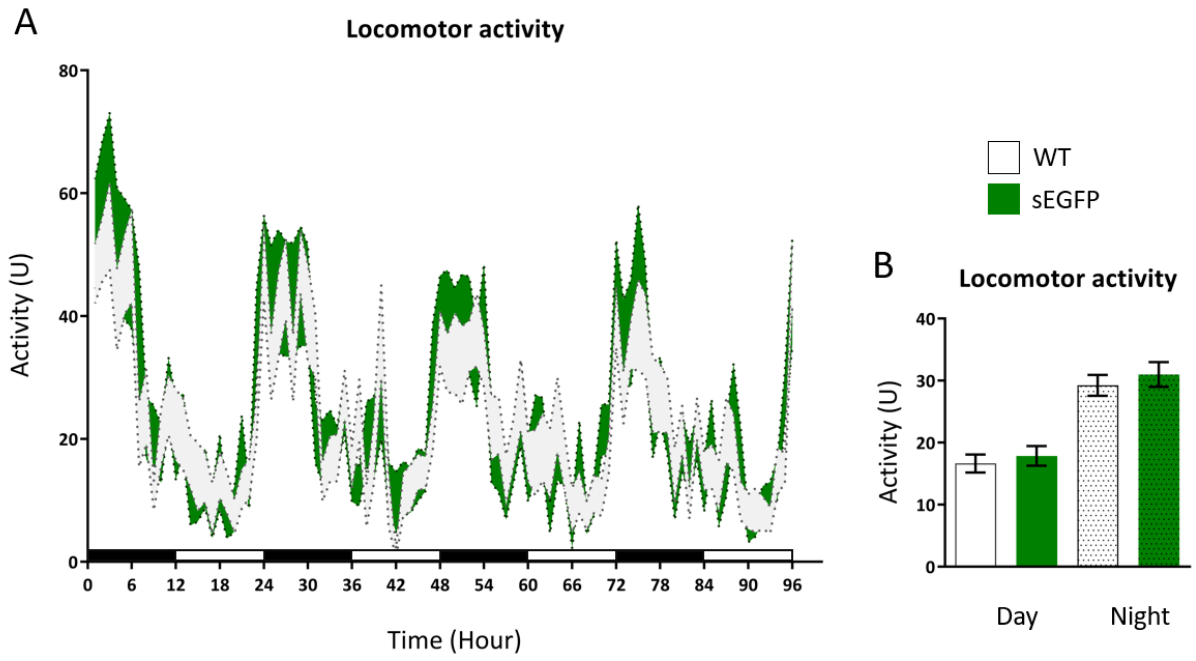

Figure 28. Home cage locomotor activity of the sEGFP mice. (A) Representation of the hourly locomotor activity throughout 72 hours. White and black bars at the bottom represent day and night hours respectively. (B) Average activity during the day and night cycles. Data is represented as mean ± SEM (n_{WT}:17, n_{sEGFP}:16).

The HCL test showed that the sEGFP mice do not present an alteration of their home cage locomotion neither during the day nor the night cycles (Figure 28 A-B). In terms of anxiety phenotypes, overexpression of P2X7R and P2X4R did not alter the parameters measured in the OFT: total distance covered (Figure 29 A), time spent in the center area (Figure 29 B), and number of entries to the center (Figure 29 C); in the EPM: time spent in the open arms (Figure 29 D), number of entries to the open arms (Figure 29 E), and latency to the first entry to an open arm (Figure 29 F); or in the LDB: time spent in the lit area (Figure 29 G), latency to the first entry to this area (Figure 29 H), and number of entries to the lit box (Figure 29 I). Anhedonic behavior was also unaltered in the sEGFP mice, as shown by the parameters

measured in the NSF: latency to first eating event (Figure 29 J), time spent eating (Figure 29 K), and number of eating events (Figure 29 L); as well as in the SPT (Figure 29 M-N). Although immobility time did not significantly vary in the sEGFP mice (Figure 29 O), the time spent struggling was elevated in these mice (Unpaired T-test; p=0.014) (Figure 29 P), and the time spent swimming was significantly decreased (Unpaired T-test; p=0.0004) (Figure 29 Q).

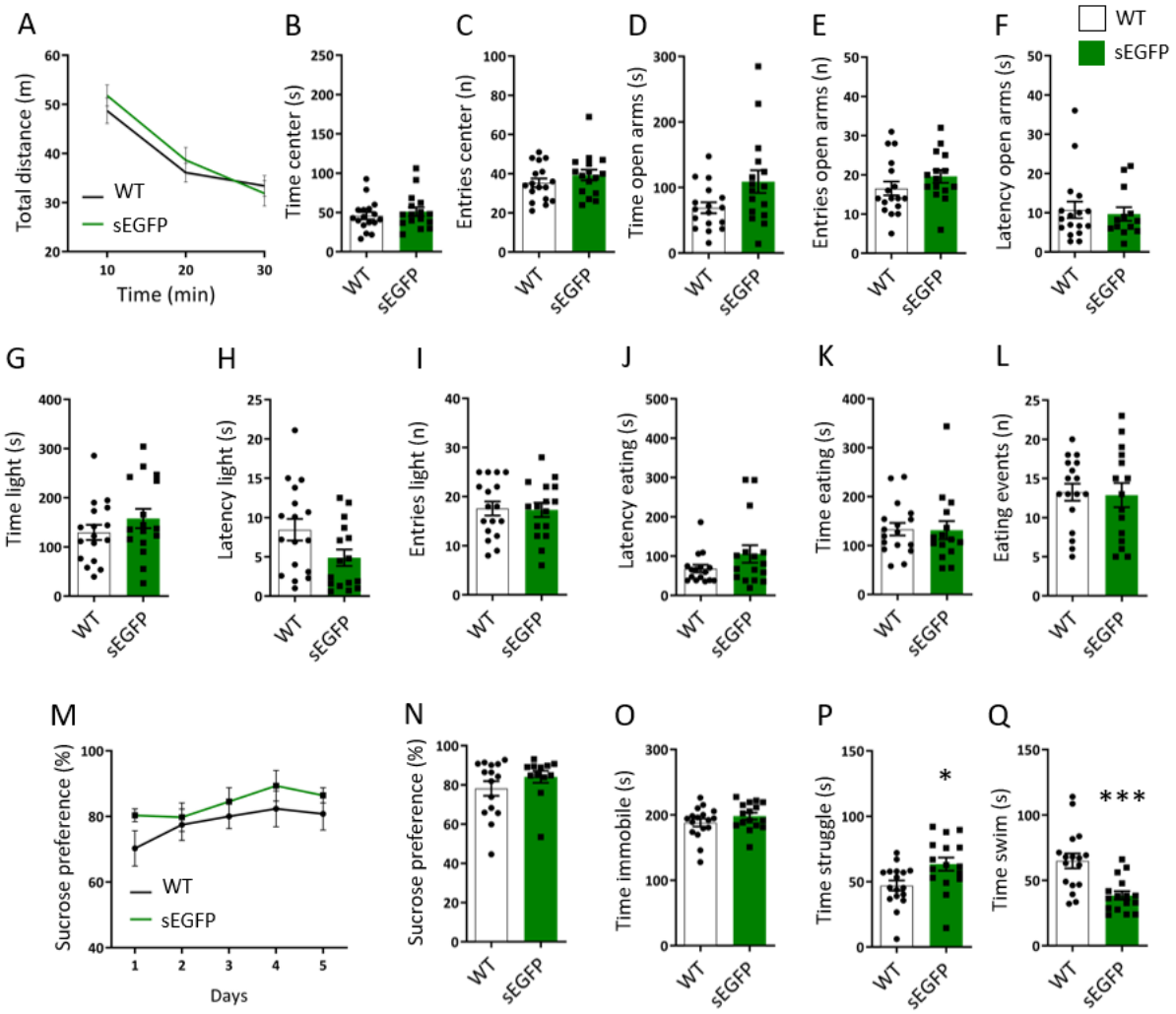

Figure 29. Assessment of anxiety- and depressive-like behavior in sEGFP mice under baseline conditions. (A) Total distance covered throughout the 30 minutes in 10 min intervals, (B) time spent in center in the first 10 minutes, and (C) entries to the center in the first 10 minutes of OFT. (D) Time spent in the open arms, (E) entries to the open arms, and (F) latency to the first entry to an open arm in the EPM. (G) Time spent in the lit compartment, (H) latency to the first entry to the lit compartment, and (I) number of entries to the lit compartment in the LDB. (J) Latency to the first eating event, (K) time spent eating, and (L) number of eating events in the NSF. (M) Daily sucrose preference during the 5 days of SPT. (N) Average sucrose preference throughout the SPT. Time spent (O) floating, (P) struggling, and (Q) swimming in the FST. Data is represented as mean ± SEM. Unpaired T-Test (n_{WT}:17, n_{sEGFP}:16). Genotype ***: p<0.001; *: p<0.05.

These results show that ectopic overexpression of P2X7R, accompanied by parallel overexpression of P2X4R does not have any impact on locomotion, anxiety, and anhedonia, and has a limited influence on coping behaviors under baseline conditions.

7.3.5 *Analysis of murine P2X7R mRNA splice variant expression*

Studies of the expression pattern of P2X7R in humanized mice showed specific P2X7R mRNA expression in the CA3 of the hippocampus, which had previously been assigned to glutamatergic neurons (Figure 30 A)(Metzger et al., 2017). This pattern reflects the endogenous P2X7R expression pattern observed in the hippocampus of WT mice (Metzger et al., 2017, https://mouse.brain-map.org/experiment/show/75551477). In this transgenic mouse line, the introduction of the human cDNA covering exon 2-13 at the position of mouse exon 2, which is followed by a strong transcriptional terminator, prevents the expression of all endogenously active murine splice variants. Therefore, the signal that was observed in the CA3 of the hWT animals corresponded to the humanized P2X7R-A variant.

On the other hand, previously published IHC analysis of the P2X7-EGFP mice did not show an elevated EGFP signal in the CA3 region, or colocalization with neuronal markers in this area (Kaczmarek-Hajek et al., 2018; Ramírez-Fernández et al., 2020). The BAC construct used to generate the P2X7-EGFP mouse line integrates the EGFP directly at the C-terminus of the P2X7R. Thus, this conformation allows only monitoring of the P2X7R splice variants A and K but not of variants, B, C or D as they will not contain the EGFP reporter. Therefore, it was decided to analyze whether this difference with the hWT and P2X7-EGFP mice could be due to alternative variant expression in the P2X7-EGFP mice. To understand the expression levels of the different variants in the brain, an analysis of all the murine variants was carried out in cortex samples. It was observed that variants A and C presented a relatively high expression, while the transcripts for the B, D and K variants were virtually not present (Figure 30 B). To validate these results, a nested PCR amplification was carried on the same samples confirming the low expression of B and D variants in the brain which were only detectable after another round of PCR amplification (Figure 30 C).

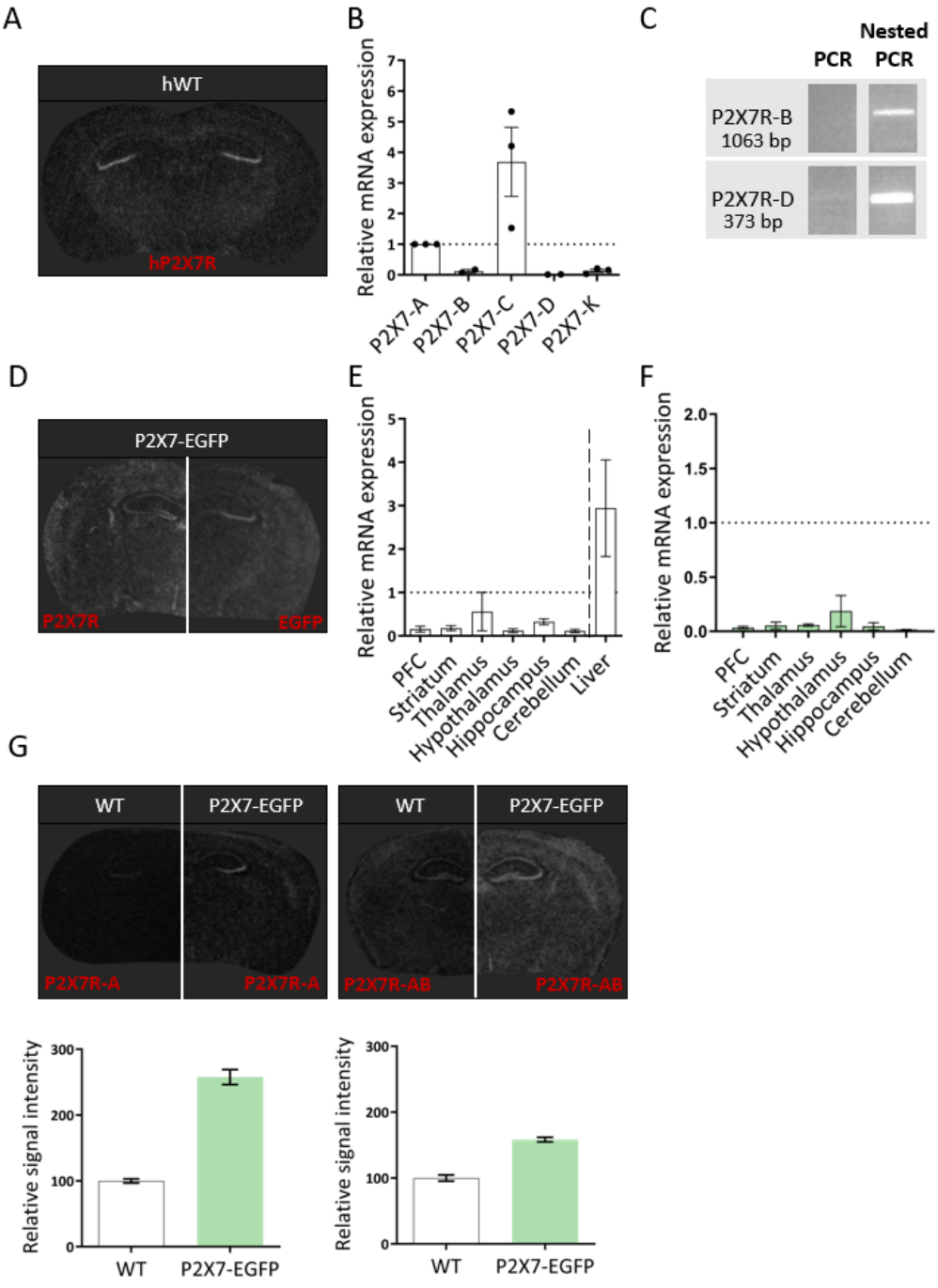

Figure 30. Analysis of the expression levels and pattern of the P2X7R and its splice variants. (A) Representative coronal section showing the mRNA expression pattern of hP2X7R mRNA in the hWT mouse line. (B) RT-qPCR analysis of the murine variants of P2X7R in WT cortex extracts (n=2-3). All variants were measured in PFC samples and normalized with the housekeeping gene HPRT, as well as to levels of P2X7R-A, which is marked in a dotted line (C) Standard (left) and nested PCR (right) for the B and D variants in cortex extracts. The size of the amplicons is shown under each variant's name. (D) Representative coronal section showing the mRNA expression pattern of P2X7R (left) and EGFP (right) mRNA in the P2X7-EGFP mouse line. (E-F) RT-qPCR analysis of the A and K variants of P2X7R in WT and P2X7-EGFP cortex extracts (n=2-3). Samples were normalized with the housekeeping gene HPRT, as well as to levels of P2X7R-A, which is marked in a dotted line. (G) Representative coronal sections showing the mRNA expression of the A (left) and the A and B (right) variants in WT and P2X7-EGFP mice. Quantifications are shown in the graphs below. Bars represent mean ± SEM.

Although initial ISH assays failed to show the P2X7R and EGFP mRNA signal in the CA3 in the P2X7-EGFP mice, subsequent analyses were able to detect the CA3-specific signal in brains hybridized with the EGFP probe (Figure 30 D). Therefore, the detection of the EGFP signal in the CA3 region of P2X7-EGFP mice by ISH, strongly suggests that this expression is mainly based on the P2X7R A or K splice variants. To unveil which of these could be responsible for the CA3 signal, a RT-qPCR was carried out for these two variants throughout the brain. We could observe that the K variant was expressed at very low levels in all the regions measured, including the hippocampus in both WT and P2X7-EGFP mice (Figure 30 E-F). We also analyzed liver samples, where the K variant is known to be abundant validating the methodology (Figure 30 E). These results point towards the A variant as the source of signal in the CA3 region.

Following these assays, further ISH analyses were performed. However, due to the necessity for riboprobes of sufficient length for this experiment (around 800 bp) and the high similarity between the variants, there was only the possibility to create probes detecting specifically variant A, detecting both variants A and B, and detecting specifically variant C. The latter was a relatively short probe (around 200 bp) which ended up not producing enough signal to be detected. However, what could be observed was a clear signal in the CA3 with the A probe, even in the WT mouse, which was less prominent in the AB probe treated sample (Figure 30 G). Given the reduced amount of variant B in the brain, confirmed through our previous analysis, it was inferred that the visual difference in signal between the samples analyzed with the A and the AB probes, was not due to the presence of variant B in the brain. In fact, after normalizing with the background and the WT samples, the increase in P2X7R intensity was higher in the sample hybridized with the A specific probe, compared to the sample hybridized with the probe detecting variants A and B simultaneously.

These findings confirmed that the P2X7R signal in the CA3 region corresponds to the P2X7R-A variant. Furthermore, the results propose that the background noise was the main reason why the CA3-specific signal was less intense when employing the AB probe and why this signal was not previously detected with the P2X7R probe (Figure 30 D). However, the reason why the P2X7-EGFP mice do not present this CA3-specific signal at the protein level remains unanswered.

7.4 *Analysis of a novel P2X7-CreERT2 mouse line*

A P2X7-CreERT2 mouse line, which had been generated by the EUCOMMTOOLS program, was characterized, as it was expected to express CreERT2 and EGFP under the control of the P2X7R promoter. This mouse line would represent a valuable tool as it would provide genetic access to P2X7R expressing cells. Initial analysis of EGFP expression using immunohistochemistry revealed that EGFP co-localized exclusively with neuronal markers, but not with microglial, oligodendrocytic or astrocytic markers (Figure 31 A). Given the fact that P2X7R is known to be expressed in microglia, astrocytes, and oligodendrocytes but only scarcely in neurons, it was hypothesized that the reporter mouse was not working as expected.

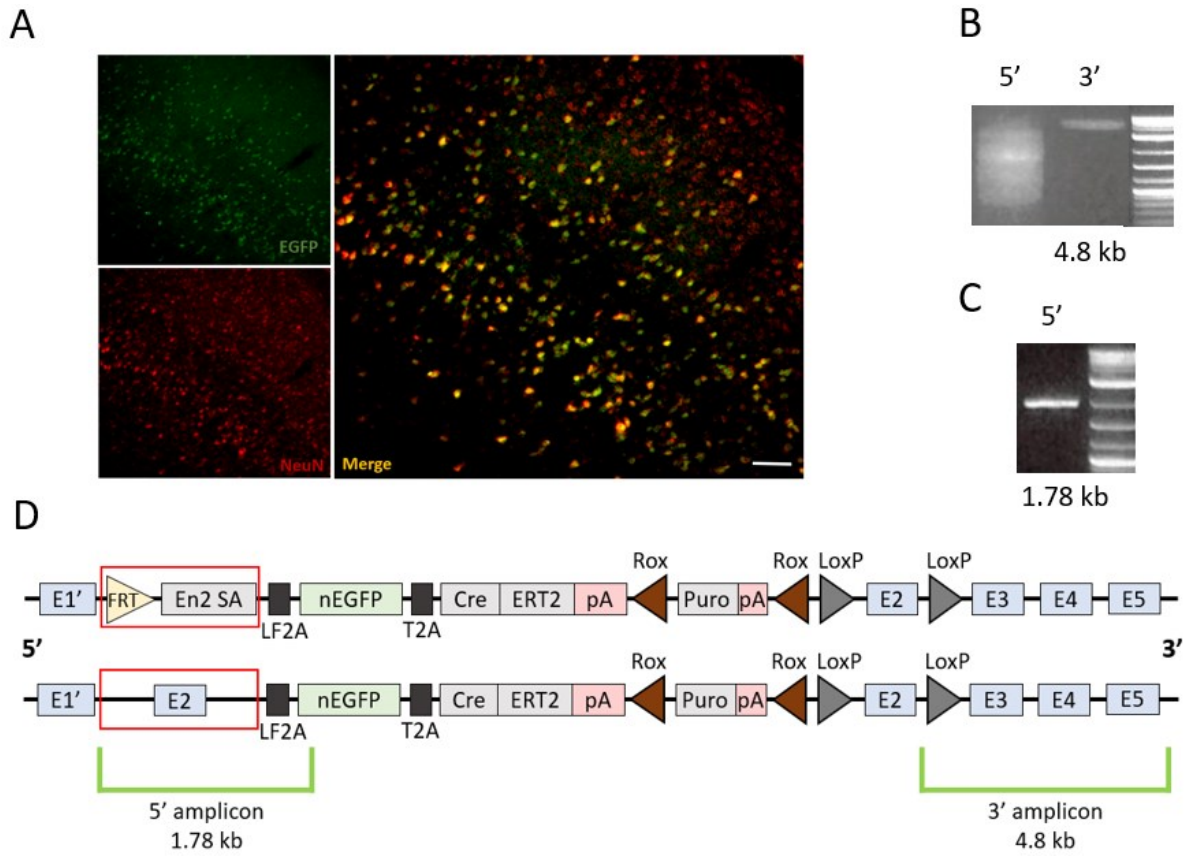

Figure 31. Analysis of the P2X7-CreERT2 mouse line. (A) Immunohistochemical analysis of the cortex region. Colocalization of EGFP (green) with neuronal marker NeuN (red). The scale bar corresponds to 200 µm. (B) Long-range PCR testing the 5´and 3´ insertion site of the transgenic construct. (C) Long range PCR with corrected primers for the 5' insertion site. (D) Scheme of the expected (top) and sequenced (bottom) fragments in the P2X7-CreERT2 mouse. In red the 5´area depicting the aberrant insertion of the targeting vector. In green marked the locations for the primers employed for the analysis of the insertion site, as well as the size of the amplicon. pA: poly A signal.

Along these lines, breeding of P2X7-CreERT2 mice to Ai9 reporter mice did not result in any TdTomato reporter gene expression following tamoxifen-treatment (data not shown). Therefore, the insertion site of the CreERT2 expression cassette in the P2X7R locus was analyzed in detail to detect possible errors during the production of this mouse line. A long-range PCR in the 5' and 3' regions of the insert was carried out. While the expected PCR amplicon of 4.8 kb was obtained in the 3' region, this was not achieved in the 5' region (Figure 31 B). As a consequence, it was questioned whether there was an issue with the insertion site in the 5' region. After a redesign of the primers on regions surrounding the problematic area (Figure 31 D, in red), the fragment was amplified and sequenced (Figure 31 C).

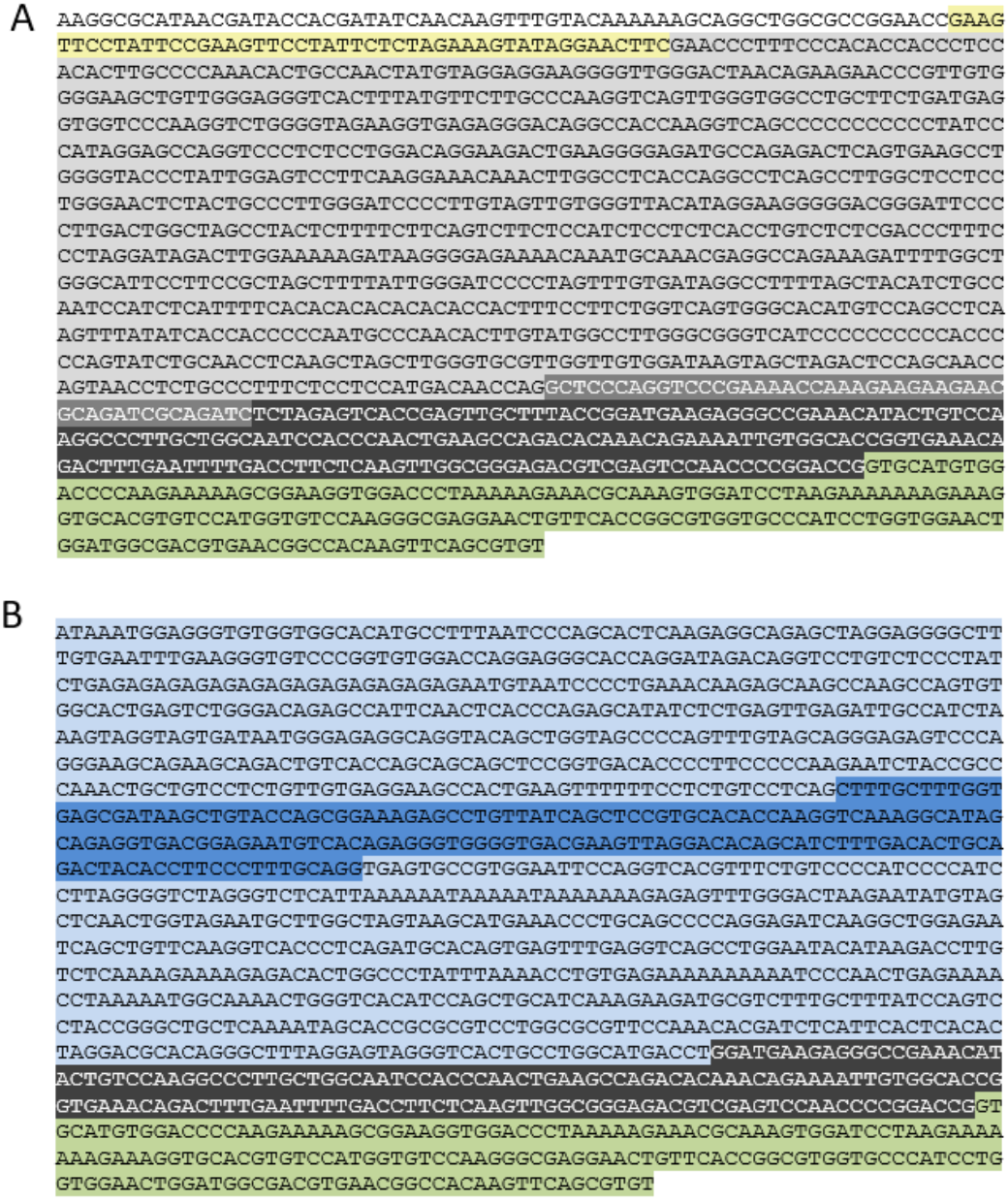

Figure legend on the next page

Figure 32. Expected and sequenced 5' fragment in the P2X7-CreERT2 mouse. (A) This 5' fragment was meant to be 1059 bp long and contain the FRT sequence (yellow), followed by the intronic and exonic regions for the EN2 splice acceptor (grey and dark grey respectively), the LF2A self-cleaving peptide (black), and finally the nEGFP sequence. (B) The sequencing result showed a 1135 bp long fragment containing the sequences for P2X7R intron 1 (light blue), exon 2 (dark blue) and intron 2 (light blue), followed by a partial LF2A and the nEGFP sequence.

The sequencing results showed that in the location where there was meant to be an FRT site and splice acceptor (En2 SA), there was a fragment of the P2X7R gene which included exon 2 suggesting an aberrant insertion involving partial duplication of the locus and 5´-deletions within the CreERT2 cassette (Figure 31 D, Figure 32). Consequently, correct in-frame splicing of P2X7R upstream exons to the CreERT2 cassette cannot occur, which explains why the transgenic mouse line was not functioning as expected.

8. Discussion

MDD is a highly prevalent disorder that affects millions of people worldwide and has a relatively high mortality rate, with an average of 1.4% worldwide (Bachmann, 2018). Although there is extensive research on the matter, only 30-50% of treated patients will experience full remission, while approximately 30 % of MDD patients will show no response to multiple therapeutic interventions, including newer generation antidepressants (Little, 2009; McIntyre et al., 2014). This leaves a great subset of the population suffering from treatment-resistant depression. Therefore, there is a clear need for new pharmacological compounds that may work either in a stand-alone manner, or in combination with currently available antidepressant treatments. A drug target that has been widely studied in the context of CNS pathology is the purinergic receptor P2X7. P2X7R is a ligand gated ion channel that has a key role in gatekeeping the immune response in the CNS (Savio et al., 2018). In the context of MDD, linkage analyses, as well as basic research conducted in rodents and human subjects, indicate that this receptor is potentially involved in the development of depression (reviewed in Ribeiro et al., 2019). Therefore, there is a need to understand the physiology and the pathophysiology of P2X7R to further substantiate whether it can be relied on as a drug target for MDD.

8.1 *The impact of P2X7R inactivation on anxiety- and depressive-like phenotypes*

8.1.1 *Analysis of humanized, full KO and microglia-specific P2X7R-KO mice*

There are numerous studies showing the impact of fully inactivating P2X7R on coping and anxiety phenotypes in mice (Basso et al., 2009; Boucher et al., 2011; Csölle, Andó, et al., 2013; Csölle, Baranyi, et al., 2013; Gao et al., 2018; Yue et al., 2017). Our first goal was to evaluate the replicability of these results in a full P2X7R-KO mice. To that end, a constitutive knockout mouse line based on the conditional humanized allele was generated by breeding to a Cre deleter line (hWT/hKO). Previous unpublished experiments carried out in our institute showed no effect of fully inactivating P2X7R on anxiety- nor depressive-like phenotypes under baseline conditions (Metzger, 2016). The limited effect of P2X7R inactivation on these phenotypes could be explained by the low impact of P2X7R activity on basal physiology. Therefore, it was hypothesized that induction of stress might be needed to unveil the potential effect of inactivating the receptor on behavioral readouts. Tests to assess locomotion, anxiety, stress coping and anhedonia were carried out on the humanized and full KO mice under acute and

chronic stress conditions. Acute stress did not reveal a differential behavioral response between hWT and hKO, and chronic social defeat stress (CSDS) caused moderate alterations in anxiety phenotypes, but not with regards to locomotion, anhedonia or coping behavior.

The relationship between inflammatory processes and depression in human subjects has been widely studied (Capuron & Miller, 2004; Dowlati et al., 2010; Köhler, Krogh, Mors, Benros, et al., 2016; Margaretten et al., 2011). Being P2X7R a key player in neuroinflammation, it was hypothesized that the activation of the receptor, namely in microglial cells, could have a significant role in the development of depressive-like symptoms. To evaluate this theory, a microglia-specific knockout mouse line was generated by breeding the conditional humanized P2X7R allele to Cx3cr1-CreERT2 mice. Compared to full, constitutive inactivation, cell type-specific inactivation of P2X7R has the benefit that blockade of the gene can be carried out during adulthood. This prevents unexpected compensatory mechanisms as a consequence of the absence of the receptor during development. Furthermore, inactivating P2X7R in a specific cell type allows to pinpoint the origin of the behavioral alterations and prevents potential pleiotropic effects resulting from a full inactivation. Assays using primary glial cell cultures derived from this mouse line proved the effectiveness of receptor inactivation upon tamoxifen treatment. P2X7R inactivation resulted in quantifiable physiological changes in microglia, such as a significant reduction in IL-1β secretion into the ECS, increased survivability and decreased morphological changes after exposure to the P2X7R agonist BzATP, with or without previous LPS priming.

To assess whether inactivation of microglial P2X7R expression could have an effect on anxiety- and depression-related phenotypes, locomotion, anxiety, stress coping behavior and anhedonia were evaluated in the microglia-specific P2X7R KO mice. The results obtained under baseline conditions proved that there was no significant effect caused by microglia inactivation of P2X7R on anxiety, stress coping behavior or anhedonia. However, mice lacking P2X7R in microglia presented an increase of overall locomotion in the home cage during the day and night cycles. Our next goal was to understand whether P2X7R could potentially have an impact on these behavioral readouts upon stress induction. Mice were subjected to CSDS, but no effects of P2X7R inactivation were observed when assessing anxiety phenotypes, coping behaviors or anhedonia under these conditions.

8.1.2 *Analysis of previously published P2X7R-KO studies*

Based on our findings, it cannot be confirmed that microglia-specific or full inactivation of P2X7R leads to a clear behavioral effect with respect to anxiety- or depressive-like phenotypes, neither in baseline nor chronic stress conditions. These results seem to contradict the previously published studies which proved that genetic inactivation or pharmacological inhibition of P2X7R could produce significant effects on some anxiety-related phenotypes (Table 13).

Upon thorough examination of these experiments, certain inconsistencies were detected, which are worth mentioning. Some studies assert that pharmacological inhibition of P2X7R with Coomassie Brilliant Blue G (BBG) leads to a decrease of immobility time in the TST, as well as to a decrease of anhedonic behavior in the SPT (Csölle, Andó, et al., 2013; Csölle, Baranyi, et al., 2013). However, BBG is known to bind to targets other than P2X7R such as P2X1R and P2X4R, therefore producing unexpected effects that are not limited to P2X7R dependent pathways (Greve et al., 2017). One of these studies also included in their experiments a specific P2X7R inhibitor, AZ-10606120, which improved anhedonic behavior in WT animals, and not in KO mice (Csölle, Baranyi, et al., 2013). Nevertheless, this study did not provide any data whether this specific inhibitor had an impact on the immobility time in the TST, a readout that was tested in BBG treated animals.

In terms of genetic inactivation, while some studies note a strong impact of P2X7R inactivation on coping behaviors under baseline conditions (Basso et al., 2009; Csölle, Andó, et al., 2013; Csölle, Baranyi, et al., 2013), others indicate that these effects can only be observed upon repetition of the behavioral test on consecutive days (Boucher et al., 2011), upon induction of stress (Yue et al., 2017), or they present instances where the differences are not significant (Csölle, Andó, et al., 2013). As for anxiety-related phenotypes, there is also a discordance, with some studies presenting a decrease of anxiety in P2X7R-KO mice (Boucher et al., 2011) while others show increased anxiety (Yue et al., 2017), or do not show a significant difference between groups (Basso et al., 2009; Csölle, Andó, et al., 2013). It is also relevant to consider that the Pfizer mouse line, which was employed in at least half of these studies (Boucher et al., 2011; Csölle, Andó, et al., 2013; Csölle, Baranyi, et al., 2013), has been proven to express active isoforms of the P2X7R, which means that they cannot be considered as full P2X7R-KO mice (Masin et al., 2012; Nicke et al., 2009).

The inconsistency between the results obtained in these studies can have several origins. First of all, the intrinsic differences between animal models, housing conditions, stress paradigms or methodologies are a primary source of discrepancies. Additionally, while some of the studies specify the use of littermates in their experiments (Csölle, Andó, et al., 2013; Csölle, Baranyi, et al., 2013), others employed C57Bl6 mice as a control group (Boucher et al., 2011; Gao et al., 2018; Yue et al., 2017), or they used separate breedings from WT or KO homozygote parents, which originated from the same heterozygote crossing (Basso et al., 2009).

Not employing littermates in these experiments has two main drawbacks. First of all, mice born from different breeding pairs could show epigenetic and environmentally-originated differences, independent from the genetic alteration that is being analyzed (Holmdahl & Malissen, 2012). For example, individual housing conditions and unexpected stressful events during development could have an impact on the outcome of the behavioral experiments. Secondly, the genetic background of the animals can have an effect on their behaviors. Employing C57Bl6 mice as controls might unveil differences between groups that could be caused solely by the genetic background, and not by the introduced gene modification (Bygrave et al., 2004; Holmdahl & Malissen, 2012). These two factors can influence the behavioral outputs and should be considered when contrasting experiments that use separate breedings for their control and subject groups. Using littermates should be the standard procedure, as it ensures that both the genetic and environmental backgrounds are comparable between groups.

Another aspect that can have an impact on the behavioral outcome of an experiment is the age and sex of the animals. The publications that specify the age of the subjects, employ mice from 2 to 5 months old. However, a study carried out in a CRISPR-induced P2X7R-KO line, shows that young, adult, and aged mice present different responses to P2X7R inactivation. While the young KO (2-month-old) present an increase in passive coping behavior and anhedonia, the adult (10-month-old) and old mice (18-month-old) present a reduction in both of these readouts upon inactivation of P2X7R (Gao et al., 2018). Furthermore, the sex of the mice employed for the behavioral experiments can also impact the baseline readouts, as well as the response to the different conditions. It is known that male and female mice can have significantly different baseline and anxiety responses (Davis et al., 2021; Lovick & Zangrossi, 2021). Additionally, the estrous cycle in female mice was found to significantly impact behavioral outcomes in anxiety, exploratory behavior and coping mechanisms (Lovick &

Zangrossi, 2021; Meziane et al., 2007; Palanza et al., 2001). All publications employing P2X7R-KO in the context of anxiety and depression are summarized in Table 13.

Table 13. Summary of all publications regarding P2X7R inactivation in murine models

Source	Mice	Results		
		Anxiety	Passive coping	Anhedonia
(Basso et al., 2009)	· Lexicon Genetics KO · 3-5 months · Males · Not littermates (P2X7 $^{+/+}$)	OFT: = EPM: =	FST: ↓ TST: ↓	NSF: =
(Boucher et al., 2011)	· Pfizer KO · 2-3 months · Females · Not littermates (C57Bl/6)	LDB: = EPM: ↓	FST: ↓ (days 2 and 3)	Not tested
(Csölle, Baranyi, et al., 2013)	· Pfizer KO / BBG and AZ-10606120 · 2-3 months · Males · Littermates (P2X7 $^{+/+}$)	Not tested	TST: ↓ (BL); ↓ (LPS)	SPT: = (BL); ↓ (LPS); ↓ (WT-BBG); ↓ (WT-AZ)
(Csölle, Andó, et al., 2013)	· Pfizer KO / BBG · 2-3 months · Males · Littermates (P2X7 $^{+/+}$)	OFT: = (BL) EPM: = (BL)	FST: = TST: ↓ (KO); ↓ (WT-BBG)	Not tested
(Yue et al., 2017)	· Unspecified KO · Age unspecified · Males and females · Not littermates (C57Bl/6)	OFT: = (BL); = (CUS) EPM: ↑ (BL); = (CUS)	FST: = (BL); ↓ (CUS)	Not tested
(Gao et al., 2018)	· CRISPS-Cas P2X7R deletion · 2-month (Y), 10-month (A), and 18-month-old (O) · Females · Not littermates (C57Bl/6)	OFT: = (Y); = (A); = (O)	FST: ↑ (Y); ↓ (A); ↓ (O)	FST: ↑ (Y); ↓ (A); ↓ (O)

"=": no significant difference. "↑": phenotype is elevated. "↓":phenotype is reduced. BL: baseline conditions. AZ: treated with AZ-10606120; CUS: chronic unpredictable stressors.

8.1.3 *The strengths of this study*

Throughout this project, it was attempted to emulate and expand the previous studies, while maintaining the highest standards of scientific practice to reduce the variability and increase the validity of the resulting data. All the mice that underwent behavioral analysis were males, and the experiments and analyses were carried out with the experimenter blinded to the genotype of each mouse, with all exclusion parameters decided beforehand. An extensive battery of behavioral tests was carried out to analyze different phenotypes that are often linked with depression (locomotion, anxiety, anhedonia, stress coping behavior), and all the parameters relevant to depressive-like behavior, which were decided in advance, were presented. Furthermore, in each experiment there was always a control group for every condition, composed by littermates of the subject group, which helped to both compare the results with the KO group and to assess whether the stress paradigms functioned as expected. This practice reduced the variability that can be manifested naturally between different batches of experiments due to unnoticed environmental factors.

Our first goal was to replicate the results obtained in previous publications with the full KO mouse line, which, in contrast to the Pfizer mouse, does not express active P2X7R splice variants. Furthermore, we also employed a conditional KO mouse line, which bears benefits over the constitutive KO lines. First, the production of a constitutive KO mouse line can give rise to physiological changes due to lack of P2X7R during development. Inhibiting the expression of the receptor throughout the span of a few weeks prevents the long-term physiological changes that could happen in constitutive KO mouse lines through unknown compensating mechanisms.

Although pharmacological inhibition could be a way to circumvent this problem, it is known that BBG, a compound used as a P2X7R inhibitor, does not present a high specificity for the receptor. This means that one cannot be certain that the behavioral effects observed are caused specifically by the blockade of P2X7R. Although one of the studies also used a specific P2X7R inhibitor, AZ-10606120, they did not present any data regarding coping mechanisms in the TST or the FST, as they did with BBG. Therefore, a conditional KO ensures that the P2X7R is inactive, and not presenting any residual activity in the CNS without having to consider off-target interactions, pharmacodynamics, or penetrance to the CNS. In addition, the creation of a cell type-specific KO line allowed to inactivate P2X7R, specifically in microglia. This guarantees that the effects that are observed are caused by the influence of this specific cell

type, avoiding pleiotropic effects that could arise from fully inactivating P2X7R in the whole organism.

8.1.4 *Outlook and future directions*

Our aim in this project was to create a valid paradigm to assess the impact of P2X7R in anxiety and depressive-like phenotypes. However, our results contrasted greatly with those of previous studies. We hypothesized there could be two main reasons for that. First, our behavioral stress paradigms may not be strong enough or not relevant enough in the physiology of P2X7R to unveil a significant effect as a consequence of its blockade. Second, P2X7R is theorized to be a contributing factor and not a sole originator of anxiety- and depressive-like behaviors. Therefore, its absence could have too limited effects on the behavioral readouts analyzed to produce significant alterations. In conclusion, the stress paradigms and behavioral readouts that were employed did not function as indicators of P2X7R activity. Consequently, the next goal in this research line should be to find different ways to assess the role of P2X7R in the context of stress and depression.

The reason why P2X7R inactivation may not have a significant impact on our behavioral readouts can have several origins. There is a possibility that the stressors that we employed are not strong enough. Although it is known that CSDS produces microglial activation and the release of inflammatory molecules such as IL-1β, TNF-α, IL-6 and ROS (Ramirez et al., 2015; Stein et al., 2017; Zhu et al., 2019), studies show that a two-hit paradigm is more effective in activating microglia in adult mice (Calcia et al., 2016). This would consist of subjecting the mice to early life stress to sensitize microglia, and then carry out a chronic stress paradigm in adulthood, such as CSDS or CUS, to produce microglia stimulation and subsequent neuroimmune activation. Secondly, a chronic social stress paradigm might be activating the immune response through additional pathways independent of P2X7R, for example, through activation of mineralocorticoid or glucocorticoid receptors present in microglia (Sierra et al., 2008). Therefore, upon CSDS there could be a number of systems, independent to P2X7R, producing physiological changes that could cloak the potential effects caused by the activity of the receptor. To circumvent this issue, a more direct approach to activate the neuroinflammatory response could be employed, which would emulate the cases of MDD that are originated by inflammatory processes (Lee & Giuliani, 2019). Previous studies have employed acute and subacute LPS treatments to simulate a depressive episode, which was

ameliorated by P2X7R inhibitors (Csölle, Baranyi, et al., 2013). Therefore, this type of stimulus could be applied to assess the effect of P2X7R inactivation in mice in a more direct manner in contrast to CSDS. Finally, another possible approach would be to measure other parameters within alternative behavioral paradigms. One example would be analyzing sleep patterns, which was previously proved to significantly change in humans and mice carrying a vulnerability SNP (Metzger et al., 2018).

P2X7R is known to have a role in the physiology of microglia and the immune response, which is closely linked to MDD. Therefore, it is important to continue examining this receptor from the perspective of mood disorders. Finding out how to measure its impact on anxiety and other depressive-related phenotypes is crucial if its potential as a therapeutic target is to be explored. The results shown in this dissertation, combined with the great variability in the data of the available studies drives us to believe that the effect of P2X7R inactivation might not be as strong as once thought. Our extensive data shows that these behavioral paradigms do not attain the readout that was anticipated from previous studies, neither in baseline nor acute or chronic stress conditions. As a consequence, further studies need to be carried out to find replicable behavioral data that can be used to assess the impact of P2X7R on depressive phenotypes.

8.2 *Characterization of the P2X7R reporter/overexpressing mouse lines*

8.2.1 *Functional analysis*

One of the main problems encountered when attempting to detect P2X7R is the lack of specific antibodies. That is why the particular regions and cell types that are expressing the receptor in the CNS have been highly debated (M. Khan et al., 2017). To solve this problem, mouse lines were created, which express reporter proteins such as enhanced green fluorescent protein (EGFP) when the expression of P2X7R is activated. In this project, I focused on two of the currently available reporter mice. The soluble EGFP mouse (sEGFP), which expresses a soluble EGFP under the control of the P2X7R promoter and the more recently developed EGFP tagged P2X7R mouse (P2X7-EGFP), which overexpresses an active form of P2X7R with an EGFP tag at the C-terminal region of the receptor (Figure 5) (GENSAT project, Kaczmarek-Hajek et al., 2018)

The sEGFP reporter mouse line has been employed for over a decade in several studies on the expression pattern and function of P2X7R (Engel et al., 2012; García-Huerta et al., 2012; Hirayama et al., 2015; Jimenez-Mateos et al., 2015; Martínez-Frailes et al., 2019; Sebastián-Serrano et al., 2016; Xiong et al., 2018). However, upon further analysis, it presented certain irregularities in the expression of P2X7R, which were inspected in detail (Ramírez-Fernández et al., 2020). The results from the sEGFP line were contrasted to those of the P2X7-EGFP line. RT-qPCR and ISH assays showed that these reporter mice were overexpressing P2X7R as well as P2X4R, and that the expression pattern of both receptors is highly inhomogeneous throughout the brain in the sEGFP mice, which was additionally confirmed through IHC analysis. In contrast, the P2X7-EGFP mouse line presented the expected homogeneous overexpression of P2X7R as well as EGFP, but not P2X4R. It is relevant to point out that the BAC fragment employed to produce the sEGFP contained the P2X4R gene downstream of the P2X7R gene. Furthermore, although the genetic alteration of the BAC was meant to produce a halt in the transcription downstream of EGFP, a duplication was detected in the insertion site, which complemented the P2X7R ATG and enabled its transcription. As a consequence, the P2X7R and P2X4R copies that resided in the BAC construct were expressed as well. Due to the fact that several copies of the construct are inserted in the genome, an overexpression of both genes occurs in the sEGFP mouse. Moreover, the inhomogeneous expression of the receptors as well as EGFP in the sEGFP, as opposed to the P2X7-EGFP mice, led us to believe that there was also a problem with the functionality of the insert, which caused ectopic reporter expression. In conclusion, these results proved that the sEGFP has a leaking reporter gene as well as aberrant overexpression of P2X7R and P2X4R, as opposed to the P2X7-EGFP line, which expresses EGFP and overexpresses P2X7R in a homogeneous fashion, matching the endogenous expression pattern of P2X7R.

Another highly relevant factor to analyze was whether the EGFP expression is indeed representative for P2X7R expression *in vivo*. In the P2X7-EGFP mouse line, there was colocalization of the reporter protein with microglial, astrocytic and oligodendrocytic markers, but not with neuronal markers (Ramírez-Fernández et al., 2020). In contrast, in the sEGFP, approximately 80% of neuronal cells were expressing EGFP, and virtually no microglia, astrocytes or oligodendrocytes. Single cell data shows that P2X7R is expressed in microglia, perivascular macrophages, oligodendrocytes, astrocytes and ependymal cells, and to a lesser extent, in excitatory neurons in the cortex and hippocampus (Zeisel et al., 2018). Therefore,

the fact that there is virtually no reporter expression in these glial cells in the sEGFP mouse led to the conclusion that this reporter mouse line is not expressing EGFP specifically in cells that express P2X7R, but rather in an unspecific, deviant pattern.

More recently, a novel combined reporter and Cre driver mouse line was produced to detect P2X7R expression and to genetically target P2X7R-expressing cells (P2X7-CreERT2). In this mouse line a construct was used which simultaneously expresses nuclear EGFP and CreERT2. In contrast to the BAC transgenic mouse lines discussed above, this mouse line is generated applying a knock-in strategy. The construct was inserted in the P2X7R locus by homologous recombination, disrupting endogenous P2X7R expression. This technology presents benefits to the BAC-induced transgenics. First, it prevents insertions in unknown areas of the genome. This guarantees the expression of the transgene since the regulatory regions are present in the mutated locus. Furthermore, random insertion of the BAC fragment could potentially disrupt an intrinsic region that is relevant for the animal's physiology. With a targeted mutation strategy, these disruptions are prevented. Secondly, while in BAC transgenics the native gene will still be expressed, in the knock-in animals there is a substitution of the native gene by the transgene, therefore ensuring that the gene of interest is the only one being expressed. Finally, BAC transgenics often present multiple insertions in the genome. Therefore, these animals will be likely to present overexpression of the gene of interest, which might cause unwanted physiological alterations.

In the P2X7-CreERT2 mouse line, EGFP and CreERT2 should be expressed under the control of the endogenous P2X7R promoter. Since the P2X7R expression level is generally rather low, it was expected that the detection of EGFP expression would require antibody staining. However, breeding to a Cre-dependent reporter should allow detection of P2X7R-expressing cells with high sensitivity. When the EGFP expression pattern was analyzed in this mouse line, it was observed that it was mainly expressed in neuronal cells, with no EGFP signal detectable in glial cells. Moreover, tamoxifen treatment did not activate expression of a Cre-dependent reporter, suggesting the lack of Cre expression. Detailed analysis of the sequence revealed an aberrant integration at the 5' insertion site. Instead of the engrailed 2 splice acceptor, there was a partial duplicate of the exon 2 region of P2X7R. The identification and specification of aberrant integration, leading to a failure to express CreERT2, opens up possibilities to correct the problem. Nowadays, RNA-guided nucleases such as the Crispr/Cas9 system allow to

actively engineer genome sequences. Once a corrected insertion is confirmed the functionality of the Cre driver/reporter mouse line needs to be reassessed.

Transgenic mouse lines are highly useful tools in basic biomedical research. However, without a proper characterization, unexpected alterations can be overlooked and result in studies containing erroneous conclusions. In fact, the importance of thoroughly analyzing the transgenic mouse lines employed in a study with complementary methodologies has been emphasized (Chen et al., 2015; Lammel et al., 2015). As previously stated, there are several factors that one must consider when employing a newly produced BAC transgenic mouse line (Johansson et al., 2010). Deletions or duplications of important regions, unwanted overexpression of the gene of interest, disruption of the host genome or lack of expression due to lack of regulatory regions are some of the potential errors that might occur during the development of a BAC transgenic (Beil et al., 2012).

These facts, in addition to our experience with the P2X7R reporter mouse lines, stress the importance of properly and thoroughly characterizing the features of a novel transgenic mouse before employing it to reach conclusions about the physiological role of a gene of interest. In the case of the P2X7R-CreERT2 line, an insertion error was quickly identified, which allows to work towards fixing it before further analysis. In contrast, regarding the sEGFP line, many studies were carried out since it was produced, before the anomalies in its gene expression were detected (Engel et al., 2012; García-Huerta et al., 2012; Hirayama et al., 2015; Jimenez-Mateos et al., 2015; Martínez-Frailes et al., 2019; Sebastián-Serrano et al., 2016; Xiong et al., 2018). As a consequence, considering the newly found features of the sEGFP mouse line, it comes into question whether some of the conclusions reached in these studies should be reassessed. This creates an additional economic and professional burden that could have been minimized if the mouse line had been properly characterized beforehand.

The expression pattern of P2X7R in the CNS has still not been fully elucidated. Reporter mouse lines are essential tools that make up for the lack of effective antibodies against the receptor and have allowed us to visually assess the presence of P2X7R in specific cell types and brain regions. Using functional reporter mouse lines in combination with RNA expression assays such as ISH or RT-qPCR, we strive towards growing our understanding of the impact of P2X7R activity in the CNS in both baseline and pathological conditions.

8.2.2 *The impact of P2X7R overexpression in anxiety- and depressive-like phenotypes*

Although there are numerous studies showing the impact of P2X7R genetic inactivation or pharmacological inhibition on anxiety- and depressive-like phenotypes, the effects of P2X7R overexpression still have not been explored. To this end, it was decided to employ the P2X7-EGFP and sEGFP mouse lines. Given the published data linking P2X7R inactivation with higher resilience to anxiety- and depressive-like behaviors, it was hypothesized that P2X7R overexpression could produce sensitivity to these phenotypes. To evaluate this theory, P2X7-EGFP and sEGFP mice were subjected to a battery of behavioral experiments to assess locomotion, anxiety, anhedonia, and coping mechanisms in baseline conditions. The results obtained from these assays showed that P2X7-EGFP had a slightly reduced anxiety-related phenotype in the OFT, but no other effects were detected in any other test measuring anxiety, anhedonia, locomotion or coping behavior. On the other hand, the sEGFP mice presented an increased struggle time, and a decreased swim time in the FST, but there was no effect on immobility time in this test, or in any other behavioral readouts. Therefore, neither native overexpression of P2X7R, nor ectopic overexpression of P2X7R and P2X4R cause a strong effect on anxiety- and depression-related phenotypes

P2X4R is involved in a multitude of processes, which include, muscle contraction, synaptic transmission and wound healing, but it is also involved in inflammation and activation of immune cells, which overlaps with P2X7R function (Suurväli et al., 2017). In fact, P2X4R expression is known to be altered in P2X7R-KO mice (Craigie et al., 2013; Weinhold et al., 2010). Furthermore, P2X4R is approximately one thousand times more sensitive to ATP than P2X7R. Although no effect in anxiety-related phenotypes was noted under baseline conditions upon P2X4R inactivation, it did have an impact on social interaction (Wyatt et al., 2013). No research has been carried out previously on the impact of P2X4R overexpression on anxiety and coping behaviors. However, the similarity of P2X4R to P2X7R, their overlap in function, and its intrinsic behavioral effects make this mouse model inadequate to study P2X7R pathophysiology. Therefore, it can be concluded that the sEGFP line is not an ideal tool to study the pathophysiology of P2X7R, as it would be challenging to pinpoint the origin of the potential behavioral or physiological readouts to P2X7R alone.

P2X7R upregulation has been observed in several neural disorders, and it seems to contribute to disease progression (Savio et al., 2018). Although there is no consensus on whether P2X7R is up or downregulated in depressive patients (Iacob et al., 2013; Lei Zhang et al., 2011), there

is proof that chronic stress produces an enhanced expression of the receptor in hippocampus and cortex in mice, an effect that was attenuated by antidepressant treatment (Su et al., 2018; Tan et al., 2017).Theoretically, employing an overexpressing model would potentially emulate this stressed state in mice. However, this is not the outcome reached in our behavioral observations. The main reason for this lack of effect might be that, although P2X7R is overexpressed, it is not necessarily activated. Therefore, in the absence of stimuli, the overexpression of P2X7R would not have a large effect on the physiology of the mice, as these receptors would not be activated. The next step for this research line would be to analyze these mouse lines again, in the presence of chronic stress or upon treatment with an inflammatory agent such as LPS. This way it would be possible to assess whether overexpression of P2X7R could produce a significant effect in locomotion, anxiety, anhedonia, and coping behaviors. We believe that the P2X7-EGFP mouse line has a great potential, not yet explored, in the field of depression and anxiety. Further analysis in different conditions and paradigms could contribute to unveiling the pathophysiology of P2X7R in MDD.

9. Conclusions

The purinergic receptor P2X7R is a relevant target in several disorders of the central nervous system due to its demonstrated involvement in response to cellular stress. It activates the production of inflammatory mediators, which have been associated with MDD, suggesting the possibility that interfering with the physiology of P2X7R may have an impact on MDD development and progression. Although P2X7R has been widely studied, there are still many unanswered questions related to it. First, there are studies that link certain P2X7R SNPs to MDD, but the underlying consequences of these associations are still not fully understood. In fact, the expression pattern of P2X7R has not been fully elucidated yet, and therefore, the physiological and pathophysiological pathways in which it is involved still need to be thoroughly analyzed. In this project I decided to approach the P2X7R in the context of MDD from two different angles.

First, available reporter mouse lines were characterized. The results showed that the sEGFP mouse line presents an aberrant expression pattern of P2X7R and P2X4R and a leaky EGFP reporter which does not reflect endogenous P2X7R expression in physiological conditions. In contrast, the P2X7-EGFP mouse line showed reporter gene expression which is consistent with endogenous P2X7R expression in WT mice. Furthermore, these mouse lines are overexpressing P2X7R, which allowed assessing the impact of P2X7R overexpression on anxiety- and depressive-like behaviors under baseline conditions. Overexpression of P2X7R, alone or in combination with P2X4R, did not have any significant impact on these behavioral readouts. It is still pertinent to work towards developing a reporter mouse line that does not present altered P2X7R physiology. That is why the P2X7-CreERT2 mouse line was generated as an alternative strategy, which still holds the potential for correction via modern genetic engineering tools.

Secondly, we attempted to replicate and expand the previously published results which had revealed that P2X7R inactivation had a significant impact on anxiety- and depression-related behaviors. Throughout the project, it was demonstrated that inactivating P2X7R, fully or specifically in microglia, did not lead to strong effects in these phenotypes under baseline, acute stress, or chronic stress conditions. P2X7R is an element believed to contribute to disease etiology. Therefore, it is important to explore alternative paradigms, such as direct immune challenge, to elucidate in a replicable way the role of P2X7R in MDD.

10. References

Abkevich, V., Camp, N. J., Hensel, C. H., Neff, C. D., Russell, D. L., Hughes, D. C., Plenk, A. M., Lowry, M. R., Richards, R. L., Carter, C., Frech, G. C., Stone, S., Rowe, K., Chau, C. A., Cortado, K., Hunt, A., Luce, K., O'Neil, G., Poarch, J., … Cannon-Albright, L. (2003). Predisposition locus for major depression at chromosome 12q22-12q23.2. *American Journal of Human Genetics*, *73*(6), 1271–1281. https://doi.org/10.1086/379978

Adinolfi, E., Cirillo, M., Woltersdorf, R., Falzoni, S., Chiozzi, P., Pellegatti, P., Callegari, M. G., Sandonà, D., Markwardt, F., Schmalzing, G., & Di Virgilio, F. (2010). Trophic activity of a naturally occurring truncated isoform of the P2X7 receptor. *The FASEB Journal*, *24*(9), 3393–3404. https://doi.org/10.1096/fj.09-153601

Amodeo, G., Allegra Trusso, M., & Fagiolini, A. (2018). Depression and Inflammation: Disentangling a Clear Yet Complex and Multifaceted Link. *Neuropsychiatry*, *7*(4), 448–457. https://doi.org/10.4172/Neuropsychiatry.1000236

Anderson, C. M., & Nedergaard, M. (2006). Emerging challenges of assigning P2X7 receptor function and immunoreactivity in neurons. *Trends in Neurosciences*, *29*(5), 257–262. https://doi.org/10.1016/j.tins.2006.03.003

Aricioglu, F., Ozkartal, C. S., Bastaskin, T., Tüzün, E., Kandemir, C., Sirvanci, S., Kucukali, C. I., & Utkan, T. (2019). Antidepressant-like Effects Induced by Chronic Blockade of the Purinergic 2X7 Receptor through Inhibition of Non-like Receptor Protein 1 Inflammasome in Chronic Unpredictable Mild Stress Model of Depression in Rats. *Clinical Psychopharmacology and Neuroscience : The Official Scientific Journal of the Korean College of Neuropsychopharmacology*, *17*(2), 261–272. https://doi.org/10.9758/cpn.2019.17.2.261

Bachmann, S. (2018). Epidemiology of suicide and the psychiatric perspective. *International Journal of Environmental Research and Public Health*, *15*(7), 1–23. https://doi.org/10.3390/ijerph15071425

Barden, N., Harvey, M., Gagné, B., Shink, E., Tremblay, M., Raymond, C., Labbé, M., Villeneuve, A., Rochette, D., Bordeleau, L., Stadler, H., Holsboer, F., & Müller-Myhsok, B. (2006). Analysis of single nucleotide polymorphisms in genes in the chromosome 12Q24.31 region points to P2RX7 as a susceptibility gene to bipolar affective disorder. *American Journal of Medical Genetics, Part B: Neuropsychiatric Genetics*, *141*(4), 374–382. https://doi.org/10.1002/ajmg.b.30303

Barros-Barbosa, A. R., Lobo, M. G., Ferreirinha, F., Correia-de-Sá, P., & Cordeiro, J. M. (2015). P2X7 receptor activation downmodulates Na+-dependent high-affinity GABA and glutamate transport into rat brain cortex synaptosomes. *Neuroscience*, *306*, 74–90. https://doi.org/10.1016/j.neuroscience.2015.08.026

Barros-Barbosa, Aurora R., Oliveira, Â., Lobo, M. G., Cordeiro, J. M., & Correia-de-Sá, P. (2018). Under stressful conditions activation of the ionotropic P2X7 receptor differentially regulates GABA and glutamate release from nerve terminals of the rat cerebral cortex. *Neurochemistry International*, *112*, 81–95. https://doi.org/10.1016/j.neuint.2017.11.005

Bartlett, R., Stokes, L., & Sluyter, R. (2014). The P2X7 Receptor Channel: Recent Developments and the Use of P2X7 Antagonists in Models of Disease. *Pharmacological Reviews*, *66*(3), 638–675. https://doi.org/10.1124/pr.113.008003

Bartlett, R., Yerbury, J. J., & Sluyter, R. (2013). P2X7 receptor activation induces reactive oxygen species formation and cell death in murine eoc13 microglia. *Mediators of Inflammation*, *2013*(271813), 1–18. https://doi.org/10.1155/2013/271813

Basso, A. M., Bratcher, N. A., Harris, R. R., Jarvis, M. F., Decker, M. W., & Rueter, L. E. (2009). Behavioral profile of P2X7 receptor knockout mice in animal models of depression and anxiety: Relevance for neuropsychiatric disorders. *Behavioural Brain Research*, *198*(1), 83–90. https://doi.org/10.1016/J.BBR.2008.10.018

Beil, J., Fairbairn, L., Pelczar, P., & Buch, T. (2012). Is BAC transgenesis obsolete? State of the art in the era of designer nucleases. *Journal of Biomedicine and Biotechnology*, *2012*(308414), 1–5. https://doi.org/10.1155/2012/308414

Berton, O., & Nestler, E. J. (2006). New approaches to antidepressant drug discovery: beyond monoamines. *Nature Reviews Neuroscience*, *7*(2), 137–151. https://doi.org/10.1038/nrn1846

Bhattacharya, A., & Ceusters, M. (2020). *Targeting neuroinflammation with brain penetrant P2X7 antagonists as novel therapeutics for neuropsychiatric disorders Biological fi ngerprints for psychosis*. *42*, 234–235.

Bhattacharya, A., Lord, B., Grigoleit, J. S., He, Y., Fraser, I., Campbell, S. N., Taylor, N., Aluisio, L., O'Connor, J. C., Papp, M., Chrovian, C., Carruthers, N., Lovenberg, T. W., & Letavic, M. A. (2018). Neuropsychopharmacology of JNJ-55308942: evaluation of a clinical candidate targeting P2X7 ion channels in animal models of neuroinflammation and anhedonia. *Neuropsychopharmacology*, *43*(13), 2586–2596. https://doi.org/10.1038/s41386-018-0141-6

Bhattacharya, A., Wang, Q., Ao, H., Shoblock, J. R., Lord, B., Aluisio, L., Fraser, I., Nepomuceno, D., Neff, R. A., Welty, N., Lovenberg, T. W., Bonaventure, P., Wickenden, A. D., Letavic, M. A., Area, N. T., & Pharmaceutical, J. (2013). Pharmacological characterization of a novel centrally permeable P2X7 receptor antagonist: JNJ-47965567. *British Journal of Pharmacology*, *170*(3), 624–640. https://doi.org/10.1111/bph.12314

Boucher, A. A., Arnold, J. C., Hunt, G. E., Spiro, A., Spencer, J., Brown, C., McGregor, I. S., Bennett, M. R., & Kassiou, M. (2011). Resilience and reduced c-Fos expression in P2X7 receptor knockout mice exposed to repeated forced swim test. *Neuroscience*, *189*, 170–177. https://doi.org/10.1016/j.neuroscience.2011.05.049

Burnstock, G. (2006). Purinergic signalling. *British Journal of Pharmacology*, *147*, 172–181. https://doi.org/10.1038/sj.bjp.0706429

Bygrave, A. E., Rose, K. L., Cortes-Hernandez, J., Warren, J., Rigby, R. J., Terence Cook, H., Walport, M. J., Vyse, T. J., & Botto, M. (2004). Spontaneous autoimmunity in 129 and C57BL/6 mice-implications for autoimmunity described in gene-targeted mice. *PLoS Biology*, *2*(8), 1081–1090. https://doi.org/10.1371/journal.pbio.0020243

Calcia, M. A., Bonsall, D. R., Bloomfield, P. S., Selvaraj, S., Barichello, T., & Howes, O. D. (2016). Stress and neuroinflammation: a systematic review of the effects of stress on microglia and the implications for mental illness. *Psychopharmacology*, *233*, 1637–1650. https://doi.org/10.1007/s00213-016-4218-9

Capuron, L., & Miller, A. H. (2004). Cytokines and psychopathology: Lessons from interferon-α. *Biological Psychiatry*, *56*(11), 819–824. https://doi.org/10.1016/j.biopsych.2004.02.009

Cassano, P., & Fava, M. (2004). Tolerability issues during long-term treatment with antidepressants. *Annals of Clinical Psychiatry : Official Journal of the American Academy of Clinical Psychiatrists*, *16*(1), 15–25. https://doi.org/10.1080/10401230490281618

Castrén, E. (2013). Neuronal Network Plasticity and Recovery From Depression. *JAMA Psychiatry*, *70*(9), 983–989. https://doi.org/10.1001/jamapsychiatry.2013.1

Castrén, E., & Rantamäki, T. (2010). The role of BDNF and its receptors in depression and antidepressant drug action: Reactivation of developmental plasticity. *Developmental Neurobiology*, *70*(5), 289–297. https://doi.org/10.1002/dneu.20758

Cheewatrakoolpong, B., Gilchrest, H., Anthes, J. C., & Greenfeder, S. (2005). Identification and characterization of splice variants of the human P2X 7 ATP channel. *Biochemical and Biophysical Research Communications*, *332*(1), 17–27. https://doi.org/10.1016/j.bbrc.2005.04.087

Chen, Y., Molet, J., Gunn, B. G., Ressler, K., & Baram, T. Z. (2015). Diversity of reporter expression patterns in transgenic mouse lines targeting corticotropin- releasing hormone-expressing neurons. *Endocrinology*, *156*(12), 4769–4780. https://doi.org/10.1210/en.2015-1673

Chessell, I. P., Hatcher, J. P., Bountra, C., Michel, A. D., Hughes, J. P., Green, P., Egerton, J., Murfin, M., Richardson, J., Peck, W. L., Grahames, C. B. A., Casula, M. A., Yiangou, Y., Birch, R., Anand, P., & Buell, G. N. (2005). Disruption of the P2X7 purinoceptor gene abolishes chronic inflammatory and neuropathic pain. *Pain*, *114*(3), 386–396. https://doi.org/10.1016/j.pain.2005.01.002

Cho, J. H., Choi, I. S., & Jang, I. S. (2010). P2X7 receptors enhance glutamate release in hippocampal hilar neurons. *NeuroReport*, *21*(13), 865–870. https://doi.org/10.1097/WNR.0b013e32833d9142

Chow, W., Doane, M. J., Sheehan, J., Alphs, L., & Le, H. (2019). Economic burden among patients with major depressive disorder: An analysis of healthcare resource use, work productivity, and direct and indirect costs by depression severity. *American Journal of Managed Care*, *Feb*, 1–3.

Chrousos, G. (1995). They hypothalamic-pituitary-adrenal axis and immune-mediated inflammation. *RadioGraphics*, *332*(20), 489–492.

Chrovian, C. C., Soyode-Johnson, A., Peterson, A. A., Gelin, C. F., Deng, X., Dvorak, C. A., Carruthers, N. I., Lord, B., Fraser, I., Aluisio, L., Coe, K. J., Scott, B., Koudriakova, T., Schoetens, F., Sepassi, K., Gallacher, D. J., Bhattacharya, A., & Letavic, M. A. (2018). A Dipolar Cycloaddition Reaction to Access 6-Methyl-4,5,6,7-tetrahydro-1H-[1,2,3]triazolo[4,5-c]pyridines Enables the Discovery Synthesis and Preclinical Profiling of a P2X7 Antagonist Clinical Candidate. *Journal of Medicinal Chemistry*, *61*(1), 207–223. https://doi.org/10.1021/acs.jmedchem.7b01279

Colonna, M., & Butovsky, O. (2017). Microglia Function in the Central Nervous System During Health and Neurodegeneration. *Annual Review of Immunology*, *35*(1), 441–468. https://doi.org/10.1146/annurev-immunol-051116-052358

Craigie, E., Birch, R. E., Unwin, R. J., & Wildman, S. S. (2013). The relationship between P2X4

and P2X7: A physiologically important interaction? *Frontiers in Physiology*, *4*(216), 1–6. https://doi.org/10.3389/fphys.2013.00216

Csölle, C., Andó, R. D., Kittel, Á., Gölöncsér, F., Baranyi, M., Soproni, K., Zelena, D., Haller, J., Németh, T., Mócsai, A., & Sperlágh, B. (2013). The absence of P2X7 receptors (P2rx7) on non-haematopoietic cells leads to selective alteration in mood-related behaviour with dysregulated gene expression and stress reactivity in mice. *International Journal of Neuropsychopharmacology*, *16*(1), 213–233. https://doi.org/10.1017/S1461145711001933

Csölle, C., Baranyi, M., Zsilla, G., Kittel, Á., Gölöncsér, F., Illes, P., Papp, E., Vizi, E. S., Sperlágh, B., Kittel, A. ´, & Lö Ncsér, G. (2013). Neurochemical Changes in the Mouse Hippocampus Underlying the Antidepressant Effect of Genetic Deletion of P2X7 Receptors. *PLoS ONE*, *8*(6), 1–18. https://doi.org/10.1371/journal.pone.0066547

Cuijpers, P., Noma, H., Karyotaki, E., Vinkers, C. H., Cipriani, Andrea, & Furukawa, T. A. (2020). A network meta-analysis of the effects of psychotherapies, pharmacotherapies and their combination in the treatment of adult depression. *World Psychiatry*, *19*(1), 92–107. https://doi.org/10.1002/wps.20701

Curtis, D., Kalsi, G., Brynjolfsson, J., McInnis, M., O'Neill, J., Smyth, C., Moloney, E., Murphy, P., McQuillin, A., Petursson, H., & Gurling, H. (2003). Genome scan of pedigrees multiply affected with bipolar disorder provides further support for the presence of a susceptibility locus on chromosome 12q23-q24, and suggests the presence of additional loci on 1p and 1q. *Psychiatric Genetics*, *13*(2), 77–84. https://doi.org/10.1097/01.ypg.0000056684.89558.d2

Czamara, D., Müller-Myhsok, B., & Lucae, S. (2018). The P2RX7 polymorphism rs2230912 is associated with depression: A meta-analysis. *Progress in Neuro-Psychopharmacology and Biological Psychiatry*, *82*, 272–277. https://doi.org/10.1016/J.PNPBP.2017.11.003

Danquah, W., Meyer-Schwesinger, C., Rissiek, B., Pinto, C., Serracant-Prat, A., Amadi, M., Iacenda, D., Knop, J.-H., Hammel, A., Bergmann, P., Schwarz, N., Assuncao, J., Rotthier, W., Haag, F., Tolosa, E., Bannas, P., Boue-Grabot, E., Magnus, T., Laeremans, T., … Koch-Nolte, F. (2016). Nanobodies that block gating of the P2X7 ion channel ameliorate inflammation. *Science Translational Medicine*, *8*(366), 1–12. https://doi.org/10.1126/scitranslmed.aaf8463

Dantzer, R., O'Connor, J. C., Freund, G. G., Johnson, R. W., & Kelley, K. W. (2008). From inflammation to sickness and depression: when the immune system subjugates the brain. *Nature Reviews. Neuroscience*, *9*(1), 46–56. https://doi.org/10.1038/nrn2297

Davis, R. L., McCracken, K., Buck, D. J., & Curtis, J. T. (2021). Social defeat affects inflammatory signaling and exploratory behavior in mice in a sex-dependent manner. *Neuroimmunology and Neuroinflammation*, *8*, 134–145. https://doi.org/10.20517/2347-8659.2020.20

De Kloet, E. R., Joëls, M., & Holsboer, F. (2005). Stress and the brain: From adaptation to disease. *Nature Reviews Neuroscience*, *6*(6), 463–475. https://doi.org/10.1038/nrn1683

Dean, J., & Keshavan, M. (2017). The neurobiology of depression: An integrated view. *Asian Journal of Psychiatry*, *27*, 101–111. https://doi.org/10.1016/j.ajp.2017.01.025

Degn, B., Lundorf, M. D., Wang, A., Vang, M., Mors, O., Kruse, T. A., & Ewald, H. (2001). Further evidence for a bipolar risk gene on chromosome 12q24 suggested by investigation of haplotype sharing and allelic association in patients from the Faroe Islands. *Molecular*

Psychiatry, *6*(4), 450–455. https://doi.org/10.1038/sj.mp.4000882

Di Benedetto, S., Müller, L., Wenger, E., Düzel, S., & Pawelec, G. (2017). Contribution of neuroinflammation and immunity to brain aging and the mitigating effects of physical and cognitive interventions. *Neuroscience and Biobehavioral Reviews*, *75*, 114–128. https://doi.org/10.1016/j.neubiorev.2017.01.044

Di Virgilio, F., Giuliani, A. L., Vultaggio-Poma, V., Falzoni, S., & Sarti, A. C. (2018). Non-nucleotide Agonists Triggering P2X7 Receptor Activation and Pore Formation. *Frontiers in Pharmacology*, *9*(39), 1–10. https://doi.org/10.3389/fphar.2018.00039

DiSabato, D. J., Quan, N., & Godbout, J. P. (2016). Neuroinflammation: the devil is in the details. *Journal of Neurochemistry*, *139*, 136–153. https://doi.org/10.1111/jnc.13607

Dong, X. X., Wang, Y., & Qin, Z. H. (2009). Molecular mechanisms of excitotoxicity and their relevance to pathogenesis of neurodegenerative diseases. *Acta Pharmacologica Sinica*, *30*(4), 379–387. https://doi.org/10.1038/aps.2009.24

Donnelly-Roberts, D. L., Namovic, M. T., Han, P., & Jarvis, M. F. (2009). Mammalian P2X7 receptor pharmacology: Comparison of recombinant mouse, rat and human P2X7 receptors. *British Journal of Pharmacology*, *157*(7), 1203–1214. https://doi.org/10.1111/j.1476-5381.2009.00233.x

Donnelly-Roberts, D. L., Namovic, M. T., Surber, B., Vaidyanathan, S. X., Perez-Medrano, A., Wang, Y., Carroll, W. A., & Jarvis, M. F. (2009). [3H]A-804598 ([3H]2-cyano-1-[(1S)-1-phenylethyl]-3-quinolin-5-ylguanidine) is a novel, potent, and selective antagonist radioligand for P2X7 receptors. *Neuropharmacology*, *56*(1), 223–229. https://doi.org/10.1016/j.neuropharm.2008.06.012

Dowlati, Y., Herrmann, N., Swardfager, W., Liu, H., Sham, L., Reim, E. K., & Lanctôt, K. L. (2010). A Meta-Analysis of Cytokines in Major Depression. *Biological Psychiatry*, *67*(5), 446–457. https://doi.org/10.1016/j.biopsych.2009.09.033

Dube, S. R., Anda, R. F., Felitti, V. J., Chapman, D. P., Williamson, D. F., & Giles, W. H. (2001). Childhood abuse, household dysfunction, and the risk of attempted suicide throughout the life span: Findings from the adverse childhood experiences study. *Journal of the American Medical Association*, *286*(24), 3089–3096. https://doi.org/10.1001/jama.286.24.3089

Dubyak, G. R. (2012). P2X7 receptor regulation of non-classical secretion from immune effector cells. *Cellular Microbiology*, *14*(11), 1697–1706. https://doi.org/10.1111/cmi.12001

Duman, R. S., Aghajanian, G. K., Sanacora, G., & Krystal, J. H. (2016). Synaptic plasticity and depression: New insights from stress and rapid-acting antidepressants. *Nature Medicine*, *22*(3), 238–249. https://doi.org/10.1038/nm.4050

Dunn, A. (2006). Cytokine Activation of the HPA Axis. *Annals of the New York Academy of Sciences*, *917*(1), 608–617. https://doi.org/10.1111/j.1749-6632.2000.tb05426.x

Engel, T., Gomez-Villafuertes, R., Tanaka, K., Mesuret, G., Sanz-Rodriguez, A., Garcia-Huerta, P., Miras-Portugal, M. T., Henshall, D. C., & Diaz-Hernandez, M. (2012). Seizure suppression and neuroprotection by targeting the purinergic P2X7 receptor during status epilepticus in mice. *The FASEB Journal*, *26*(4), 1616–1628. https://doi.org/10.1096/fj.11-196089

Farooq, R. K., Tanti, A., Ainouche, S., Roger, S., Belzung, C., & Camus, V. (2018). A P2X7 receptor antagonist reverses behavioural alterations, microglial activation and neuroendocrine dysregulation in an unpredictable chronic mild stress (UCMS) model of depression in mice. *Psychoneuroendocrinology*, *97*, 120–130. https://doi.org/10.1016/j.psyneuen.2018.07.016

Farrington, G. K., Caram-Salas, N., Haqqani, A. S., Brunette, E., Eldredge, J., Pepinsky, B., Antognetti, G., Baumann, E., Ding, W., Garber, E., Jiang, S., Delaney, C., Boileau, E., Sisk, W. P., & Stanimirovic, D. B. (2014). A novel platform for engineering blood-brain barrier-crossing bispecific biologics. *The FASEB Journal*, *28*(11), 4764–4778. https://doi.org/10.1096/fj.14-253369

Felger, J. C., & Lotrich, F. E. (2013). Inflammatory cytokines in depression: Neurobiological mechanisms and therapeutic implications. *Neuroscience*, *246*, 199–229. https://doi.org/10.1016/j.neuroscience.2013.04.060

Fellin, T., Pozzan, T., & Carmignoto, G. (2006). Purinergic receptors mediate two distinct glutamate release pathways in hippocampal astrocytes. *The Journal of Biological Chemistry*, *281*(7), 4274–4284. https://doi.org/10.1074/jbc.M510679200

Feng, W. P., Zhang, B., Li, W., & Liu, J. (2014). Lack of association of P2RX7 gene rs2230912 polymorphism with mood disorders: A meta-analysis. *PLoS ONE*, *9*(2), 1–6. https://doi.org/10.1371/journal.pone.0088575

Feng, Y.-H., Li, X., Wang, L., Zhou, L., & Gorodeski, G. I. (2006). A truncated P2X7 receptor variant (P2X7-j) endogenously expressed in cervical cancer cells antagonizes the full-length P2X7 receptor through hetero-oligomerization. *The Journal of Biological Chemistry*, *281*(25), 17228–17237. https://doi.org/10.1074/jbc.M602999200

Ferguson, J. M. (2001). SSRI Antidepressant Medications: Adverse Effects and Tolerability. *Primary Care Companion to the Journal of Clinical Psychiatry*, *3*(1), 22–27. https://doi.org/10.4088/pcc.v03n0105

Fogaça, M. V, & Duman, R. S. (2019). Cortical GABAergic Dysfunction in Stress and Depression: New Insights for Therapeutic Interventions. *Frontiers in Cellular Neuroscience*, *13*(87), 1–20. https://doi.org/10.3389/fncel.2019.00087

Fogal, B., & Hewett, S. J. (2008). Interleukin-1β: A bridge between inflammation and excitotoxicity? *Journal of Neurochemistry*, *106*(1), 1–23. https://doi.org/10.1111/j.1471-4159.2008.05315.x

Gao, L., Lin, Z., Xie, G., Zhou, T., Hu, W., Liu, C., Liu, X., Wang, X., Qian, M., & Ni, B. (2018). The effects of P2X7 receptor knockout on emotional conditions over the lifespan of mice. *NeuroReport*, *29*(17), 1479–1486. https://doi.org/10.1097/WNR.0000000000001136

García-Huerta, P., Diáz-Hernandez, M., Delicado, E. G., Pimentel-Santillana, M., Miras-Portugals, M. T., & Gońez-Villafuertes, R. (2012). The specificity protein factor Sp1 mediates transcriptional regulation of P2X7 receptors in the nervous system. *Journal of Biological Chemistry*, *287*(53), 44628–44644. https://doi.org/10.1074/jbc.M112.390971

Gölöncsér, F., Baranyi, M., Balázsfi, D., Demeter, K., Haller, J., Freund, T. F. F., Zelena, D., & Sperlágh, B. (2017). Regulation of hippocampal 5-HT release by P2X7 receptors in response to

optogenetic stimulation of median raphe terminals of mice. *Frontiers in Molecular Neuroscience*, *10*(325), 1–16. https://doi.org/10.3389/fnmol.2017.00325

Gong, S., Zheng, C., Doughty, M. L., Losos, K., Didkovsky, N., Schambra, U. B., Nowak, N. J., Joyner, A., Leblanc, G., Hatten, M. E., & Heintz, N. (2016). A gene expression atlas of the central nervous system based on bacterial artificial chromosomes. *AAPM Annual Meeting*, *425*(6961), 917–925. https://doi.org/10.1038/nature02033

Green, E. K., Grozeva, D., Raybould, R., Elvidge, G., Macgregor, S., Craig, I., Farmer, A., McGuffin, P., Forty, L., Jones, L., Jones, I., O'Donovan, M. C., Owen, M. J., Kirov, G., & Craddock, N. (2009). P2RX7: A bipolar and unipolar disorder candidate susceptibility gene? *American Journal of Medical Genetics, Part B: Neuropsychiatric Genetics*, *150*(8), 1063–1069. https://doi.org/10.1002/ajmg.b.30931

Greenberg, P. E., Fournier, A.-A. A., Sisitsky, T., Pike, C. T., & Kessler, R. C. (2015). The economic burden of adults with major depressive disorder in the United States (2005 and 2010). *Journal of Clinical Psychiatry*, *76*(2), 155–162. https://doi.org/10.4088/JCP.14m09298

Greve, A. S., Skals, M., Fagerberg, S. K., Tonnus, W., Ellermann-Eriksen, S., Evans, R. J., Linkermann, A., & Praetorius, H. A. (2017). P2X1 , P2X4 , and P2X7 Receptor Knock Out Mice Expose Differential Outcome of Sepsis Induced by α-Haemolysin Producing Escherichia coli. *Frontiers in Cellular and Infection Microbiology*, *7*(113), 1–14. https://doi.org/10.3389/fcimb.2017.00113

Grigoroiu-Serbanescu, M., Herms, S., Mühleisen, T. W., Georgi, A., Diaconu, C. C., Strohmaier, J., Czerski, P., Hauser, J., Leszczynska-Rodziewicz, A., Jamra, R. A., Babadjanova, G., Tiganov, A., Krasnov, V., Kapiletti, S., Neagu, A. I., Vollmer, J., Breuer, R., Rietschel, M., Nöthen, M. M., … Propping, P. (2009). Variation in *P2RX7* candidate gene (rs2230912) is not associated with bipolar I disorder and unipolar major depression in four European samples. *American Journal of Medical Genetics Part B: Neuropsychiatric Genetics*, *150B*(7), 1017–1021. https://doi.org/10.1002/ajmg.b.30952

Guadagno, J., Swan, P., Shaikh, R., & Cregan, S. P. (2015). Microglia-derived IL-1β triggers p53-mediated cell cycle arrest and apoptosis in neural precursor cells. *Cell Death and Disease*, *6*(e1779), 1–10. https://doi.org/10.1038/cddis.2015.151

Habermacher, C., Dunning, K., Chataigneau, T., & Grutter, T. (2016). Molecular structure and function of P2X receptors. *Neuropharmacology*, *104*, 18–30. https://doi.org/10.1016/j.neuropharm.2015.07.032

Hattori, M., & Gouaux, E. (2012). Molecular mechanism of ATP binding and ion channel activation in P2X receptors. *Nature*, *485*(7397), 207–212. https://doi.org/10.1038/nature11010

He, Y., Taylor, N., Fourgeaud, L., & Bhattacharya, A. (2017). The role of microglial P2X7: modulation of cell death and cytokine release. *Journal of Neuroinflammation*, *14*(135), 1–13. https://doi.org/10.1186/s12974-017-0904-8

Hejjas, K., Szekely, A., Domotor, E., Halmai, Z., Balogh, G., Schilling, B., Sarosi, A., Faludi, G., Sasvari-Szekely, M., & Nemoda, Z. (2009). Association between depression and the Gln460Arg polymorphism of P2RX7 gene: A dimensional approach. *American Journal of Medical Genetics, Part B: Neuropsychiatric Genetics*, *150*(2), 295–299. https://doi.org/10.1002/ajmg.b.30799

Hewinson, J., & MacKenzie, A. B. (2007). P2X7 receptor-mediated reactive oxygen and nitrogen species formation: From receptor to generators. *Biochemical Society Transactions*, *35*(5), 1168–1170. https://doi.org/10.1042/BST0351168

Hirayama, Y., Ikeda-Matsuo, Y., Notomi, S., Enaida, H., Kinouchi, H., & Koizumi, S. (2015). Astrocyte-mediated ischemic tolerance. *Journal of Neuroscience*, *35*(9), 3794–3805. https://doi.org/10.1523/JNEUROSCI.4218-14.2015

Holmdahl, R., & Malissen, B. (2012). The need for littermate controls. *European Journal of Immunology*, *42*(1), 45–47. https://doi.org/10.1002/eji.201142048

Iacob, E., Light, K. C., Tadler, S. C., Weeks, H. R., White, A. T., Hughen, R. W., VanHaitsma, T. A., Bushnell, L., & Light, A. R. (2013). Dysregulation of leukocyte gene expression in women with medication-refractory depression versus healthy non-depressed controls. *BMC Psychiatry*, *13*(273), 1–10. https://doi.org/10.1186/1471-244X-13-273

Illes, P., Khan, T. M., & Rubini, P. (2017). Neuronal P2X7 Receptors Revisited: Do They Really Exist? *The Journal of Neuroscience*, *37*(30), 7049–7062. https://doi.org/10.1523/JNEUROSCI.3103-16.2017

Illes, P., Verkhratsky, A., Burnstock, G., & Franke, H. (2012). P2X receptors and their roles in astroglia in the central and peripheral nervous system. *Neuroscientist*, *18*(5), 422–438. https://doi.org/10.1177/1073858411418524

Iwata, M., Ota, K. T., Li, X.-Y. Y., Sakaue, F., Li, N., Dutheil, S., Banasr, M., Duric, V., Yamanashi, T., Kaneko, K., Rasmussen, K., Glasebrook, A., Koester, A., Song, D., Jones, K. A., Zorn, S., Smagin, G., & Duman, R. S. (2016). Psychological stress activates the inflammasome via release of adenosine triphosphate and stimulation of the purinergic type 2X7 receptor. *Biological Psychiatry*, *80*(1), 12–22. https://doi.org/10.1016/j.biopsych.2015.11.026

Jick, H., Kaye, J. A., & Jick, S. S. (2004). Antidepressants and the Risk of Suicidal Behaviors. *JAMA*, *292*(3), 338–343. https://doi.org/10.1001/jama.292.3.338

Jimenez-Mateos, E. M., Arribas-Blazquez, M., Sanz-Rodriguez, A., Concannon, C., Olivos-Ore, L. A., Reschke, C. R., Mooney, C. M., Mooney, C., Lugara, E., Morgan, J., Langa, E., Jimenez-Pacheco, A., Silva, L. F. A., Mesuret, G., Boison, D., Miras-Portugal, M. T., Letavic, M., Artalejo, A. R., Bhattacharya, A., … Engel, T. (2015). MicroRNA targeting of the P2X7 purinoceptor opposes a contralateral epileptogenic focus in the hippocampus. *Scientific Reports*, *5*(17486), 1–17. https://doi.org/10.1038/srep17486

Jin, Y., Sun, L. H., Yang, W., Cui, R. J., & Xu, S. B. (2019). The role of BDNF in the neuroimmune axis regulation of mood disorders. *Frontiers in Neurology*, *10*(515), 1–10. https://doi.org/10.3389/fneur.2019.00515

Johansson, T., Broll, I., Frenz, T., Hemmers, S., Becher, B., Zeilhofer, H. U., & Buch, T. (2010). Building a zoo of mice for genetic analyses: A comprehensive protocol for the rapid generation of BAC transgenic mice. *Genesis*, *280*(48), 264–280. https://doi.org/10.1002/dvg.20612

Kaczmarek-Hajek, K., Zhang, J., Kopp, R., Grosche, A., Rissiek, B., Saul, A., Bruzzone, S., Engel, T., Jooss, T., Krautloher, A., Schuster, S., Magnus, T., Stadelmann, C., Sirko, S., Koch-Nolte, F., Eulenburg, V., & Nicke, A. (2018). Re-evaluation of neuronal P2X7 expression using novel mouse models and a P2X7-specific nanobody. *ELife*, *7*. https://doi.org/10.7554/eLife.36217

Karasawa, A., & Kawate, T. (2016). Structural basis for subtype-specific inhibition of the P2X7 receptor. *ELife*, *5*. https://doi.org/10.7554/eLife.22153

Keller, J., Gomez, R., Williams, G., Lembke, A., Lazzeroni, L., Murphy, G. M., Schatzberg, A. F., & Schatzberg, A. F. (2017). HPA axis in major depression: cortisol, clinical symptomatology and genetic variation predict cognition. *Molecular Psychiatry*, *22*(4), 527–536. https://doi.org/10.1038/mp.2016.120

Kendler, K. S., Gatz, M., Gardner, C. O., & Pedersen, N. L. (2006). A Swedish National Twin Study of Lifetime Major Depression. *American Journal of Psychiatry*, *163*(1), 109–114. https://doi.org/10.1176/appi.ajp.163.1.109

Kessler, R. C., McGonagle, K. A., Swartz, M., Blazer, D. G., & Nelson, C. B. (n.d.). Sex and depression in the National Comorbidity Survey. I: Lifetime prevalence, chronicity and recurrence. *Journal of Affective Disorders*, *29*(2–3), 85–96. https://doi.org/10.1016/0165-0327(93)90026-g

Kessler, R. C., Zhao, S., Blazer, D. G., & Swartz, M. (1997). Prevalence, correlates, and course of minor depression and major depression in the National Comorbidity Survey. *Journal of Affective Disorders*, *45*(1–2), 19–30. https://doi.org/10.1016/s0165-0327(97)00056-6

Khakh, B. S., & North, R. A. (2012). Neuromodulation by extracellular ATP and P2X receptors in the CNS. *Neuron*, *76*(1), 51–69. https://doi.org/10.1016/j.neuron.2012.09.024

Khan, M., Rubini, P., Teresa Miras-Portugal, X. M., Lvaro Sebastián-Serrano, A. ´, De, L., García, D., & Díaz-Hernández, X. (2017). Dual Perspectives Dual Perspectives Companion Paper: Neuronal P2X7 Receptors Revisited: Do They Really Exist?, by Peter Illes, Tahir Neuronal P2X7 Receptor: Involvement in Neuronal Physiology and Pathology. *The Journal of Neuroscience*, *37*(30), 7063–7072. https://doi.org/10.1523/JNEUROSCI.3104-16.2017

Khan, M. T., Deussing, J., Tang, Y., & Illes, P. (2018). Astrocytic rather than neuronal P2X7 receptors modulate the function of the tri-synaptic network in the rodent hippocampus. *Brain Research Bulletin*, *151*(Sep), 164–173. https://doi.org/10.1016/j.brainresbull.2018.07.016

Koch-Nolte, F., Eichhoff, A., Pinto-Espinoza, C., Schwarz, N., Schäfer, T., Menzel, S., Haag, F., Demeules, M., Gondé, H., & Adriouch, S. (2019). Novel biologics targeting the P2X7 ion channel. *Current Opinion in Pharmacology*, *47*, 110–118. https://doi.org/10.1016/j.coph.2019.03.001

Köhler, O., Benros, M. E., Nordentoft, M., Farkouh, M. E., Iyengar, R. L., Mors, O., & Krogh, J. (2014). Effect of Anti-inflammatory Treatment on Depression, Depressive Symptoms, and Adverse Effects. *JAMA Psychiatry*, *71*(12), 1381–1391. https://doi.org/10.1001/jamapsychiatry.2014.1611

Köhler, O., Krogh, J., Mors, O., & Benros, M. E. (2016). Inflammation in Depression and the Potential for Anti-Inflammatory Treatment. *Current Neuropharmacology*, *14*, 732–742. https://doi.org/10.2174/1570159X14666151208113

Köhler, O., Krogh, J., Mors, O., Benros, M. E., Kohler, O., Krogh, J., Mors, O., & Eriksen Benros, M. (2016). Inflammation in Depression and the Potential for Anti-Inflammatory Treatment. *Current Neuropharmacology*, *14*, 732–742. https://doi.org/10.2174/1570159X14666151208113

Kraus, C., Kadriu, B., Lanzenberger, R., Zarate, C. A., & Kasper, S. (2019). Prognosis and improved outcomes in major depression: a review. *Translational Psychiatry*, *9*(127), 1–17. https://doi.org/10.1038/s41398-019-0460-3

Kupfer, D. J., Frank, E., & Phillips, M. L. (2012). Major depressive disorder: new clinical, neurobiological, and treatment perspectives. *Lancet (London, England)*, *379*(9820), 1045–1055. https://doi.org/10.1016/S0140-6736(11)60602-8

Lammel, S., Steinberg, E., Földy, C., Wall, N., Beier, K., Luo, L., & Malenka, R. (2015). Diversity of Transgenic Mouse Models for Selective Targeting of Midbrain Dopamine Neurons. *Neuron*, *85*(2), 429–438. https://doi.org/10.1016/j.neuron.2014.12.036.Diversity

Lee, C.-H. H., & Giuliani, F. (2019). The Role of Inflammation in Depression and Fatigue. *Frontiers in Immunology*, *10*(1696), 1–12. https://doi.org/10.3389/fimmu.2019.01696

Li, T., Bourgeois, J.-P., Celli, S., Glacial, F., Le Sourd, A.-M., Mecheri, S., Weksler, B., Romero, I., Couraud, P.-O., Rougeon, F., & Lafaye, P. (2012). Cell-penetrating anti-GFAP VHH and corresponding fluorescent fusion protein VHH-GFP spontaneously cross the blood-brain barrier and specifically recognize astrocytes: application to brain imaging. *The FASEB Journal*, *26*(10), 3969–3979. https://doi.org/10.1096/fj.11-201384

Little, A. (2009). Treatment-resistant depression. *American Family Physician*, *80*(2), 167–172. https://doi.org/10.9740/mhc.n207177

Liu, J. J., Wei, Y. Bin, Strawbridge, R., Bao, Y., Chang, S., Shi, L., Que, J., Gadad, B. S., Trivedi, M. H., Kelsoe, J. R., & Lu, L. (2019). Peripheral cytokine levels and response to antidepressant treatment in depression: a systematic review and meta-analysis. *Molecular Psychiatry*, *25*(2), 339–350. https://doi.org/10.1038/s41380-019-0474-5

Liu, R. J., & Aghajanian, G. K. (2008). Stress blunts serotonin- and hypocretin-evoked EPSCs in prefrontal cortex: Role of corticosterone-mediated apical dendritic atrophy. *Proceedings of the National Academy of Sciences of the United States of America*, *105*(1), 359–364. https://doi.org/10.1073/pnas.0706679105

Liu, X., Zhao, Z., Ji, R., Zhu, J., Sui, Q.-Q., Knight, G. E., Burnstock, G., He, C., Yuan, H., & Xiang, Z. (2017). Inhibition of P2X7 receptors improves outcomes after traumatic brain injury in rats. *Purinergic Signalling*, *13*(4), 529–544. https://doi.org/10.1007/s11302-017-9579-y

Liu, Y., Zhao, J., & Guo, W. (2018). Emotional Roles of Mono-Aminergic Neurotransmitters in Major Depressive Disorder and Anxiety Disorders. *Frontiers in Psychology*, *9*(2201), 1–8. https://doi.org/10.3389/fpsyg.2018.02201

Livak, K. J., & Schmittgen, T. D. (2001). Analysis of relative gene expression data using real-time quantitative PCR and the 2-ΔΔCT method. *Methods*, *25*(4), 402–408. https://doi.org/10.1006/meth.2001.1262

Lopizzo, N., Bocchio Chiavetto, L., Cattane, N., Plazzotta, G., Tarazi, F. I., Pariante, C. M., Riva, M. A., & Cattaneo, A. (2015). Gene-environment interaction in major depression: focus on experience-dependent biological systems. *Frontiers in Psychiatry*, *6*(68), 1–12. https://doi.org/10.3389/fpsyt.2015.00068

Lovick, T. A., & Zangrossi, H. (2021). Effect of Estrous Cycle on Behavior of Females in Rodent

Tests of Anxiety. *Frontiers in Psychiatry*, *12*(711065), 1–20. https://doi.org/10.3389/fpsyt.2021.711065

Lucae, S., Salyakina, D., Barden, N., Harvey, M., Gagné, B., Labbé, M., Binder, E. B., Uhr, M., Paez-Pereda, M., Sillaber, I., Ising, M., Brückl, T., Lieb, R., Holsboer, F., & Müller-Myhsok, B. (2006). P2RX7, a gene coding for a purinergic ligand-gated ion channel, is associated with major depressive disorder. *Human Molecular Genetics*, *15*(16), 2438–2445. https://doi.org/10.1093/hmg/ddl166

Lyman, M., Lloyd, D. G., Ji, X., Vizcaychipi, M. P., & Ma, D. (2014). Neuroinflammation: The role and consequences. *Neuroscience Research*, *79*, 1–12. https://doi.org/10.1016/J.NEURES.2013.10.004

Ma, M., Ren, Q., Zhang, J. C., & Hashimoto, K. (2014). Effects of brilliant blue G on serum tumor necrosis factor-α levels and depression-like behavior in mice after lipopolysaccharide administration. *Clinical Psychopharmacology and Neuroscience*, *12*(1), 31–36. https://doi.org/10.9758/cpn.2014.12.1.31

Machado-Vieira, R., Baumann, J., Wheeler-Castillo, C., Latov, D., Henter, I., Salvadore, G., & Zarate, C. (2010). The Timing of Antidepressant Effects: A Comparison of Diverse Pharmacological and Somatic Treatments. *Pharmaceuticals*, *3*(1), 19–41. https://doi.org/10.3390/ph3010019

Mackenzie, A. B., Young, M. T., Adinolfi, E., & Surprenant, A. (2005a). Pseudoapoptosis induced by brief activation of ATP-gated P2X7 receptors. *Journal of Biological Chemistry*, *280*(40), 33968–33976. https://doi.org/10.1074/jbc.M502705200

Mackenzie, A. B., Young, M. T., Adinolfi, E., & Surprenant, A. (2005b). Pseudoapoptosis Induced by Brief Activation of ATP-gated P2X $_7$ Receptors. *Journal of Biological Chemistry*, *280*(40), 33968–33976. https://doi.org/10.1074/jbc.M502705200

Magariñ̃os, A. M., & McEwen, B. S. (1995). Stress-induced atrophy of apical dendrites of hippocampal CA3c neurons: Comparison of stressors. *Neuroscience*, *69*(1), 83–88. https://doi.org/10.1016/0306-4522(95)00256-I

Malberg, J. E., & Duman, R. S. (2003). Cell proliferation in adult hippocampus is decreased by inescapable stress: Reversal by fluoxetine treatment. *Neuropsychopharmacology*, *28*(9), 1562–1571. https://doi.org/10.1038/sj.npp.1300234

Margaretten, M., Julian, L., Katz, P., & Yelin, E. (2011). Depression in patients with rheumatoid arthritis: Description, causes and mechanisms. *International Journal of Clinical Rheumatology*, *6*(6), 617–623. https://doi.org/10.2217/ijr.11.62

Martínez-Frailes, C., Di Lauro, C., Bianchi, C., De Diego-García, L., Sebastián-Serrano, Á., Boscá, L., & Díaz-Hernández, M. (2019). Amyloid peptide induced neuroinflammation increases the P2X7 receptor expression in microglial cells, impacting on its functionality. *Frontiers in Cellular Neuroscience*, *13*(143), 1–15. https://doi.org/10.3389/fncel.2019.00143

Masin, M., Young, C., Lim, K., Barnes, S. J., Xu, X. J., Marschall, V., Brutkowski, W., Mooney, E. R., Gorecki, D. C., & Murrell-Lagnado, R. (2012). Expression, assembly and function of novel C-terminal truncated variants of the mouse P2X7 receptor: re-evaluation of P2X7 knockouts. *British Journal of Pharmacology*, *165*(4), 978–993. https://doi.org/10.1111/J.1476-

5381.2011.01624.X

Masuch, A., Shieh, C. H., van Rooijen, N., van Calker, D., & Biber, K. (2016). Mechanism of microglia neuroprotection: Involvement of P2X7, TNFα, and valproic acid. *Glia*, *64*(1), 76–89. https://doi.org/10.1002/glia.22904

Matute, C., Torre, I., Pérez-Cerdá, F., Pérez-Samartín, A., Alberdi, E., Etxebarria, E., Arranz, A. M., Ravid, R., Rodríguez-Antigüedad, A., Sánchez-Gómez, M. V., & Domercq, M. (2007). P2X7 receptor blockade prevents ATP excitotoxicity in oligodendrocytes and ameliorates experimental autoimmune encephalomyelitis. *Journal of Neuroscience*, *27*(35), 9525–9533. https://doi.org/10.3390/ijms22063054

McCarthy, A. E., Yoshioka, C., & Mansoor, S. E. (2019). Full-Length P2X7 Structures Reveal How Palmitoylation Prevents Channel Desensitization. *Cell*, 1–12. https://doi.org/10.1016/j.cell.2019.09.017

McGuffin, P., Knight, J., Breen, G., Brewster, S., Boyd, P. R., Craddock, N., Gill, M., Korszun, A., Maier, W., Middleton, L., Mors, O., Owen, M. J., Perry, J., Preisig, M., Reich, T., Rice, J., Rietschel, M., Jones, L., Sham, P., & Farmer, A. E. (2005). Whole genome linkage scan of recurrent depressive disorder from the depression network study. *Human Molecular Genetics*, *14*(22), 3337–3345. https://doi.org/10.1093/hmg/ddi363

McIntyre, R. S., Filteau, M.-J. J., Martin, L., Patry, S., Carvalho, A., Cha, D. S., Barakat, M., & Miguelez, M. (2014). Treatment-resistant depression: Definitions, review of the evidence, and algorithmic approach. *Journal of Affective Disorders*, *156*, 1–7. https://doi.org/10.1016/j.jad.2013.10.043

Mead, E. L., Mosley, A., Eaton, S., Dobson, L., Heales, S. J., & Pocock, J. M. (2012). Microglial neurotransmitter receptors trigger superoxide production in microglia; consequences for microglial-neuronal interactions. *Journal of Neurochemistry*, *121*(2), 287–301. https://doi.org/10.1111/j.1471-4159.2012.07659.x

Metzger, M. . (2016). *The P2X7 receptor and its functional involvement in mood and neurodegenerative disorders* (pp. 1–171).

Metzger, M. W., Walser, S. M., Aprile-Garcia, F., Dedic, N., Chen, A., Holsboer, F., Arzt, E., Wurst, W., & Deussing, J. M. (2017). Genetically dissecting P2rx7 expression within the central nervous system using conditional humanized mice. *Purinergic Signalling*, *13*(2), 153–170. https://doi.org/10.1007/s11302-016-9546-z

Metzger, M. W., Walser, S. M., Dedic, N., Aprile-Garcia, F., Jakubcakova, V., Adamczyk, M., Webb, K. J., Uhr, M., Refojo, D., Schmidt, M. V., Friess, E., Steiger, A., Kimura, M., Chen, A., Holsboer, F., Arzt, E., Wurst, W., & Deussing, J. M. (2017). Heterozygosity for the mood disorder-associated variant Gln460Arg alters P2X7 receptor function and sleep quality. *The Journal of Neuroscience*, *37*(48), 11688–11700. https://doi.org/10.1523/JNEUROSCI.3487-16.2017

Meziane, H., Ouagazzal, A. M., Aubert, L., Wietrzych, M., & Krezel, W. (2007). Estrous cycle effects on behavior of C57BL/6J and BALB/cByJ female mice: Implications for phenotyping strategies. *Genes, Brain and Behavior*, *6*(2), 192–200. https://doi.org/10.1111/j.1601-183X.2006.00249.x

Miller, G. E., Stetler, C. A., Carney, R. M., Freedland, K. E., & Banks, W. A. (2002). Clinical depression and inflammatory risk markers for coronary heart disease. *The American Journal of Cardiology*, *90*(12), 1279–1283. https://doi.org/10.1016/S0002-9149(02)02863-1

Miras-Portugal, M. T., Sebastián-Serrano, Á., de Diego García, L., & Díaz-Hernández, M. (2017). Neuronal P2X7 Receptor: Involvement in Neuronal Physiology and Pathology. *The Journal of Neuroscience*, *37*(30), 7063–7072. https://doi.org/10.1523/JNEUROSCI.3104-16.2017

Monif, M., Reid, C. A., Powell, K. L., Drummond, K. J., O'Brien, T. J., & Williams, D. A. (2016). Interleukin-1β has trophic effects in microglia and its release is mediated by P2X7R pore. *Journal of Neuroinflammation*, *13*(1), 1–15. https://doi.org/10.1186/s12974-016-0621-8

Moore, S. F., & MacKenzie, A. B. (2008). Species and agonist dependent zinc modulation of endogenous and recombinant ATP-gated P2X7 receptors. *Biochemical Pharmacology*, *76*(12), 1740–1747. https://doi.org/10.1016/j.bcp.2008.09.015

Mori, T., Koichi, T., Buffo, A., Wurst, W., Kühn, R., & Götz, M. (2006). Inducible Gene Deletion in Astroglia and Radial Glia. *Glia*, *54*, 21–34. https://doi.org/10.1002/glia

Mulinari, S. (2012). Monoamine theories of depression: Historical impact on biomedical research. *Journal of the History of the Neurosciences*, *21*(4), 366–392. https://doi.org/10.1080/0964704X.2011.623917

Muyldermans, S. (2013). Nanobodies: Natural Single-Domain Antibodies. *Annual Review of Biochemistry*, *82*(1), 775–797. https://doi.org/10.1146/annurev-biochem-063011-092449

Nagy, G., Ronai, Z., Somogyi, A., Sasvari-Szekely, M., Rahman, O. A., Mate, A., Varga, T., & Nemoda, Z. (2008). P2RX7 Gln460Arg polymorphism is associated with depression among diabetic patients. *Progress in Neuro-Psychopharmacology and Biological Psychiatry*, *32*(8), 1884–1888. https://doi.org/10.1016/j.pnpbp.2008.08.021

Nicke, A., Kuan, Y.-H., Masin, M., Rettinger, J., Marquez-Klaka, B., Bender, O., Górecki, D. C., Murrell-Lagnado, R. D., & Soto, F. (2009). A functional P2X7 splice variant with an alternative transmembrane domain 1 escapes gene inactivation in P2X7 knock-out mice. *The Journal of Biological Chemistry*, *284*(38), 25813–25822. https://doi.org/10.1074/jbc.M109.033134

Otrokocsi, L., Kittel, Á., & Sperlágh, B. (2017). P2X7 receptors drive spine synapse plasticity in the learned helplessness model of depression. *International Journal of Neuropsychopharmacology*, *20*(10), 813–822. https://doi.org/10.1093/ijnp/pyx046

Otte, C., Gold, S. M., Penninx, B. W., Pariante, C. M., Etkin, A., Fava, M., Mohr, D. C., & Schatzberg, A. F. (2016). Major depressive disorder. *Nature Reviews Disease Primers*, *2*(16065), 1–20. https://doi.org/10.1038/nrdp.2016.65

Pace, T. W. W., & Miller, A. H. (2007). Cytokine-Effects on Glucocorticoid Receptor Function: Relevance to Glucocorticoid Resistance and the Pathophysiology and Treatment of Major Depression. *Brain Behavior Immunology*, *21*(1), 9–19.

Palanza, P., Gioiosa, L., & Parmigiani, S. (2001). Social stress in mice: Gender differences and effects of estrous cycle and social dominance. *Physiology and Behavior*, *73*(3), 411–420. https://doi.org/10.1016/S0031-9384(01)00494-2

Parkhurst, C. N., Yang, G., Ninan, I., Savas, J. N., Yates, J. R., Lafaille, J. J., Hempstead, B. L.,

Littman, D. R., Gan, W.-B., & Gan, W.-B. (2013). Microglia promote learning-dependent synapse formation through brain-derived neurotrophic factor. *Cell*, *155*(7), 1596–1609. https://doi.org/10.1016/j.cell.2013.11.030

Pegoraro, A., De Marchi, E., & Adinolfi, E. (2021). P2X7 Variants in Oncogenesis. *Cells*, *10*(1). https://doi.org/10.3390/cells10010189

Peterson, R. E., Cai, N., Dahl, A. W., Bigdeli, T. B., Edwards, A. C., Webb, B. T., Bacanu, S.-A., Zaitlen, N., Flint, J., & Kendler, K. S. (2018). Molecular Genetic Analysis Subdivided by Adversity Exposure Suggests Etiologic Heterogeneity in Major Depression. *American Journal of Psychiatry*, *175*(6), 545–554. https://doi.org/10.1176/appi.ajp.2017.17060621

Raison, C. L., Capuron, L., & Miller, A. H. (2006). Cytokines sing the blues: inflammation and the pathogenesis of depression. *Trends in Immunology*, *27*(1), 24–31. https://doi.org/10.1016/j.it.2005.11.006

Raison, C. L., Rutherford, R. E., Woolwine, B. J., Shuo, C., Schettler, P., Drake, D. F., Haroon, E., & Miller, A. H. (2013). A randomized controlled trial of the tumor necrosis factor antagonist infliximab for treatment-resistant depression: the role of baseline inflammatory biomarkers. *JAMA Psychiatry*, *70*(1), 31–41. https://doi.org/10.1001/2013.jamapsychiatry.4

Ramírez-Fernández, A., Urbina-Treviño, L., Conte, G., Alves, M., Rissiek, B., Durner, A., Scalbert, N., Zhang, J., Magnus, T., Koch-Nolte, F., Plesnila, N., Deussing, J. M., Engel, T., Kopp, R., & Nicke, A. (2020). Deviant reporter expression and P2X4 passenger gene overexpression in the soluble EGFP BAC transgenic P2X7 reporter mouse model. *Scientific Reports*, *10*(1), 1–17. https://doi.org/10.1038/s41598-020-76428-0

Ramirez, C., Shea, D., McKim, D., & Sheridan, J. (2015). Imipramine attenuates neuroinflammatory signaling and reverses stress-induced social avoidance. *Brain Behav Immun*, *176*(1), 100–106. https://doi.org/10.1016/j.bbi.2015.01.016.Imipramine

Ribeiro, Deidiane E, Müller, H. K., Elfving, B., Eskelund, A., Joca, S. R., & Wegener, G. (2019). Antidepressant-like effect induced by P2X7 receptor blockade in FSL rats is associated with BDNF signalling activation. *Journal of Psychopharmacology*, *33*(11), 1436–1446. https://doi.org/10.1177/0269881119872173

Ribeiro, Deidiane Elisa, Roncalho, A. L., Glaser, T., Ulrich, H., Wegener, G., & Joca, S. (2019). P2X7 Receptor Signaling in Stress and Depression. *International Journal of Molecular Sciences*, *20*(2778), 1–26. https://doi.org/10.3390/ijms20112778

Riedel, T., Schmalzing, G., & Markwardt, F. (2007). Influence of extracellular monovalent cations on pore and gating properties of P2X7 receptor-operated single-channel currents. *Biophysical Journal*, *93*(3), 846–858. https://doi.org/10.1529/biophysj.106.103614

Rohden, A. I., Benchaya, M. C., Camargo, R. S., Moreira, T. de C., Barros, H. M. T., & Ferigolo, M. (2017). Dropout Prevalence and Associated Factors in Randomized Clinical Trials of Adolescents Treated for Depression: Systematic Review and Meta-analysis. *Clinical Therapeutics*, *39*(5), 971-992.e4. https://doi.org/10.1016/j.clinthera.2017.03.017

Rosenblat, J. D., Brietzke, E., Mansur, R. B., Maruschak, N. A., Lee, Y., & Mcintyre, R. S. (2015). Inflammation as a neurobiological substrate of cognitive impairment in bipolar disorder: Evidence, pathophysiology and treatment implications. *Journal of Affective Disorders*, *188*,

149–159. https://doi.org/10.1016/j.jad.2015.08.058

Sanacora, G., Treccani, G., & Popoli, M. (2012). Towards a glutamate hypothesis of depression: An emerging frontier of neuropsychopharmacology for mood disorders. *Neuropharmacology*, *62*(1), 63–77. https://doi.org/10.1016/j.neuropharm.2011.07.036

Santarelli, L. (2003). Requirement of Hippocampal Neurogenesis for the Behavioral Effects of Antidepressants. *Science*, *301*(5634), 805–809. https://doi.org/10.1126/science.1083328

Sassarini, D. J. (2016). Depression in midlife women. *Maturitas*, *94*, 149–154. https://doi.org/10.1016/j.maturitas.2016.09.004

Savio, L. E. B., de Andrade Mello, P., da Silva, C. G., & Coutinho-Silva, R. (2018). The P2X7 Receptor in Inflammatory Diseases: Angel or Demon? *Frontiers in Pharmacology*, *9*(52), 1–31. https://doi.org/10.3389/fphar.2018.00052

Schwarz, N., Drouot, L., Nicke, A., Fliegert, R., Boyer, O., Guse, A. H., Haag, F., Adriouch, S., & Koch-Nolte, F. (2012). Alternative splicing of the N-terminal cytosolic and transmembrane domains of P2X7 controls gating of the ion channel by ADP-ribosylation. *PloS One*, *7*(7), 1–9. https://doi.org/10.1371/journal.pone.0041269

Sebastián-Serrano, Á., Engel, T., de Diego-García, L., Olivos-Oré, L. A., Arribas-Blázquez, M., Martínez-Frailes, C., Pérez-Díaz, C., Millán, J. L., Artalejo, A. R., Miras-Portugal, M. T., Henshall, D. C., & Díaz-Hernández, M. (2016). Neurodevelopmental alterations and seizures developed by mouse model of infantile hypophosphatasia are associated with purinergic signalling deregulation. *Human Molecular Genetics*, *25*(19), 4143–4156. https://doi.org/10.1093/hmg/ddw248

Sen, S., Duman, R., & Sanacora, G. (2008). Serum BDNF, Depression and Anti-Depressant Medications: Meta-Analyses and Implications. *Biological Psychiatry*, *64*(6), 527–532. https://doi.org/10.1016/j.biopsych.2008.05.005

Shabab, T., Khanabdali, R., Moghadamtousi, S. Z., Kadir, H. A., & Mohan, G. (2017). Neuroinflammation pathways: a general review. *International Journal of Neuroscience*, *127*(7), 624–633. https://doi.org/10.1080/00207454.2016.1212854

Shadrina, M., Bondarenko, E. A., & Slominsky, P. A. (2018). Genetics Factors in Major Depression Disease. *Frontiers in Psychiatry*, *9*(334), 1–18. https://doi.org/10.3389/fpsyt.2018.00334

Shink, E., Morissette, J., Sherrington, R., & Barden, N. (2005). A genome-wide scan points to a susceptibility locus for bipolar disorder on chromosome 12. *Molecular Psychiatry*, *10*(6), 545–552. https://doi.org/10.1038/sj.mp.4001601

Sierra, A., Gottfried-Blackmore, A., Milner, T. A., McEwen, B. S., & Bulloch, K. (2008). Steroid hormone receptor expression and function in microglia. *Glia*, *56*(6), 659–674. https://doi.org/10.1002/glia.20644

Simon, G. E., Savarino, J., Operskalski, B., Wang, P. S., Ph, D., Operskalski, B., & Wang, P. S. (2006). Suicide risk during antidepressant treatment. *American Journal of Psychiatry*, *163*(1), 41–47. https://doi.org/10.1176/appi.ajp.163.1.41

Sluyter, R. (2017). The P2X7 receptor. *Advances in Experimental Medicine and Biology*,

1051(July), 17–53. https://doi.org/10.1007/5584_2017_59

Sluyter, R., & Stokes, L. (2011). Significance of P2X7 receptor variants to human health and disease. *Recent Patents on DNA & Gene Sequences*, *5*(1), 41–54.

Solle, M., Labasi, J., Perregaux, D. G., Stam, E., Petrushova, N., Koller, B. H., Griffiths, R. J., & Gabel, C. A. (2001). Altered cytokine production in mice lacking P2X(7) receptors. *The Journal of Biological Chemistry*, *276*(1), 125–132. https://doi.org/10.1074/jbc.M006781200

Soronen, P., Mantere, O., Melartin, T., Suominen, K., Vuorilehto, M., Rytsälä, H., Arvilommi, P., Holma, I., Holma, M., Jylhä, P., Valtonen, H. M., Haukka, J., Isometsä, E., & Paunio, T. (2011). P2RX7 gene is associated consistently with mood disorders and predicts clinical outcome in three clinical cohorts. *American Journal of Medical Genetics Part B: Neuropsychiatric Genetics*, *156*(4), 435–447. https://doi.org/10.1002/ajmg.b.31179

Stahl, E. A., Breen, G., Forstner, A. J., McQuillin, A., Ripke, S., Trubetskoy, V., Mattheisen, M., Wang, Y., Coleman, J. R. I., Gaspar, H. A., de Leeuw, C. A., Steinberg, S., Pavlides, J. M. W., Trzaskowski, M., Byrne, E. M., Pers, T. H., Holmans, P. A., Richards, A. L., Abbott, L., … Sklar, P. (2019). Genome-wide association study identifies 30 loci associated with bipolar disorder. *Nature Genetics*, *51*(5), 793–803. https://doi.org/10.1038/s41588-019-0397-8

Stein, D. J., Vasconcelos, M. F., Albrechet-Souza, L., Ceresér, K. M. M., & De Almeida, R. M. M. (2017). Microglial over-activation by social defeat stress contributes to anxiety-and depressive-like behaviors. *Frontiers in Behavioral Neuroscience*, *11*(207), 1–10. https://doi.org/10.3389/fnbeh.2017.00207

Steiner, J., Bielau, H., Brisch, R., Danos, P., Ullrich, O., Mawrin, C., Bernstein, H.-G., & Bogerts, B. (2008). Immunological aspects in the neurobiology of suicide: Elevated microglial density in schizophrenia and depression is associated with suicide. *Journal of Psychiatric Research*, *42*(2), 151–157. https://doi.org/10.1016/j.jpsychires.2006.10.013

Stetler, C., & Miller, G. E. (2011). Depression and hypothalamic-pituitary-adrenal activation: A quantitative summary of four decades of research. *Psychosomatic Medicine*, *73*(2), 114–126. https://doi.org/10.1097/PSY.0b013e31820ad12b

Stokes, L., Fuller, S. J., Sluyter, R., Skarratt, K. K., Gu, B. J., & Wiley, J. S. (2010). Two haplotypes of the P2X $_7$ receptor containing the Ala-348 to Thr polymorphism exhibit a gain-of-function effect and enhanced interleukin-1β secretion. *The FASEB Journal*, *24*(8), 2916–2927. https://doi.org/10.1096/fj.09-150862

Su, W. J., Zhang, T., Jiang, C. L., & Wang, W. (2018). Clemastine alleviates depressive-like behavior through reversing the imbalance of microglia-related pro-inflammatory state in mouse hippocampus. *Frontiers in Cellular Neuroscience*, *12*(412), 1–11. https://doi.org/10.3389/fncel.2018.00412

Suadicani, S. O., Brosnan, C. F., & Scemes, E. (2006). P2X7 receptors mediate ATP release and amplification of astrocytic intercellular Ca2+ signaling. *The Journal of Neuroscience : The Official Journal of the Society for Neuroscience*, *26*(5), 1378–1385. https://doi.org/10.1523/JNEUROSCI.3902-05.2006

Sullivan, P. F., Neale, M. C., & Kendler, K. S. (2000). Genetic epidemiology of major depression: Review and meta-analysis. *American Journal of Psychiatry*, *157*(10), 1552–1562.

https://doi.org/10.1176/appi.ajp.157.10.1552

Surprenant, A., Rassendren, F., Kawashima, E., North, R. A., & Buell, G. (1996). The Cytolytic P2Z Receptor for Extracellular ATP Identified as a P2X Receptor (P2X7). *Science*, *272*(May), 5–8. https://doi.org/10.1126/science.272.5262.735

Suurväli, J., Boudinot, P., Kanellopoulos, J., & Rüütel Boudinot, S. (2017). P2X4: A fast and sensitive purinergic receptor. *Biomedical Journal*, *40*(5), 245–256. https://doi.org/10.1016/j.bj.2017.06.010

Taliaz, D., Stall, N., Dar, D. E., & Zangen, A. (2010). Knockdown of brain-derived neurotrophic factor in specific brain sites precipitates behaviors associated with depression and reduces neurogenesis. *Molecular Psychiatry*, *15*(1), 80–92. https://doi.org/10.1038/mp.2009.67

Tan, S., Wang, Y., Chen, K., Long, Z., & Zou, J. (2017). Ketamine alleviates depressive-like behaviors via down-regulating inflammatory cytokines induced by chronic restraint stress in mice. *Biological and Pharmaceutical Bulletin*, *40*(8), 1260–1267. https://doi.org/10.1248/bpb.b17-00131

Tewari, M., & Seth, P. (2015). Emerging role of P2X7 receptors in CNS health and disease. *Ageing Research Reviews*, *24*, 328–342. https://doi.org/10.1016/j.arr.2015.10.001

Thomas, A. J., Davis, S., Morris, C., Jackson, E., Harrison, R., & O'Brien, J. T. (2005). Increase in Interleukin-1β in Late-Life Depression. *American Journal of Psychiatry*, *162*(1), 175–177. https://doi.org/10.1176/appi.ajp.162.1.175

Timmers, M., Ravenstijn, P., Xi, L., Triana-Baltzer, G., Furey, M., Van Hemelryck, S., Biewenga, J., Ceusters, M., Bhattacharya, A., van den Boer, M., van Nueten, L., & de Boer, P. (2018). Clinical pharmacokinetics, pharmacodynamics, safety, and tolerability of JNJ-54175446, a brain permeable P2X7 antagonist, in a randomised single-ascending dose study in healthy participants. *Journal of Psychopharmacology*, *32*(12), 1341–1350. https://doi.org/10.1177/0269881118800067

Tong, L., Aleph Prieto, G., Kramár, E. A., Smith, E. D., Cribbs, D. H., Lynch, G., & Cotman, C. W. (2012). Brain-derived neurotrophic factor-dependent synaptic plasticity is suppressed by interleukin-1β via p38 mitogen-activated protein kinase. *Journal of Neuroscience*, *32*(49), 17714–17724. https://doi.org/10.1523/JNEUROSCI.1253-12.2012

Troubat, R., Leman, S., Pinchaud, K., Surget, A., Barone, P., Roger, S., Le Guisquet, A. M., Brizard, B., Belzung, C., & Camus, V. (2021). Brain immune cells characterization in UCMS exposed P2X7 knock-out mouse. *Brain, Behavior, and Immunity*, *94*(April 2020), 159–174. https://doi.org/10.1016/j.bbi.2021.02.012

Van der Meij, A., Comijs, H. C., Dols, A., Janzing, J. G. E., & Oude Voshaar, R. C. (2014). BDNF in late-life depression: Effect of SSRI usage and interaction with childhood abuse. *Psychoneuroendocrinology*, *43*, 81–89. https://doi.org/10.1016/j.psyneuen.2014.02.001

Vereczkei, A., Abdul-Rahman, O., Halmai, Z., Nagy, G., Szekely, A., Somogyi, A., Faludi, G., & Nemoda, Z. (2019). Association of purinergic receptor P2RX7 gene polymorphisms with depression symptoms. *Progress in Neuro-Psychopharmacology and Biological Psychiatry*, *92*, 207–216. https://doi.org/10.1016/j.pnpbp.2019.01.006

Viikki, M., Kampman, O., Anttila, S., Illi, A., Setälä-Soikkeli, E., Huuhka, M., Mononen, N., Lehtimäki, T., & Leinonen, E. (2011). P2RX7 polymorphisms Gln460Arg and His155Tyr are not associated with major depressive disorder or remission after SSRI or ECT. *Neuroscience Letters*, *493*(3), 127–130. https://doi.org/10.1016/j.neulet.2011.02.023

Volonte, C., Apolloni, S., D. Skaper, S., & Burnstock, G. (2012). P2X7 Receptors: Channels, Pores and More. *CNS & Neurological Disorders - Drug Targets*, *11*(6), 705–721. https://doi.org/10.2174/187152712803581137

Wei, L., Syed Mortadza, S. A., Yan, J., Zhang, L., Wang, L., Yin, Y., Li, C., Chalon, S., Emond, P., Belzung, C., Li, D., Lu, C., Roger, S., & Jiang, L. H. (2018). ATP-activated P2X7 receptor in the pathophysiology of mood disorders and as an emerging target for the development of novel antidepressant therapeutics. *Neuroscience and Biobehavioral Reviews*, *87*(2010), 192–205. https://doi.org/10.1016/j.neubiorev.2018.02.005

Weinhold, K., Krause-Buchholz, U., Rödel, G., Kasper, M., & Barth, K. (2010). Interaction and interrelation of P2X7 and P2X4 receptor complexes in mouse lung epithelial cells. *Cellular and Molecular Life Sciences*, *67*(15), 2631–2642. https://doi.org/10.1007/s00018-010-0355-1

Wook Koo, J., & Duman, R. S. (2008). IL-1β is an essential mediator of the antineurogenic and anhedonic effects of stress. *Proceedings of the National Academy of Sciences of the United States of America*, *105*(2), 751–756. https://doi.org/10.1073/pnas.0708092105

World Health Organizaton. (2017). Depression and Other Common Mental Disorders: Global Health Estimates. Geneva: *Geneva: World Health Organization*, *CC BY-NC-S*.

Wray, N. R., Ripke, S., Mattheisen, M., Trzaskowski, M., Byrne, E. M., Abdellaoui, A., Adams, M. J., Agerbo, E., Air, T. M., Andlauer, T. M. F., Bacanu, S. A., Bækvad-Hansen, M., Beekman, A. F. T., Bigdeli, T. B., Binder, E. B., Blackwood, D. R. H., Bryois, J., Buttenschøn, H. N., Bybjerg-Grauholm, J., … Sullivan, P. F. (2018). Genome-wide association analyses identify 44 risk variants and refine the genetic architecture of major depression. *Nature Genetics*, *50*(5), 668–681. https://doi.org/10.1038/s41588-018-0090-3

Wyatt, L. R., Godar, S. C., Khoja, S., Jakowec, M. W., Alkana, R. L., Bortolato, M., & Davies, D. L. (2013). Sociocommunicative and sensorimotor impairments in male P2X4-deficient mice. *Neuropsychopharmacology*, *38*(10), 1993–2002. https://doi.org/10.1038/npp.2013.98

Xia, J., Lim, J. C., Lu, W., Beckel, J. M., Macarak, E. J., Laties, A. M., & Mitchell, C. H. (2012). Neurons respond directly to mechanical deformation with pannexin-mediated ATP release and autostimulation of P2X 7 receptors. *Journal of Physiology*, *590*(10), 2285–2304. https://doi.org/10.1113/jphysiol.2012.227983

Xiong, Y., Teng, S., Zheng, L., Sun, S., Li, J., Guo, N., Li, M., Wang, L., Zhu, F., Wang, C., Rao, Z., & Zhou, Z. (2018). Stretch-induced Ca2+ independent ATP release in hippocampal astrocytes. *Journal of Physiology*, *596*(10), 1931–1947. https://doi.org/10.1113/JP275805

Ye, L., Huang, Y., Zhao, L., Li, Y., Sun, L., Zhou, Y., Qian, G., & Zheng, J. C. (2013). IL-1β and TNF-α induce neurotoxicity through glutamate production: a potential role for neuronal glutaminase NIH Public Access. *J Neurochem*, *125*(6), 897–908. https://doi.org/10.1111/jnc.12263

Young, C. N. J., & Górecki, D. C. (2018). P2RX7 Purinoceptor as a Therapeutic Target-The

Second Coming? *Frontiers in Chemistry*, *6*(248), 1–14. https://doi.org/10.3389/fchem.2018.00248

Young, C. N., Sinadinos, A., Lefebvre, A., Chan, P., Arkle, S., Vaudry, D., & Gorecki, D. C. (2015). A novel mechanism of autophagic cell death in dystrophic muscle regulated by P2RX7 receptor large-pore formation and HSP90. *Autophagy*, *11*(1), 113–130. https://doi.org/10.4161/15548627.2014.994402

Yue, N., Huang, H., Zhu, X., Han, Q., Wang, Y., Li, B., Liu, Q., Wu, G., Zhang, Y., & Yu, J. (2017). Activation of P2X7 receptor and NLRP3 inflammasome assembly in hippocampal glial cells mediates chronic stress-induced depressive-like behaviors. *Journal of Neuroinflammation*, *14*(102), 1–15. https://doi.org/10.1186/s12974-017-0865-y

Zeisel, A., Hochgerner, H., Lönnerberg, P., Johnsson, A., Memic, F., van der Zwan, J., Häring, M., Braun, E., Borm, L. E., La Manno, G., Codeluppi, S., Furlan, A., Lee, K., Skene, N., Harris, K. D., Hjerling-Leffler, J., Arenas, E., Ernfors, P., Marklund, U., & Linnarsson, S. (2018). Molecular Architecture of the Mouse Nervous System. *Cell*, *174*(4), 999-1014.e22. https://doi.org/10.1016/j.cell.2018.06.021

Zhang, Lei, Su, T. P., Choi, K., Maree, W., Li, C. T., Chung, M. Y., Chen, Y. S., Bai, Y. M., Chou, Y. H., Barker, J. L., Barrett, J. E., Li, X. X., Li, H., Benedek, D. M., & Ursano, R. (2011). P11 (S100A10) as a potential biomarker of psychiatric patients at risk of suicide. *Journal of Psychiatric Research*, *45*(4), 435–441. https://doi.org/10.1016/j.jpsychires.2010.08.012

Zhang, Lijuan, Fu, T., Yin, R., Zhang, Q., & Shen, B. (2017). Prevalence of depression and anxiety in systemic lupus erythematosus: a systematic review and meta-analysis. *BMC Psychiatry*, *17*(70), 1–14. https://doi.org/10.1186/s12888-017-1234-1

Zhao, Y. F., Tang, Y., & Illes, P. (2021). Astrocytic and Oligodendrocytic P2X7 Receptors Determine Neuronal Functions in the CNS. *Frontiers in Molecular Neuroscience*, *14*, 1–10. https://doi.org/10.3389/fnmol.2021.641570

Zhu, C. Bin, Blakely, R. D., & Hewlett, W. A. (2006). The proinflammatory cytokines interleukin-1beta and tumor necrosis factor-alpha activate serotonin transporters. *Neuropsychopharmacology*, *31*(10), 2121–2131. https://doi.org/10.1038/sj.npp.1301029

Zhu, Y., Klomparens, E. A., Guo, S., & Geng, X. (2019). Neuroinflammation caused by mental stress: the effect of chronic restraint stress and acute repeated social defeat stress in mice. *Neurological Research*, *41*(8), 762–769. https://doi.org/10.1080/01616412.2019.1615670

11. Acknowledgements

To Jan Deussing for giving me the opportunity to work in this project, for the guidance and for all his unconditional support.

To Annette Nicke and Carsten Wotjak for their time and valuable contributions.

To the PurinesDX network for the funding, fresh ideas, and good times.

To the Graduate School of Neuroscience for the structure and guidance.

To my colleagues, past and present, for the interesting discussions, friendly ears and helping hands.

To all my people, for always having their hand tended to me. This would have been much more difficult without you.

A mi familia, por hacer que todo esto sea posible y por estar siempre conmigo. Sin vosotros habría sido imposible.